

Thèse de Doctorat

Yue PENG

*Mémoire présenté en vue de l'obtention
du grade de Docteur de l'Université de Nantes
Sous le label de l'Université Nantes Angers Le Mans*

École doctorale Sciences et Technologies de l'Information et Mathématiques (STIM)

*Discipline : Electronique
Laboratoire : IETR UMR 6164*

Soutenance le 9 novembre 2015

Energy optimisation of communication techniques between communicating objects

JURY

Président	M. Kosaï RAOOF , Professeur, ENSIM, Université du Maine
Rapporteur	M. Olivier BERDER , Professeur, IUT de Lannion
Rapporteur	M. Yannis POUSSET , Professeur, Université de Poitiers
Examineur	M. Jean-Yves BAUDAIS , Chargé de Recherche CNRS/HDR, IETR, Rennes
Directeur de Thèse	M. Jean-François DIOURIS , Professeur, Ecole polytechnique de l'université de Nantes
Encadrant	M. Guillaume ANDRIEUX , Maître de Conférences, IUT de la Roche s/Yon

Acknowledgments

Have a lot of wonderful memories, I went through four years journey in Nantes. The people I met here is really unbelievable. A few words mentioned here cannot capture all my appreciation to your supports and the pleasure you brought to me.

First of all, I would like to express my great thanks to my advisor, Professor Jean-François Diouris. It has been a pleasant experience of working with him. I want to thank him for his gentleness, encouragement and inspiration. I have benefited tremendously from that, not only at the academic research but also on the personal growth. This impact will go along with me throughout my life.

I would also like to thank Guillaume Andrieux, Assistant Professor, for many contributions of his perspective to refine the works of my thesis and for his countless help during the writing of my thesis.

Grateful acknowledgments are also given to Professor Yannis Pousset and Professor Olivier Berder, the reviewers of my thesis, for their acceptance of being the reviewer of my thesis.

The IETR lab has provided a great collegial environment for academic research. I thank Professor Yide Wang, for his tremendous supports and also good care for my daily life. The works in IETR cannot be so efficient without help from Sandrine Charlier, secretary of IETR, Marc Brunet, engineer of IETR. They deserve many thanks.

At last, for my family and my friends, I want to thank Zhu QI, Ting Zhang, Xiaoting Xiao, Zhaoxin Chen, Hong kun... We had a wonderful memory of both working and traveling in Europe.

Contents

1	Introduction	15
1.1	Energy conservation in Wireless Sensor Networks	16
1.2	Objectives of the work	19
1.3	The outline of the thesis	19
2	Energy efficient transmission techniques	21
2.1	Fundamental Shannon limit	22
2.2	Modulation	26
2.2.1	Binary phase-shift keying (BPSK)	26
2.2.2	OOK	27
2.2.3	Orthogonal modulation	27
2.3	Minimum energy coding schemes	31
2.3.1	Minimum energy coding	31
2.3.2	Modified minimum energy coding	34
2.4	Error control scheme	37
2.4.1	Overview of error control	37
2.4.2	Example of error-correction code: Hamming code	38
2.4.3	Error correction in ME-Coding	40
2.4.4	Error correction codes combined with ME-Coding	42
2.5	ME-coding on different communication channels	43
2.5.1	AWGN channel and Rayleigh fading channel	44
2.5.2	Error probability in AWGN channel and Rayleigh fading channel	46
2.5.3	Simulation results versus theoretic results	55
2.6	Summary	57
3	Energy consumption models	59
3.1	The architecture of a typical wireless sensor node	60
3.2	General energy consumption model	62

3.2.1	General energy consumption model of fully-functioning node	63
3.2.2	General power consumption model of communication link . . .	65
3.2.3	Application of the model to based OOK ME Coding	67
3.3	OOK matched energy consumption models	69
3.3.1	Normal energy consumption model	69
3.3.2	Condition and analysis of the proposed model	74
3.3.3	Shutdown energy consumption model	78
3.4	Conclusion	82
4	Energy efficiency of Minimum Energy coding	83
4.1	Description of the studied devices	84
4.1.1	The first OOK transmitter	84
4.1.2	High performance OOK transmitter	85
4.1.3	OOK receiver	86
4.2	Energy consumption study of a realistic transmitter	87
4.2.1	Minimum energy coding and BER analysis	88
4.2.2	Energy consumption model	89
4.2.3	Energy Consumption Analysis	94
4.2.4	Conclusion	97
4.3	Energy analysis of a high performance transmitter	98
4.3.1	Energy consumption model of the 52pJ/bit OOK transmitter	98
4.3.2	Energy consumption improvement	101
4.3.3	Optimization of the coding size	103
4.3.4	Conclusion	106
4.4	Receiver energy consumption	106
4.4.1	Energy consumption Model	107
4.4.2	Energy consumption of the receiver	108
4.5	Conclusion	111
5	Error control schemes and Application	115
5.1	Error Control Protocols	116
5.1.1	Automatic repeat request Protocol	116
5.1.2	Energy consumption performance analysis	118
5.1.3	Numerical results	120
5.1.4	Conclusion	124
5.2	Self powered Energy Efficient OOK Transmitter	124

<i>CONTENTS</i>	7
5.2.1 Optimization of the autonomous transmitter	125
5.3 Summary	134
6 Conclusion and future works	137
6.1 Conclusion	137
6.2 Future works	139
A Index of value definition	141
B Optimization of the coding size	143
C Résumé étendu (French extended abstract)	147
D Research and Published Papers	153

List of Tables

2.1	Minimum-Energy Code table for $k = 2$ and 3	33
3.1	System parameter	68
3.2	The simulation parameter	75
3.3	The simulation parameter	80
4.1	The parameter of the transmitter	100
4.2	The transmit parameter of the transmitter	101
4.3	The parameter of particular case	106
4.4	Energy per codeword in shutdown mode	108
5.1	The circuit parameters	123
5.2	<i>PIC12LF1501</i> power consumption as the function of the DC voltage using the low energy $31kHz$ internal oscillator	128
5.3	RT40-433 power model parameters	128
5.4	Required $r(M)$ in dB for M orthogonal modulations	130

List of Figures

1.1	Taxonomy of approaches to energy savings in sensor networks.	17
2.1	Trade-off between energy efficiency and bandwidth efficiency.	24
2.2	Transmit and total energy per bit as a function of the bit rate	25
2.3	Constellation diagram example for BPSK.	26
2.4	The probability of bit error for orthogonal modulations.	29
2.5	Trade-off between energy efficiency and spectrum efficiency for orthogonal modulations	30
2.6	Typical OOK Modulation Scheme.	31
2.7	Block Diagram of ME Mapping Scheme.	32
2.8	Flow of chip-by-chip detection process.	34
2.9	The principle of MME coding.	35
2.10	Receive MME to ME energy gain.	37
2.11	Bit error probability for Hamming code and BPSK modulation.	40
2.12	Error Correction with Code-by-Code Detection.	41
2.13	AWGN Channel	44
2.14	Example of hard decision process for ME-Coding	49
2.15	Performance of ME-coding in AWGN channel	56
2.16	Performance of ME-coding in Rayleigh fading channel	56
3.1	The architecture of a typical wireless sensor node.	60
3.2	Power consumption of a typical wireless sensor node.	61
3.3	Block diagram of a fully-functioning node.	62
3.4	A link model.	63
3.5	A model of the microsensor node.	63
3.6	Burst receive/transmit cycle for Bluetooth Transceiver.	65
3.7	Transmitter Circuit Blocks (Analog).	66
3.8	Receiver Circuit Blocks.	66

3.9	Energy consumption comparison	68
3.10	Transmitter circuit analog blocks	70
3.11	OOK Receiver circuit	70
3.12	Definition of the switch time	71
3.13	Total power consumption versus output power (circuit MAX1472, from datasheet)	75
3.14	Total power consumption of the MAX1472 using the proposed model (without switch time)	76
3.15	Demodulation of the output signal of the MAX1472 transmitter from circuit data sheet. Data rate = 100kbit/s	76
3.16	Total power consumption of the MAX1472 using the proposed model (with switch time= $0.5\mu s$)	77
3.17	Transmitter circuit analog blocks - shutdown mode	78
3.18	Transmit time of bit '1' and bit '0' in shutdown mode	78
3.19	Total power consumption of the MAX1472 using the shutdown mode	81
3.20	Comparison of the total power consumption of the MAX1472 using the shutdown mode and the normal mode	81
4.1	The analog block (a) Typical Application Circuit (b)Functional Dia- gram	85
4.2	The block diagram of the second OOK transmitter	86
4.3	Functional diagram of MAX7033 receiver	87
4.4	OOK transceiver developed in the laboratory	88
4.5	BER performance of ME-Coding	89
4.6	The equivalent analog block of the simple OOK model	90
4.7	Supply current vs.output power (a) CW and 0.5 duty cycle (b) Cubic polynomial curve fitting for different duty cycles	92
4.8	The equivalent analog block of <i>SDOWN</i> model	93
4.9	(a) Transmit energy per bit with $R=100\text{kbit/s}$ (b) Total energy con- sumption per bit with $R = 100\text{kbit/s}$	95
4.10	Total energy consumption per bit with MAX1472 with $R=1\text{ kbit/s}$	96
4.11	Relationship between energy consumption and bit rate, for $d = 10\text{m}$	97
4.12	The block diagram of the ook transmitter	98
4.13	Oscillator output	99
4.14	Total power consumption	102
4.15	Total energy consumption per source bit	102

4.16	Total energy consumption as a function of k	103
4.17	The signal to noise ratio r_0 versus coding size k	104
4.18	The transmit range versus coding size k	105
4.19	Activity of the receiver in shutdown mode	107
4.20	The energy consumption of the receiver in normal mode	109
4.21	The energy consumption of the receiver in shutdown mode	109
4.22	The energy consumption for $R = 100kbit/s$	110
4.23	The energy consumption with shutdown mode for $R = 100kbit/s$	111
4.24	The energy consumption with shutdown mode for $R = 1kbit/s$	112
4.25	The total energy consumption VS the symbol rate	112
5.1	Transmission model	119
5.2	Illustration of the working of a simple ARQ protocol	119
5.3	Average transmission times required for a successful reception as a function of the output power for sending a 1, using OOK	121
5.4	Average transmission times required for a successful reception as a function of the output power, using ME(7,3)	122
5.5	Average transmission times required for a successful reception as a function of the output power, using ME(63,6)	122
5.6	Average total energy per bit as a function of the output power, using OOK	123
5.7	Average total energy per bit as a function of the output power, using ME(7,3)	124
5.8	Average total energy per bit as a function of the output power, using ME(63,6)	125
5.9	Block diagram of an autonomous transmitter	126
5.10	Block diagram of the piezoelectric harvester	126
5.11	Capacitor voltage and stored energy	127
5.12	Energy per bit versus bit rate for different values of k , BER= 10^{-3}	130
5.13	Maximum transmit power as a function of the bit rate for different values of k , BER= 10^{-3}	131
5.14	Number of bits versus bit rate for different values of k , BER= 10^{-3}	132
5.15	Total energy per bit versus k for a fixed chip rate equal to 9600 kHz, $k = 1$ is OOK, $k > 1$ is 2^k orthogonal modulation	133
5.16	Piezo-electric transmitter	134
5.17	Led lamp receiver	135

5.18 Waveform received after OOK demodulation. The identifier is the time position of the second pulse. 135

B.1 Diagram of the real branches of the Lambert W function 144

Introduction

Wireless sensor network (WSN) technology is promising and is therefore gaining popularity day by day in a wide range of applications [1, 2, 3, 4], especially related to the civil and military operations. This technology is mainly used for sensing, data gathering or surveillance use, where low data rate of the order of few kbit/s and of transmission range of the order of few meters are involved. One of the challenging topics in wireless communication techniques to be used for WSN applications is energy efficiency. The life time of a wireless sensor node depends on available energy sources and its overall energy consumption. Furthermore, there is a limitation of the capacity of batteries because of the small size requirement of the nodes. Power efficiency at system level must be brought about by keeping in mind the circuit complexities and the circuit power consumption. Every design comes with a trade-off, hence, we have to compromise either with power, bandwidth or error. This is the main reason for us to think in terms of developing a more energy efficient wireless communication system at the expense of bandwidth and with least circuit complexities.

Energy optimization of wireless sensor networks is a vast topic that has generated interest from numerous researchers and engineers in networks, digital communication, circuit design, material technology, etc. Our work focuses on the link level but it is interesting to propose firstly a synthetic review of the research status on energy conservation in wireless sensor networks.

1.1 Energy conservation in Wireless Sensor Networks

Energy constraint has always been one of the most significant problems when developing wireless sensor networks. Many methods have been introduced to solve this problem, basically in two aspects: energy management [5, 6] and energy harvesting [7, 8, 9]. When a sensor node is depleted of energy, it will die and disconnect from the network which can significantly impact the performance of the application. Sensor network lifetime depends on the number of active nodes and connectivity of the network, so energy must be used efficiently in order to maximize the network lifetime.

The first method is energy harvesting. Energy harvesting involves nodes replenishing its energy from an energy source. Potential energy sources include solar cells [10, 11], vibration [12, 13], fuel cells, acoustic noise and a mobile supplier [14]. In terms of harvesting energy from the environment [7, 15], solar cell is the current mature technique that harvests energy from light. There is also work in using a mobile energy supplier such as a robot to replenish energy. The robots would be responsible in charging themselves with energy and then delivering energy to the nodes.

The other method is energy management. Typically, a sensor node is a tiny device that includes three basic components: a sensing subsystem for data acquisition [16] from the physical surrounding environment, a processing subsystem for local data processing and storage, and a wireless communication subsystem for data transmission. In addition, a power source supplies the energy needed by the device to perform the programmed task. This power source often consists of a battery with a limited energy budget.

The energy cost of transmitting a single bit of information is approximately the same as that needed for processing a thousand operations in a typical sensor node [17]. The energy consumption of the sensing subsystem depends on the specific sensor type. In many cases, it is negligible with respect to the energy consumed by the processing and the communication subsystems. In general, energy-saving techniques focus on two subsystems: the networking subsystem (i.e., energy management is taken into account in the operations of each single node, as well as in the design of networking protocols), and the sensing subsystem (i.e., techniques are used to reduce the amount or frequency of energy-expensive samples). The lifetime of a sensor network can be extended by jointly applying different techniques.

Several approaches have to be exploited to reduce power consumption in wireless sensor networks. At a very general level, we identify four main enabling techniques in Fig. 1.1, namely, duty cycling, data-driven approaches, mobility and link optimization.

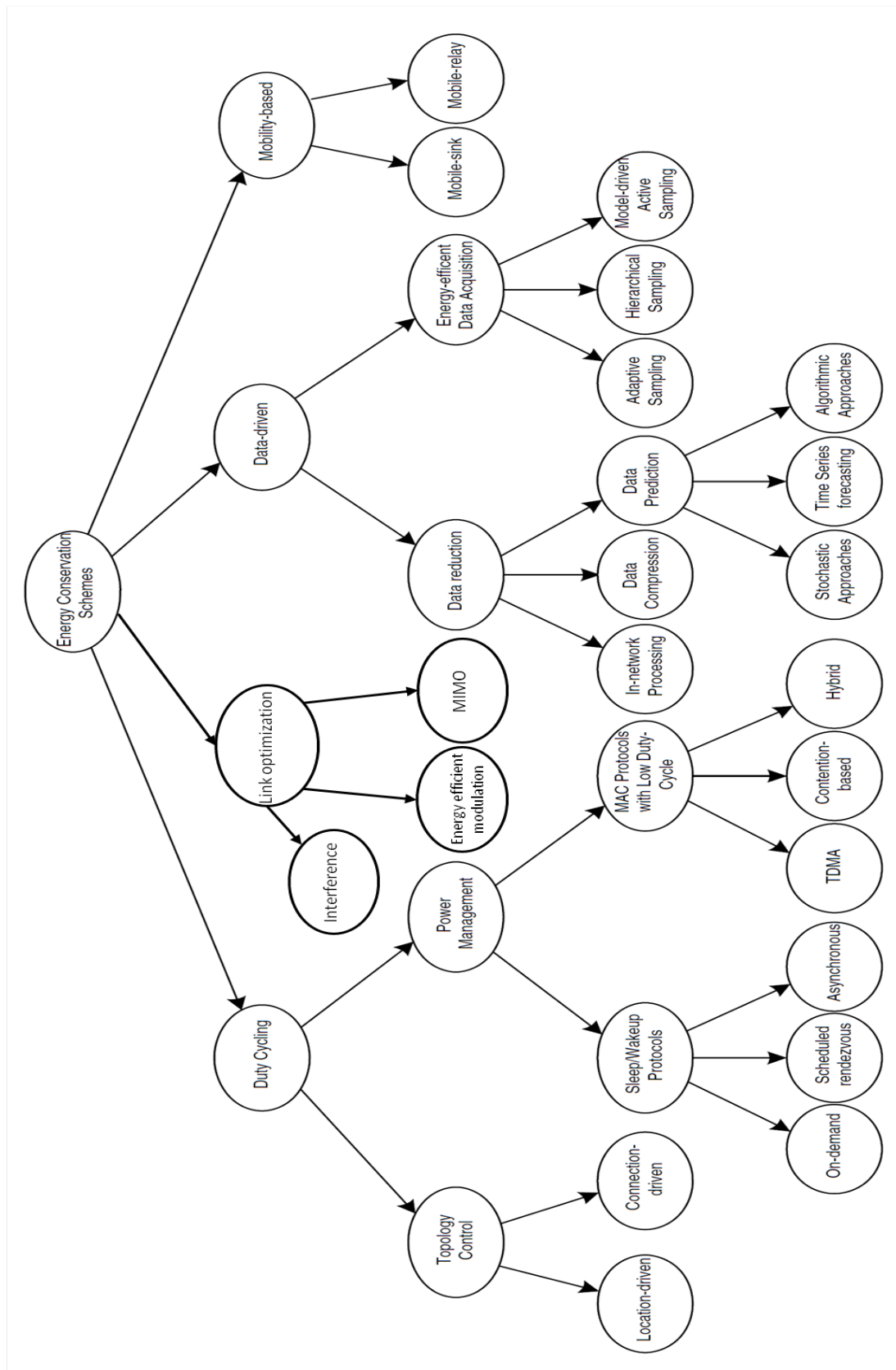


Figure 1.1: Taxonomy of approaches to energy savings in sensor networks.

Duty cycling [8, 18] is mainly focused on the networking subsystem. The most effective energy-conserving operation is putting the radio transceiver in the (low-power) sleep mode whenever communication is not required. Ideally, the radio should be switched off as soon as there is no more data to send/receive, and should be resumed as soon as a new data packet becomes ready. In this way, nodes alternate between active and sleep periods depending on network activity. This behavior is usually referred as duty cycling and duty cycle is defined as the fraction of time nodes are active during their lifetime. In Fig. 1.1, we can consider to use the effective MAC protocols [19], network protocols [20, 21, 22], error control protocols [23] to increase the network lifetime.

Duty-cycling schemes are typically oblivious to data that are sampled by sensor nodes. Hence, data-driven approaches can be used to improve the energy efficiency even more. This way to decrease the total communication traffic is using data aggregation [24, 25, 26, 27], data compression [28, 29, 30], data prediction [31, 32].

The third way is to utilize mobility to improve network lifetime. When the sensor nodes are mobile, mobility can finally be used as a tool for reducing energy consumption (beyond duty cycling and data-driven techniques). We can also divide this method into two categories: one is to use mobile agent to collect data in order to conserve energy consumption, another way is to balance the energy consumption by introducing a mobile sink [33, 34, 35]. In a static sensor network, packets coming from sensor nodes follow a multi-hop path towards the sink(s). Thus, a few paths can be more loaded than others and nodes closer to the sink have to relay more packets so that they are more subject to premature energy depletion (tunneling effect) [36].

The last way is link optimization including interference, MIMO and energy efficient modulation. We pay more attention on the energy efficient modulation, as many new coding and modulation schemes can be employed to bring about power efficiency at system level. Source coding [37, 38, 39], radio power control [40] and sleep disciplines [41] are all techniques that have been used to minimize the energy consumption of wireless sensor networks by using low energy coding schemes. The system can be made to operate with less SNR for a given error performance, but these codes are complex codes and circuit power consumption of the algorithms are increased.

There has been many recent works in the field of wireless microsensors to bring about energy efficiency at both system level and circuit level. Wang et al. [42] have discussed the issues of many low power wireless microsensor applications. They have proposed energy efficient modulations and MAC protocols for asymmetric RF microsensor systems. Comparison of various modulation techniques with respect to

transmit power and bandwidth efficiency is discussed. Methods to overcome the transmitter complexities and also the MAC protocols are described for microsensor applications.

1.2 Objectives of the work

In this thesis we focus on the physical layer and we propose to reduce the energy consumption for the transmission of small amount of information between or from communicating objects. In terms of applications, our targets are small devices like sensors, remote controls or actuators which can be scattered in different environments (houses, buildings, body, etc.) and must work autonomously with batteries or energy harvester.

We propose to use low energy coding schemes or low duty cycle modulations which can be implemented with simple (and low cost) circuits. The originality of our work is to propose an approach to the joint optimization of the transmitting techniques and circuit energy. The analysis is done using generic but also realistic models integrated in demonstrators.

1.3 The outline of the thesis

The content of the thesis is summarized as follows:

- Chapter 2 introduces energy efficient transmission techniques used in our study. The motivation is from the fundamental Shannon trade off between energy efficiency and spectrum efficiency, which is recalled. We introduce simple modulation schemes and the minimum energy efficient source coding (ME-coding) method with error control scheme. We determine the performance of the proposed methods, in terms of transmit energy, for the additive white gaussian noise channel and the Rayleigh channel;
- Chapter 3 deals with energy consumption models. We give an overview of the energy consumption in wireless sensor nodes. We introduce two general energy consumption models based on transceiver node and communication link respectively. These reference models which are used in numerous research works, are not matched to OOK modulation. So, we present new accurate energy consumption models that can be used to evaluate energy efficiency of ME-coding;
- Chapter 4 focus on the energy consumption analysis of ME-coding based on

realistic energy models of several devices. The first circuit is a low cost OOK transmitter for wide application but which has the disadvantage of having important limitations on the maximum bit rate. The second transmitter is a high performance and more energy efficient transmitter, but which is not commercially available. Besides, the method of selecting the optimal coding size is presented as well to reduce the energy consumption. The analysis is extended to the reception using another low cost circuit. In the last section, the energy consumption of a low cost receiver is studied. We propose and evaluate a method to reduce the activity of the circuit when receiving ME code-words;

- Chapter 5 presents more complex applications of the energy efficient transmission techniques. The first part describes the introduction of ME coding in an automatic repeat request error control protocol. The second part shows a realistic application of our study to a simple communicating device supplied by limited energy harvesting;
- Chapter 6 concludes on our efforts in coming up with energy efficient source coding scheme and modulation.

Energy efficient transmission techniques

In digital communication or data transmission, E_b/N_0 (the energy per bit to noise power spectral density ratio) is an important parameter. It is a normalized signal-to-noise ratio (SNR) measure, also known as the "SNR per bit". It is especially useful when comparing the bit error rate (BER) performance of different digital modulation schemes without taking bandwidth into account.

The energy E_b can be seen as the energy which is necessary to transmit one bit. It can be considered as a good metric to evaluate the energy efficiency of a transmission technique.

For a target performance (i.e bit error probability) the required E_b can be determined for a given transmission technique (modulation, demodulation, channel coding...) and channel condition.

Shannon showed there is a fundamental trade-off [43] between energy and bandwidth efficiency for reliable communications when only considering the transmit energy. Reducing the energy per bit is always obtained at the price of the bandwidth efficiency.

This important result is recalled in the next section. We include also a first model of circuit energy in order to show that considering the circuit power consumption can introduce a new optimum trade-off between energy and bandwidth efficiency. After

this theoretical approach, the rest of the chapter deals with realistic transmission techniques. Section 2.2 recalls the definition of different modulations. We focus on on-off keying modulation and orthogonal modulations which constitute the basis of our work. Section 2.3 defines the energy efficient source coding that will be used in our work. Section 2.4 is an overview of channel coding which is also an efficient method to reduce the energy per bit. In radio frequency modulation, a large part of the transmitted energy is lost in the propagation channel. Section 2.5 provides the performance of the proposed method for AWGN channel and Rayleigh channel.

2.1 Fundamental Shannon limit

One of the most famous results from information theory is the fundamental limit [43, 44], or Shannon limit, that sets requirements on the signal to noise ratio for reliable communication.

Consider a band limited Gaussian channel with bandwidth W and noise level N_0 . If the transmitted power constraint is P , then the capacity is given by

$$C = W \log_2\left(1 + \frac{P}{N_0 W}\right) \text{ [bits/s]} \quad (2.1)$$

Without other constraints, we would like to use as much bandwidth as possible. In theory the available bandwidth can be infinite, and therefore we set $W \rightarrow \infty$ in the formula.

$$C_\infty = \lim_{W \rightarrow \infty} W \log_2\left(1 + \frac{P}{N_0 W}\right) = \frac{P/N_0}{\ln 2} \quad (2.2)$$

Assigning the achieved bit rate as R_b , it is required that this value is not more than the capacity, $C_\infty \geq R_b$. Assume now that the signaling time is T_s and that in each signal, k information bits are transmitted. Then $PT_s = E_s = E_b k$ where E_s is the average energy per transmitted symbol and E_b is the average energy per information bit. The variable E_b is a very important parameter since it is something that can be compared between different systems, without having the same number of bits per symbol or even the same coding rate. Then a system independent signal to noise ratio is defined by $\text{SNR} = E_b/N_0$.

We can write the energy per bit as

$$E_b = \frac{PT_s}{k} \quad (2.3)$$

and considering the ratio between C_∞ and the bit rate R_b we get

$$\frac{C_\infty}{R_b} = \frac{P/N_0 T_s}{\ln 2} \frac{1}{k} = \frac{E_b/N_0}{\ln 2} > 1 \quad (2.4)$$

where we used that $R_b = \frac{k}{T_s}$ and we require $C_\infty > R_b$ for reliable communication. Rewriting the above equation, we can conclude that for reliable communication the SNR is required to be

$$E_b/N_0 > \ln 2 = 0.69 = -1.59 \text{ dB} \quad (2.5)$$

The value 1.6 dB is the well known Shannon limit and constitutes a hard limit for which it is possible to achieve reliable communication. If the SNR is less than this limit, it is not possible to reach error probability that tends to zero, independently of what system is used.

From this inequation we can also determine the minimum energy E_{bmin} to transmit an information bit on the additive white Gaussian noise channel. Assuming a thermal noise, defined by a power spectral density $N_0 = k_B T$ where $k_B = 1.38 \times 10^{-23} \text{ J/K}$ is the Boltzman constant and T is the temperature in Kelvin, we can express E_{bmin} as :

$$E_{bmin} = k_B T \ln 2 \quad (2.6)$$

This limit is identical to the minimum amount of energy required to erase one bit of information defined by Landauer [45]. The numerical value at 20°C (293.15 K) is very small:

$$E_{bmin} = 2.8 \times 10^{-21} \text{ J} \quad (2.7)$$

and probably unattainable in practice.

Considering now the capacity expression in Equation (2.1) for a finite bandwidth and ensuring the limit case $R_b = C$, the transmitted power constraint P can be written as:

$$P = N_0 W (2^{\frac{R_b}{W}} - 1) \quad (2.8)$$

Then the equation (2.3) can be rewritten as

$$E_b = \frac{P}{R_b} = \frac{N_0 W}{R_b} (2^{\frac{R_b}{W}} - 1) \quad (2.9)$$

$$E_b = \frac{N_0}{\eta} (2^n - 1) \quad (2.10)$$

where the bandwidth efficiency is defined as $\eta = \frac{R_b}{W}$.

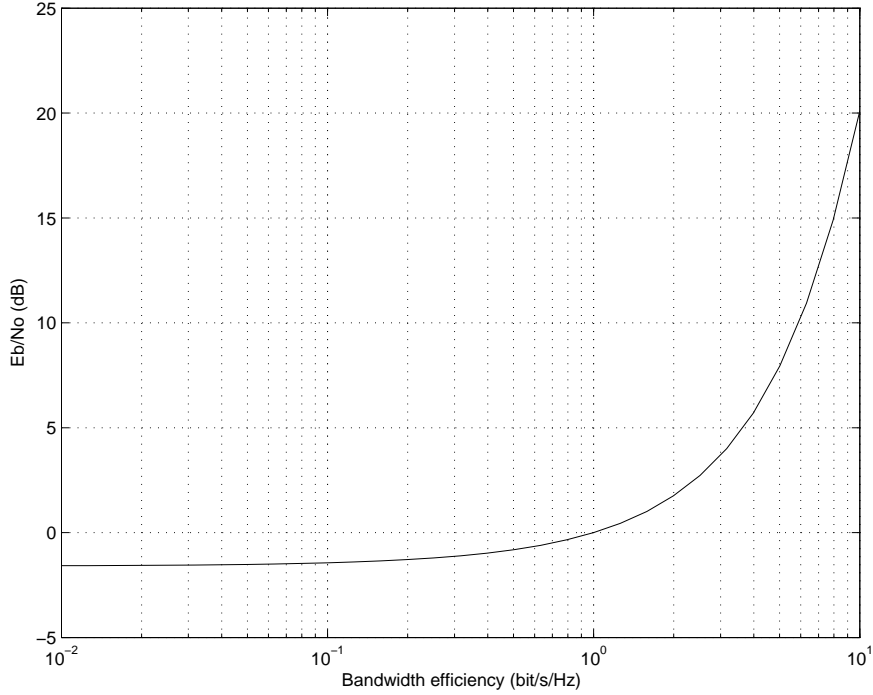


Figure 2.1: Trade-off between energy efficiency and bandwidth efficiency.

The fundamental trade-off between energy efficiency and bandwidth efficiency is plotted in the Fig. 2.1. It can be shown that reducing the energy per bit results in the reduction of the bandwidth efficiency, i.e. the increasing of the bandwidth necessary to send a given bit rate.

The energy per bit E_b represents the bit energy that is transmitted on the channel. If we consider a realistic channel, we must introduce the channel gain g and the transmit energy becomes:

$$E_b = \frac{N_0}{g\eta} (2^n - 1) \quad (2.11)$$

In a real case, the process of the information needs an additional energy that can be called circuit energy. As we want to be independent of the specific transmission scheme, we propose a model for which the circuit power is constant equal to P_c . So the total energy per bit can be written:

$$E_b = \frac{N_0}{g\eta}(2^\eta - 1) + \frac{P_c}{R_b} \quad (2.12)$$

We can also express the total bit energy as a function of the bit rate :

$$E_b = \frac{N_0}{gR_b/W}(2^{R_b/W} - 1) + \frac{P_c}{R_b} \quad (2.13)$$

For a given bandwidth W , this equation shows that the transmit energy is a growing function of the bit rate whereas the circuit energy is decreasing.

This behavior is illustrated in Fig. 2.2 which shows the transmit energy and the total energy as the function of the bit rate for a bandwidth equal to 1 MHz and $N_0 = k_B T$, where k_B is the Boltzman constant, $T = 300K$ is the temperature, and $P_c = 1\mu W$. We assume $g = -128$ dB, corresponding to a free space attenuation for a 2 GHz frequency and a transmit distance equal to 1 km plus a 30 dB margin.

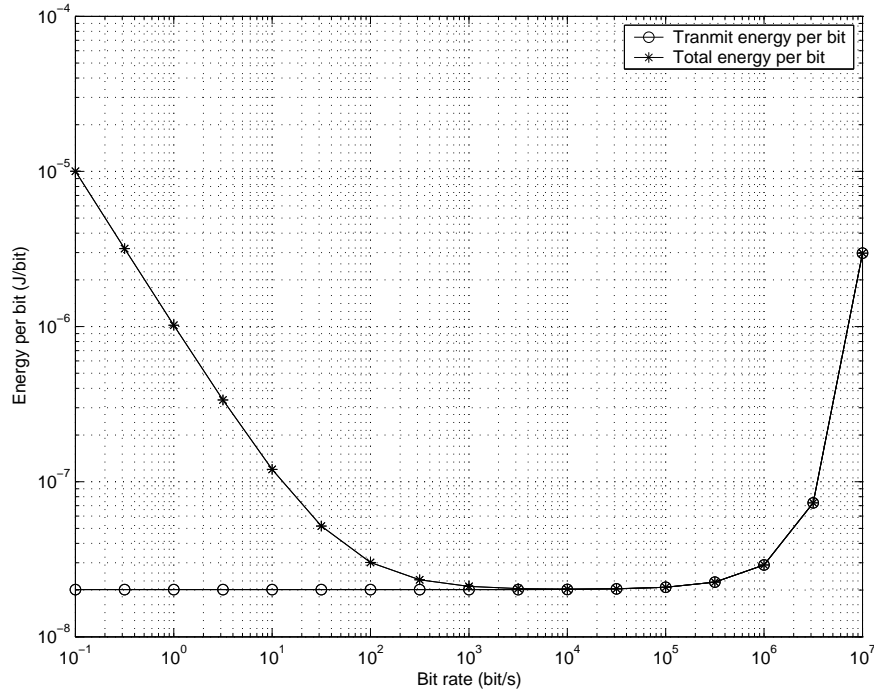


Figure 2.2: Transmit and total energy per bit as a function of the bit rate

It can be shown that the circuit energy is predominant for low bit rate whereas the transmit energy grows a lot for high bit rate. Hence, an optimal bit rate can be determined, corresponding to the minimization of the total energy. With the chosen numerical values, this optimal rate is about 10 kbit/s .

In the rest of this chapter we focus only on the transmit energy. Circuit energy will

be considered, using more realistic circuit models, in the next chapters.

2.2 Modulation

Modulation is the operation which consists in introducing the information in a signal that is matched to the bandwidth of the physical channel (for example a radio frequency channel). In the next sub-section we consider firstly the Binary Phase Shift Keying which is the simplest form of digital modulation. This modulation will be used as a reference in our study. Then, we introduce On Off Keying which is the modulation used for Minimum Energy Coding and finally the orthogonal modulation which can be used to approach C_∞ and which has also be used at the end of our study.

2.2.1 Binary phase-shift keying (BPSK)

BPSK (Binary Phase Shift Keying[46, 47], or 2PSK) is the simplest form of phase shift keying (PSK). It uses two phases which are separated by 180° and so can also be termed 2-PSK. In the figure 2.3, the two symbols are shown on the real axis, at 0° for bit 1 and 180° for bit 0. This modulation is the most robust of all the PSKs. It is, however, only able to modulate at 1 bit/symbol and so is unsuitable for high data-rate applications.

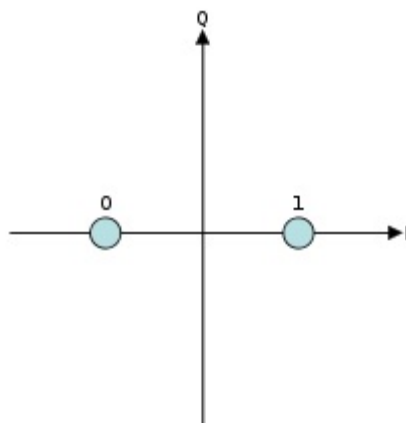


Figure 2.3: Constellation diagram example for BPSK.

In the presence of an arbitrary phase-shift introduced by the communication channel, the demodulator is unable to tell which constellation point is which. As a result, the data is often differentially encoded prior to modulation.

For BPSK modulation and without coding, suppose the signals are affected by an additive white Gaussian noise (AWGN). Then, using the coherent receiver, the bit error probability is the same as the symbol error probability [46], and is given by:

$$P_e = \frac{1}{2} \operatorname{erfc} \left(\sqrt{E_b/N_0} \right) \quad (2.14)$$

Knowing that one bit is transmitted per symbol, we deduce that the spectrum efficiency of BPSK is 1 bit/s/Hz.

2.2.2 OOK

On-Off Keying (OOK) is the simplest form of amplitude-shift keying (ASK) modulation that represents digital data as the presence or absence of a carrier wave. In its simplest form, the presence of a carrier for a specific duration represents a binary one, while its absence for the same duration represents a binary zero. It is analog to unipolar encoding line code.

OOK is most commonly used to transmit Morse code over radio frequencies, although in principle any digital encoding scheme may be used. OOK has been used in the ISM bands to transfer data between computers, for example. In addition to RF carrier waves, OOK is also used in optical communication systems.

For OOK modulation and without coding, suppose the signals are affected by an additive white Gaussian noise (AWGN), then the bit error probability [48], for a coherent receiver, is given by:

$$P_e = \frac{1}{2} \operatorname{erfc} \left(\sqrt{\frac{E_b/N_0}{2}} \right) \quad (2.15)$$

where, E_b is the average energy per bit. This equation shows that, for the same BER, a loss of 3dB is obtained in comparison to BPSK. We will see in our work that the advantage of OOK will be obtained in association with Minimum Energy Coding and taking into account the circuit energy consumption.

Similarly to BPSK, the spectrum efficiency is 1 bit/s/Hz.

2.2.3 Orthogonal modulation

Orthogonal modulation [49] with non-coherent detection is a practical choice for situations where the received signal phase cannot be reliably estimated and/or tracked. There are many important applications where this is the case. Examples include mil-

itary communications using fast frequency hopping, airborne communications with high Doppler shifts due to significant relative motion of the transmitter and receiver, and high phase noise scenarios, due to the use of inexpensive or unreliable local oscillators.

For equal-energy orthogonal signals $s_m(t)$ $m = 1, \dots, M$, the optimum receiver selects the signal resulting in the largest cross correlation between the received signal $x(t)$ and each of the M possible transmitted signals using the decision variable:

$$u_m = \frac{1}{\sqrt{E}} \int_0^T x(t)s_m(t)dt \quad m = 1, \dots, M \quad (2.16)$$

suppose that the signal s_m is transmitted. Using the orthogonality property of the symbols and assuming that the energy of $s_m(t)$ is unity, the above random variables can be written as:

$$\begin{aligned} u_1 &= \sqrt{E} + n_1 \\ u_m &= n_m, \quad m \neq 1 \end{aligned} \quad (2.17)$$

where n_m are zero-mean, mutually independent Gaussian random variables with variance $\sigma^2 = N_0/2$. The probability of correct decision is given by:

$$P_c = \int_{-\infty}^{+\infty} P((u_2 < u_1, \dots, u_M < u_1)/u_1) p(u_1) du_1 \quad (2.18)$$

since the $\{u_m\}$ are statistically independent, the joint probability factors into a product of $M - 1$ marginal probabilities of the form:

$$\begin{aligned} P(u_m < u_1/u_1) &= \frac{1}{\sqrt{\pi N_0}} \int_{-\infty}^{u_1} e^{-\frac{x^2}{N_0}} dx \\ &= 1 - \frac{1}{2} \operatorname{erfc}\left(\frac{u_1}{\sqrt{N_0}}\right) \end{aligned} \quad (2.19)$$

Therefore the symbol error probability is given by:

$$P_s = 1 - P_c = 1 - \frac{1}{\sqrt{\pi}} \int_{-\infty}^{+\infty} \left(1 - \frac{1}{2} \operatorname{erfc}(x)\right)^{M-1} e^{-(x-\sqrt{E/N_0})^2} dx \quad (2.20)$$

Since $M = 2^k$, each symbol contains k bits and is at the same distance from the others. We can then deduce the bit error probability:

$$P_{eb} = \frac{1}{k} \sum_{n=1}^k n C_k^n \frac{P_s}{2^k - 1} = \frac{2^{k-1}}{2^k - 1} P_s \quad (2.21)$$

We can also consider the union bound, resulting in a simpler formula for the symbol error probability:

$$P_s \simeq \frac{M-1}{2} \operatorname{erfc} \left(\sqrt{\frac{k E_b}{2 N_0}} \right) \quad (2.22)$$

The graphs of the probability of bit error as a function of SNR per bit E_b/N_0 are shown in Fig. 2.4 for a Gaussian channel.

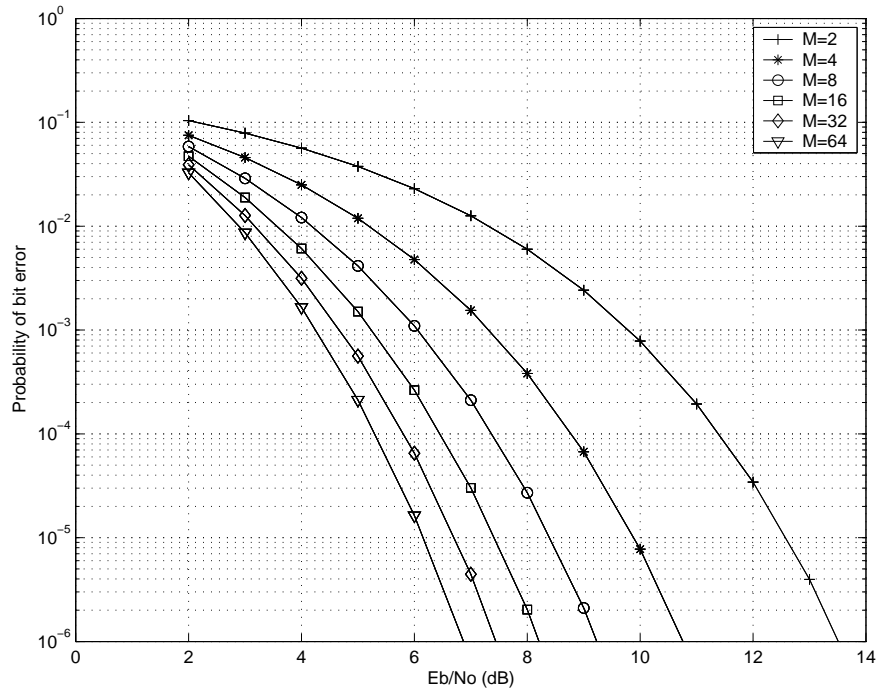


Figure 2.4: The probability of bit error for orthogonal modulations.

This figure illustrates that, by increasing the number M of waveforms, one can reduce the SNR per bit required to achieve a given probability of bit error. For example, to keep a bit error probability $P_b = 10^{-5}$, the required SNR ratio per bit is about 12.5 dB for $M = 2$, but if $M = 64$ corresponding to 6 bits per symbol, the required SNR ratio per bit is approximately 6.1 dB. Thus, a gain of 6.4 dB is realized in transmitter power to achieve $P_b = 10^{-5}$ by increasing M from 2 to 64.

The spectrum efficiency of orthogonal modulations [50] is:

$$\eta = \frac{2k}{M} \quad (2.23)$$

The Fig. 2.5 presents the trade-off between energy efficiency and spectrum efficiency when varying the number of bits per symbol and the probability of error. Increasing M allows to reduce the energy per bit but at the price of reducing the spectrum efficiency. It can be shown [46] that orthogonal modulations allow to obtain the Shannon limit for an infinite number of bits per symbol (i.e. for an infinite bandwidth). The presented results are obtained with the union bound which is not a good approximation for very large number of symbols and low SNR. So the -1.6 dB limit cannot be shown by this approximation.

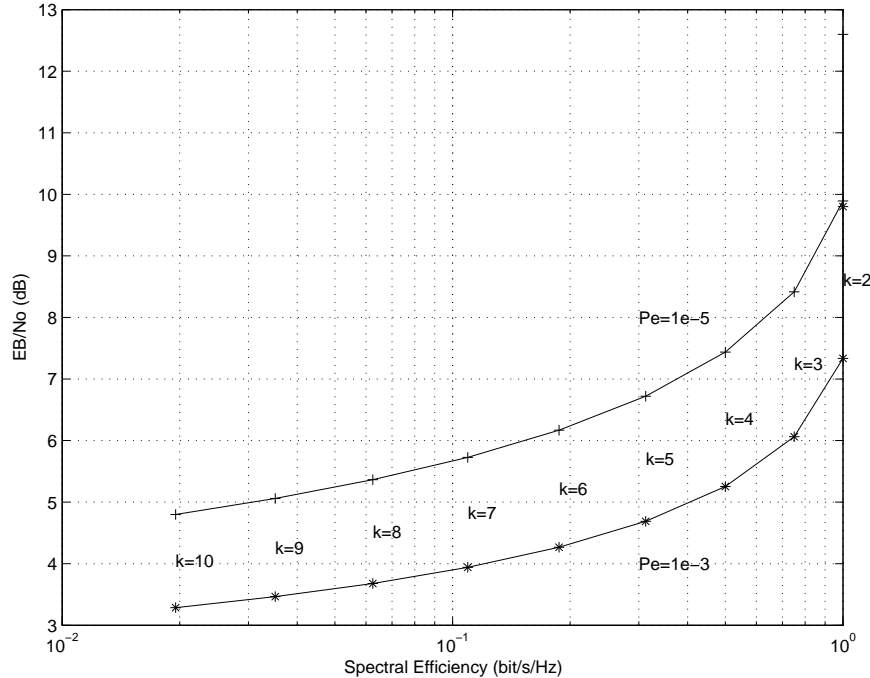


Figure 2.5: Trade-off between energy efficiency and spectrum efficiency for orthogonal modulations

2.3 Minimum energy coding schemes

2.3.1 Minimum energy coding

In OOK, a carrier signal is transmitted when a bit one is sent and no signal is transmitted when a bit zero is sent.

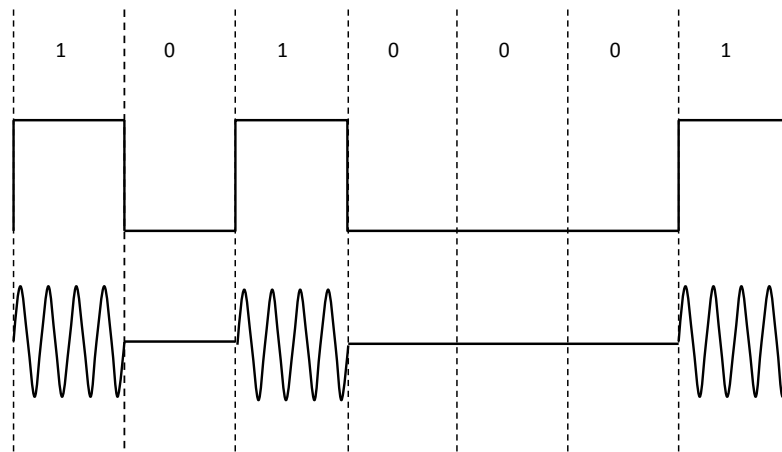


Figure 2.6: Typical OOK Modulation Scheme.

Fig. 2.6 shows OOK transmitted signals for a sequence of bits. We can assume that the transmitter expends more energy when transmitting a signal for bit one. Thus, for a system that uses OOK modulation technique, the obvious way to reduce the consumed energy would be to reduce the number of bit one. Since we have no control over the information source, the only way to reduce the high bits (bit one) would be to map a set of information bit sequence to a constant length code-word (ME-Code) which has less number of bits one in it. This is originally based on the idea proposed by Erin and Asada [51]. They have formulated the power optimization problem for wireless communication applications with message source of known statistics. They bring about the reduction in energy consumption in two steps. Firstly, use a set of codes that have less number of high bits in it. Secondly, assign these set of codes to the messages in such a way that, codes with less number of ones are assigned to messages of higher probabilities. They have also taken one step towards improving the performance of

these codes by simple concatenation process. Their approach of ME-Coding cannot be applied to sources with unknown statistics. Authors in [52] keep the basic idea of ME-Coding (source-bits mapped to code-bits) for source with unknown statistics (unknown probabilities of occurrence of symbols) and use a very simple near optimal detection process to improve the performance of ME-coding, thus proposing a new approach towards ME-coding. Besides, a theoretical framework is proposed by [53] for accurate comparison of minimum energy coding in coded division multiple access (CDMA) wireless sensor networks (WSNs).

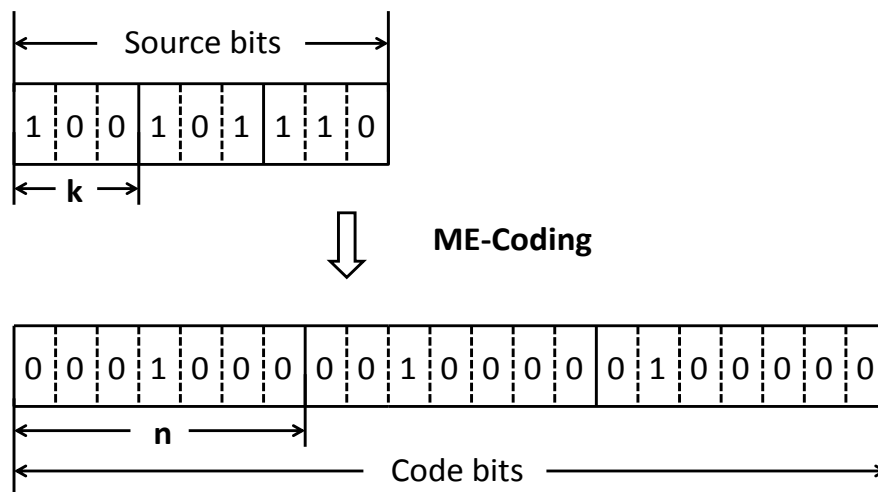


Figure 2.7: Block Diagram of ME Mapping Scheme.

The basic transmitter-side block diagram is shown in Figure 2.7. Information source produces information bits 1 and 0. The info-bits are fed to the source encoding block or the ME-Coding block. The ME encoder gives out a sequence of bits that has a reduced number of bit-1s in it. These source encoded bits are now OOK modulated in the modulator block and then transmitted by a RF transmitter bit-by-bit.

Consider k binary bits (1 and 0) from the source. ME-encoder groups these k bits together and maps it to a ME-Code word of length n , where $n > k$. Thus, there can

be a total of $M = 2^k$ possible incoming symbols mapped to M code-words that are predetermined. As already mentioned the duty cycle of the coded sequence is lower than the original sequence.

In our work, to avoid a confusion between information bits and coded bits we will call chips the bit after coding.

Our main idea is to apply the ME-coding to sources with unknown statistics (or a source with equiprobable symbols). We consider the extreme form of coding where we use a maximum of one high chip in the entire code-word sequence. The reason being, firstly, we satisfy the criterion of having less number of ones in the transmitted code-word bit sequence compared to source bit sequence. Secondly, this code-word can safely be assigned to any of the M source symbols occurring at any probability. Finally, this results in the maximum reduction of total number of ones in the transmitted code-word chip sequence. Table 2.1 [52] shows the source symbol and their corresponding code-words for $M = 4$ and 8.

Table 2.1: Minimum-Energy Code table for $k = 2$ and 3

Source bits	code-word	Source bits	code-word
00	000	000	0000000
01	001	001	0000001
10	010	010	0000010
11	100	011	0000100
		100	0001000
		101	0010000
		110	0100000
		111	1000000

For mapping $M = 2^k$ source symbols, we need a code-word of length $n = M - 1$. This is because the all-zero source symbol is mapped to an all-zero code-word sequence and the remaining $M - 1$ source symbols can be mapped to M length code-words containing only one high chip. In general, for grouping k bits we need a code length of $2^k - 1$. So, the code rate is defined by $r = k/n = k/(2^k - 1)$. We use the standard form of representation of the codes: $\text{ME}(n, k)$, where n represents the code-word length assigned to message symbol of k bits. The minimum Euclidean distance between any two code-words is $d_{min} = 1$. Strictly speaking, these codes have no capability of correction or detection of errors.

For example, if the all-zero code-word is transmitted, an error on one bit will result in a legal ME-coding code-word so that this error can not be detected.

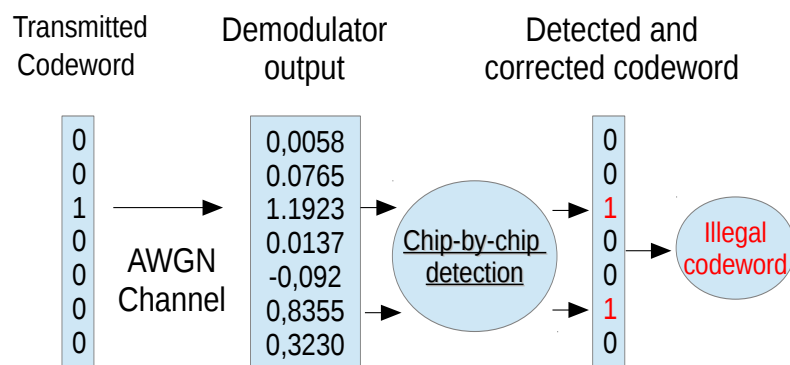


Figure 2.8: Flow of chip-by-chip detection process.

However, the basic characteristic of the code (maximum of one high chip in the code-word) makes it possible to detect errors when the receiving code-word has more than one high chip in it. i.e. if a chip-by-chip hard decision with 0.5 threshold is made on the demodulated signal, and if any code-word is detected with more than one high chip, then it can be considered as code in error and hence, all the final k message bits corresponding to that code-word at the receiver is considered to be in error. Fig. 2.8 shows an example of the process of error detection for a ME(7,3) code.

ME-coding decreases the spectrum efficiency by a factor

$$\frac{k}{n} = \frac{k}{2^k - 1} \quad (2.24)$$

So, for a given information rate the bandwidth must be largely increased. In a lot of practical cases, the bandwidth is constrained by the channel or the circuits. In that case, the information rate must be reduced when using ME coding with large n .

2.3.2 Modified minimum energy coding

In [54], the authors propose a Modified Minimum Energy Coding which can reduce the circuit energy. They use this method in CDMA and show that the multiple

access interference can be reduced because interference is only generated during the transmission of bits 1, resulting in better BER.

The principle of MME coding is depicted in Fig. 2.9. Unlike ME coding, a MME code-word is composed of several sub-frames of length $L_s + 1$. The first chip of each sub-frame indicates if there are one or more high chips in that sub-frame, i.e.

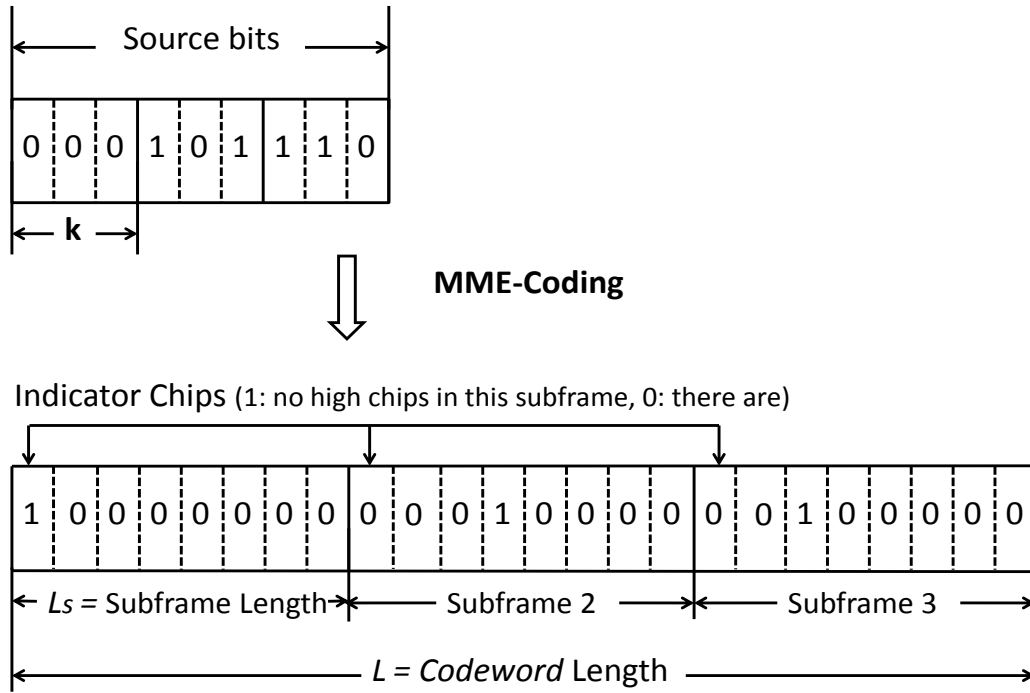


Figure 2.9: The principle of MME coding.

$$b_{ind}(l) = \begin{cases} 1, & \text{if there is no high chips in the subframe} \\ 0, & \text{if there is at least one high chip in the subframe} \end{cases} \quad (2.25)$$

where l is the subframe index (between 0 and $N_s - 1$ where $N_s = L/L_s$ is the number of subframes to transmit a codeword of L chips). The rest of the code-word is the same as the ME code-word.

The receiver first decodes the indicator bit. If it is not a '0', the receiver doesn't decode the remaining L_s chips in the subframe. In this case, the power required to decode a subframe is reduced.

To show this reduction we can calculate the mean value of the receiver on-time for

the transmission of the word :

$$T_{onRxMME} = N_s \times T_c \times [1 + P(b_{ind} = 0) \times (L_s)] \quad (2.26)$$

where $P(b_{ind} = 0)$ is the probability that $b_{ind} = 0$, and T_c is the chip duration.

If we assume, like the cited authors, that α is the probability that a chip 1 is transmitted and that these chips are independent, then

$$P(b_{ind} = 0) = 1 - P(c_1 = 0, \dots, c_{L_s} = 0) \quad (2.27)$$

where the c_k are the L_s chips of the subframe. So

$$P(b_{ind} = 0) = (1 - (1 - \alpha)^{L_s}) \quad (2.28)$$

and

$$T_{onRxMME} = N_s \times T_c \times [1 + (1 - (1 - \alpha)^{L_s}) \times (L_s)] \quad (2.29)$$

This expression is slightly different from the result given in [54], because we do not consider that the index chips $b_{ind}(k)$ are information bits.

For ME coding the receiver is on during the reception of the L chips. So the receiver on time is :

$$T_{onRxME} = L \times T_c = N_s \times L_s \times T_c \quad (2.30)$$

Assuming that the power consumption of the receiver is constant, we can define the receive energy gain of MME to ME by:

$$\rho = T_{onRxME}/T_{onRxMME} = \frac{L_s}{1 + (1 - (1 - \alpha)^{L_s}) \times L_s} \quad (2.31)$$

The energy gain is plotted in figure 2.10 as the function of the subframe length L_s and α , the probability of 1 in the code. It can be shown that there is an optimum value for L_s for a given α . When L_s increases the gain decreases because the $T_{onRxMME}$ becomes longer. So a small value of L_s is preferable. It must be also noticed that the MME is only interesting when α is sufficiently low (less than 0.3). In the other case MME can be less efficient than ME.

As shown further, in the chapter 4, it is also possible to reduce the activity of the receiver during the reception of Minimum Energy codes, providing a similar energy gain.

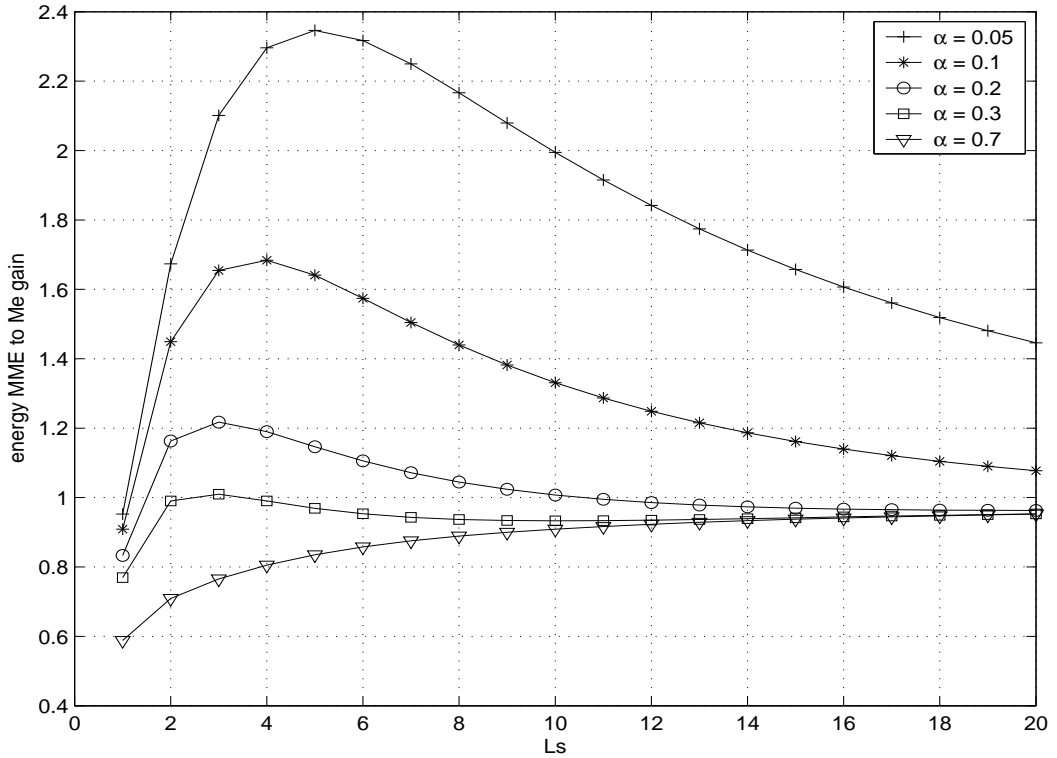


Figure 2.10: Receive MME to ME energy gain.

2.4 Error control scheme

2.4.1 Overview of error control

Error Correcting Code (ECC) [55] is the typical way used at the data link layer to perform error control for reliable wireless communication. Each kind of error control code introduces redundancy into an information message of length k by the addition of m extra bits, to form a code-word of length $n = m + k$ for the transmission. The redundancy bits allow the receiver to detect or/and correct the transmission errors. This ability to correct errors in the received message means that using an error control code over a noisy channel provides better bit error rate (BER) performance for the same signal to noise ratio (SNR) than uncoded systems. In other words, using error control coding can reduce the transmitted power for the same BER performance. However, this improvement has a cost in terms of bandwidth consumption and decoding complexity due to the redundant data added by the code. The code rate r_c defines the ratio of the number of bits before and after the coder:

$$r_c = \frac{k}{n} \quad (2.32)$$

Typically there is a trade-off between coding gain and decoder complexity. Complex codes may provide better coding gain but require more complex decoding algorithm, and need more power consumption. Therefore, when considering the error control codes used in the sensor networks, low complex codes would be advisable. In the next subsection we present the simple example of Hamming code and we show that ME-Coding can be seen as a limited error correction code.

2.4.2 Example of error-correction code: Hamming code

Hamming code is a linear binary error-correction code. For each integer $m > 1$, there is one type of code defined by:

$$(n, k) = (2^m - 1, 2^m - 1 - m) \quad (2.33)$$

Suppose the minimum distance of any error correction code is given by d_{min} , then it has the error detectability of $d_{min} - 1$ bits and error correctability of $\lfloor \frac{d_{min}-1}{2} \rfloor$ bits. The Hamming codes have a minimum distance $d_{min} = 3$, which means that they can detect 2 error bits and correct 1 error bit.

Generally, encoding and decoding of Hamming code can be expressed as matrix operation. Assuming that the code generator matrix is G , the parity-check matrix is H , the vector of k information bits is x , the vector of the encoded message bits is r and the syndrome vector is s .

To demonstrate how Hamming codes are calculated and used to detect errors, an example of Hamming (7, 4) codes is presented below. In this example, the information bits 1011 are encoded into the code-word 0110011 using the following matrix operation.

$$r = x \cdot G = \begin{bmatrix} 1 & 0 & 1 & 1 \end{bmatrix} \cdot \begin{bmatrix} 1 & 1 & 1 & 0 & 0 & 0 & 0 \\ 1 & 0 & 0 & 1 & 1 & 0 & 0 \\ 0 & 1 & 0 & 1 & 0 & 1 & 0 \\ 1 & 1 & 0 & 1 & 0 & 0 & 1 \end{bmatrix} = \begin{bmatrix} 0 & 1 & 1 & 0 & 0 & 1 & 1 \end{bmatrix} \quad (2.34)$$

Lets assume that the third bit of the code-word is corrupted. Hence, the received sequence is $r = 0100011$.

Then at the decoder side:

$$s = r \cdot H^t = \begin{bmatrix} 0 & 1 & 0 & 0 & 0 & 1 & 1 \end{bmatrix} \cdot \begin{bmatrix} 0 & 0 & 1 \\ 0 & 1 & 0 \\ 0 & 1 & 1 \\ 1 & 0 & 0 \\ 1 & 0 & 1 \\ 1 & 1 & 0 \\ 1 & 1 & 1 \end{bmatrix} = \begin{bmatrix} 0 & 1 & 1 \end{bmatrix} \quad (2.35)$$

where the binary syndrome s is equal to the decimal number 3 indicating that the third bit of the received sequence is incorrect.

Considering a code with code-word length N and error correcting capability of t bits, we can see that if the received code-word is incorrect and has distance of i , which is greater than t , to the transmitted code-word, the decoder will decode the code-word to an unexpected information bits which have a maximum difference of $i + t$ bits to the original information bits.

So, assuming a memory-less symmetric binary channel, with probability of error P_e , a bound of the bit error rate is [46]

$$P_{eb} \leq \frac{1}{N} \sum_{i=t+1}^N (i+t) C_N^i P_e^i (1-P_e)^{N-i} \quad (2.36)$$

We can get a more simpler approximation as:

$$P_{eb} \approx \frac{1}{N} (2t+1) C_N^{t+1} P_e^{t+1} \quad (2.37)$$

If the underlying channel is an additive white gaussian noise channel using BPSK modulation and a coherent detector, the probability of error of the binary channel must be taken as :

$$P_e = \frac{1}{2} \operatorname{erfc} \left(\sqrt{\frac{r_c E_b}{N_0}} \right) \quad (2.38)$$

Fig. 2.11 shows the BER performance of uncoded BPSK and Hamming coded BPSK. For sufficiently low BER, Hamming coded BPSK provides an improvement of

signal to noise ratio compared with uncoded BPSK.

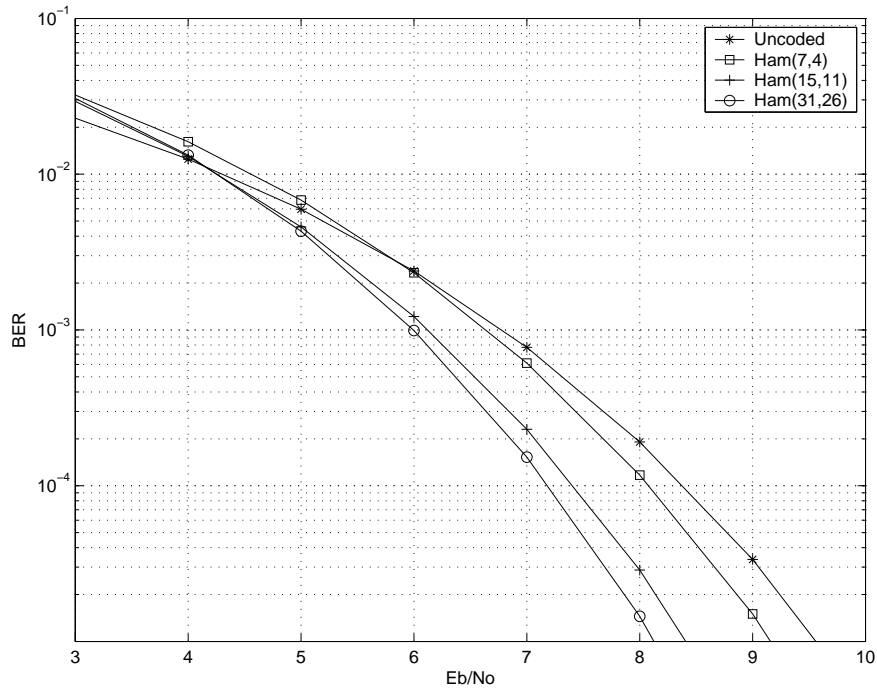


Figure 2.11: Bit error probability for Hamming code and BPSK modulation.

This improvement is obtained at the price of the reduction of the spectrum efficiency by a factor equal to the inverse of the code rate.

2.4.3 Error correction in ME-Coding

ME-Coding has been presented in the previous section with the possibility to reduce the power consumption by reducing the number of high chips. With the proposed scheme (a maximum of one high chip in each code-word), we have seen that the minimum distance between the code-words is only one. So there is no systematic capability of error detection or correction.

However we have seen that, considering a chip by chip detection, a limited error detection capability can be obtained. We show here that limited error correction can also be obtained by considering code by code detection.

The signal strengths of the demodulated chips vary due to the presence of noise in the channel, the bits may not be the same as it was sent from the transmitter. We consider Addition White Gaussian Noise (AWGN). After a chip-by-chip 0.5 threshold detection is made, a code-word bit sequence say 0010000 might be sent and may be detected as 0010010. As already discussed, the basic property of the code-word has

made it possible to detect an error in the code-word. Instead of declaring this code-word as one to be in error, [56] follow a different approach for code-word detection.

With code-by-code detection a scheme with error correction capability can be obtained. The receiver observes the energy levels of all the incoming n chips of the code-word. Then the chip with highest strength is considered as a high chip and the rest as low chip. If the chip with highest strength is lower than 0.5, it is detected as all zero code-word.

Fig. 2.12 shows the process of our code-by-code detection for a code-word. It shows a transmitted code-word 0010000. This is demodulated as 0.0058, 0.0765, 1.1923, 0.0137, -0.092 , 0.8355, 0.323. In the earlier approach of chip-by-chip detection with 0.5 threshold, it would have been detected as 0010010. Now, we look at the chip with highest strength in the entire code-word. The original high chip of energy 1.1923 is set as chip-1 and the rest is made as chip-0s. Thus, it is detected as 0100000. Since the noise is AWGN, the probability of energy of genuine chip-1 being greater than the energy of the error chip-1 is more ie. If energy of genuine chip-1 is e_i and that of the error chip-1 is e_j , then, $P(e_i > e_j)$ is more than $P(e_j > e_i)$. This fact is clear from a Gaussian distribution curve.

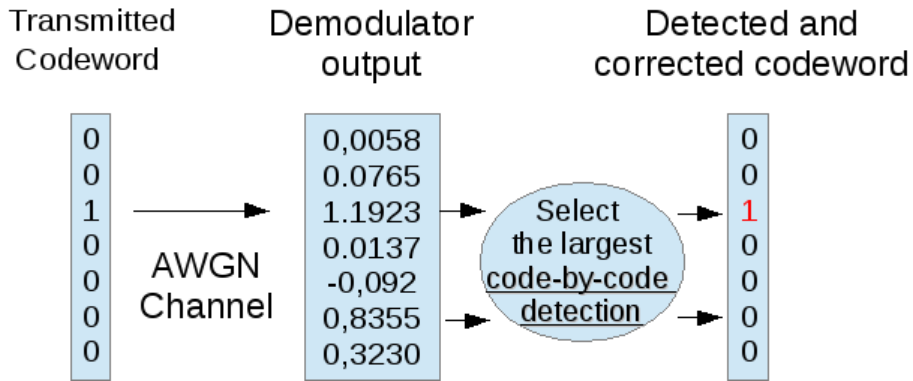


Figure 2.12: Error Correction with Code-by-Code Detection.

By code-by-code detection process we accomplish two things. Firstly, we eliminate the occurrence of an invalid code-word at the receiver and improve the error performance of ME-Coding. Secondly, this method performs exactly like an optimal detector.

In an optimal decoding scheme, the demodulator output produces the receiver code-word of length n as $r = [r_1, r_2, \dots, r_n]$. An optimal detector maximizes the prob-

ability of detecting a correct code-word $C_m = [C_{1m}, C_{2m}, \dots, C_{nm}]$ from the codeset C , given, received code r . ie.

$$\operatorname{argmax}_{m=1,2,\dots,n} Pr(C_m/r) \quad (2.39)$$

It maximizes the correlation metrics $C(r, C_m)$, which can be written

$$C(r, C_m)_{m=1,2,3,\dots,n} = r \cdot C_m^t = (r_1 C_{1m} + r_2 C_{2m} + r_3 C_{3m} \dots + r_n C_{nm}) \quad (2.40)$$

Since our code-word has only one high chip in it, $MAX[C(r, C_m)_{m=1,2,3,\dots,n}]$ is nothing but considering the highest energy chip. This method of code-by-code detection proves to be simpler than the standard optimum detection.

ME-coding has very limited detection and correction capabilities. So it can be interesting to consider additional error correction schemes. These possibilities must be considered with practical aspects. The sensor applications have transceiver with limited computing capabilities, memory resources and reduced processor speed. Another important factor to be considered is the delay in the receiver processor. There are many efficient codes with higher code gains like turbo codes to achieve energy efficiency at a system level [57]. It is complicated to generate and detect these codes. Complex algorithms take up more power in computing. Computation time also increases with complexity. Moreover, our sole idea of having less number of chip-1 in the transmitted code chip sequence must be maintained. The main objective here is to bring about a considerable conservation in the energy at a system level with algorithms of least complexities, demanding less resources and consuming lower power in the circuit level implementation.

2.4.4 Error correction codes combined with ME-Coding

Error correction schemes like Convolution codes and Block codes can be adopted to have an improvement in the error performance of the ME-coding scheme. Convolution codes are tough to be combined with ME-codes as they are generated in a finite-state machine and they do not allow a direct concatenation with ME-codes [3].

Block codes like Hamming code are used for error performance improvement in ME-coding [3]. For example, systematic binary Hamming block code scheme, say a standard (7,4) Hamming code can be combined with the ME-codes using the parity check equation $C_m H^t = 0$ (C_m is the code-word and H^t is the transpose of parity

check matrix). This effort of improving the error performance of ME-code by combining it with Hamming Code proves unsuccessful as the basic approach of ME-coding to have a reduced number of ones in the transmitted code-word chip sequence is lost. The coding gain provided by Hamming codes for smaller values of n is small and a higher circuit complexity for syndrome detection at the receiver is required [46]. It also increases the length of the ME code-word.

In Chapter 5, Automatic Repeat reQuest (ARQ) will be considered for error control scheme with the advantage that the minimum energy coding properties will be maintained.

2.5 ME-coding on different communication channels

The communication channel provides the connection between the transmitter and the receiver. The physical channel may be a pair of wires that carries the electrical signal, or an optical fiber that carries the information on a modulated light beam or an underwater ocean channel in which the information is transmitted acoustically or free space over which the information-bearing signal is radiated by use of antennas. Other media that can be characterized as communication channels are data storage media, such as magnetic tape, magnetic disks, and optical disks.

One common problem in signal transmission through any channel is additive noise. In general, additive noise is generated internally by components such as resistors and solid-state devices used to implement the communication system. This is sometimes called thermal noise. Other sources of noise and interference may arise externally to the system, such as interference from other users of the channel. When such noise and interference occupy the same frequency band as the desired signal, its effect can be minimized by proper design of the transmitted signal and its demodulator at the receiver. Other types of signal degradations that may be encountered in transmission over the channel are signal attenuation, amplitude and phase distortion, multipath distortion.

2.5.1 AWGN channel and Rayleigh fading channel

Additive White Gaussain Noise channel

The simplest mathematical model for a communication channel is the additive white gaussain noise channel, illustrated in figure 2.13. In this model, the transmit-

ted signal $s(t)$ is corrupted by an additive random noise process $n(t)$. Physically, the additive noise process may arise from electronic components and amplifiers at the receiver of the communication system, or from interference encountered in transmission.

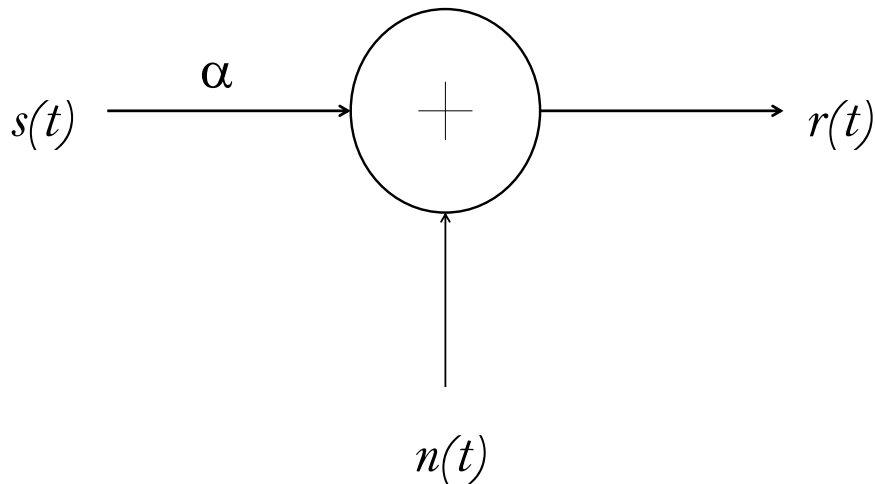


Figure 2.13: AWGN Channel

Thermal noise, introduced primarily by passive components and amplifiers at the receiver, is characterized statically as a white Gaussian noise process. Hence, the resulting mathematical model for the channel is usually called the AWGN channel. Other types of noise present in radio communication systems, like interferences etc. can also be approximately modeled by a Gaussian noise. Because this channel model applies to a broad class of physical communication channels and because of its mathematical tractability, this is the predominant channel model used in our communication system analysis and design.

Considering channel attenuation, the received signal is [46]:

$$r(t) = \alpha s(t) + n(t) \quad (2.41)$$

where α is the attenuation factor.

Zero-mean White Gaussian Noise (WGN) has the same power spectral density for all frequencies. The auto correlation function of WGN is given by the inverse Fourier transform of the noise power spectral density: the autocorrelation function is zero for all time but 0. This means that any two different samples of WGN, no matter how

close together in time they are taken, are uncorrelated. The noise signal WGN is totally decorrelated from its time shifted version.

The noises decrease the Signal to Noise Ratio (SNR) and, as shown by Shannon, limit the spectral efficiency of the system. Noise is the main detrimental effect in most radio communication systems.

Rayleigh Fading Channel

In a wireless communication channel, the transmitted signal travels from transmitter to receiver over multiple paths. This multipath propagation is the source of amplitude fluctuations, delay, phase fluctuations due to the environment evolution. For example, the transmitted signal from a BTS (Base Transceiver Station) may suffer multiple reflections from the buildings nearby, before reaching the mobile station.

The delays and other parameters associated with different signal paths change in an unpredictable manner and can only be characterized statistically. When a large number of paths is present, the central limit theorem can be applied to model the time-variant impulse response of the channel as a complex-valued Gaussian random process.

When the delay spread of the channel impulse response is much smaller than the transmitted symbol duration, the channel is described as a flat fading channel. In that case the channel model can be written [46]:

$$r(t) = \alpha(t)s(t) + n(t) \quad (2.42)$$

with the same notations that in the previous subsection but $\alpha(t)$ is a complex random variable.

So, in this model, the different paths are combined in an equivalent single path. If the random variable $\alpha(t)$ is a complex zero mean gaussian variable the channel is called a Rayleigh fading channel, because the amplitude of $\alpha(t)$ exhibits a Rayleigh distribution.

This type of channel is obtained when the different paths have about the same power, for example when there is no line of sight transmission.

2.5.2 Error probability in AWGN channel and Rayleigh fading channel

In this subsection we will recall the bit error probability of BPSK and OOK modulations for the AWGN channel and the Rayleigh fading channel. Then we will de-

termine the Bit Error Rate (BER) of ME-Coding for the same channels. Analytical expressions will be compared with simulation results.

Error probability in AWGN channel

The error probabilities of BPSK and OOK modulations in an AWGN channel were already given with the definition of these modulations in section 2.2.1 and 2.2.2. It is recalled that switching from BPSK to OOK provides a degradation of 3 dB.

Error probability in Rayleigh fading channel

We now consider the Rayleigh fading channel. We assume that the long-term variations in the channel are absorbed into ε_m , which represents the average received symbol energy (for symbol m) over the time frame for which the multipath power may be assumed to be constant. According to 2.42, the received signal is given by:

$$y(t) = \alpha(t)s(t) + n(t) \quad (2.43)$$

For slow fading, $\alpha(t)$ may be assumed to be constant over each symbol period. Thus, for memoryless modulation and symbol-by-symbol demodulation, $y(t)$ for demodulation over symbol period $[0, T_s]$ may be written as

$$y(t) = \alpha s(t) + n(t) \quad (2.44)$$

The error probability is a function of the received signal-to-noise ratio (SNR), i.e., the received symbol energy divided by the noise power spectral density. We denote the symbol SNR by γ_s , and the corresponding bit SNR by γ_b , where $\gamma_b = \gamma_s/k$, $k = \log_2 M$, and M is the number of symbols (equals to 2 for the considered modulations).

For slow, flat fading, the received SNR is

$$\gamma_s = \frac{|\alpha|^2 \varepsilon_s}{N_0} \quad (2.45)$$

The average SNR (averaging over α^2) is given by

$$\overline{\gamma_s} = E[|\alpha|^2] \frac{\varepsilon_s}{N_0} \quad (2.46)$$

We can assume, without loss of generality, that $E[|\alpha|^2] = 1$. So $\overline{\gamma_s}$ reduces to

$$\overline{\gamma_s} = \frac{\varepsilon_s}{N_0} \quad (2.47)$$

In our case, $k = 1$. Hence, the corresponding bit SNR are given by

$$\bar{\gamma}_b = \frac{\varepsilon_s}{N_0 k} = \frac{\varepsilon_b}{N_0} \quad (2.48)$$

Suppose the symbol error probability with SNR γ_s is denoted by $P_e(\gamma_s)$. Then the average error probability (averaged over the fading) is

$$\bar{P}_e = \int_0^\infty P_e(x) p_{\bar{\gamma}_s}(x) dx \quad (2.49)$$

where $p_{\bar{\gamma}_s}$ is the pdf of γ_s .

For Rayleigh fading, γ_s has a chi-square distribution with mean $\bar{\gamma}_s$, i.e.,

$$p_{\bar{\gamma}_s}(x) = \frac{1}{\bar{\gamma}_s} \exp\left[-\frac{x}{\bar{\gamma}_s}\right] \quad x \geq 0 \quad (2.50)$$

The probability of error for BPSK modulation is:

$$\bar{P}_e = \int_0^\infty \frac{1}{2} \operatorname{erfc}(\sqrt{x}) \frac{e^{-x/\bar{\gamma}_s}}{\bar{\gamma}_s} dx \quad (2.51)$$

After some calculations [46], we get

$$\bar{P}_e = \frac{1}{2} \left[1 - \sqrt{\frac{\bar{\gamma}_b}{1 + \bar{\gamma}_b}} \right] \approx \frac{1}{4\bar{\gamma}_b} \quad (\text{for large } \gamma_b) \quad (2.52)$$

For OOK modulation

$$P_b(\gamma_b) = \frac{1}{2} \operatorname{erfc}\left(\sqrt{\frac{\gamma_b}{2}}\right) \quad (2.53)$$

Here \bar{P}_e is the same as that for BPSK with $\bar{\gamma}_b$ replaced by $\bar{\gamma}_b/2$, i.e.,

$$\bar{P}_e = \frac{1}{2} \left[1 - \sqrt{\frac{\bar{\gamma}_b}{2 + \bar{\gamma}_b}} \right] \approx \frac{1}{2\bar{\gamma}_b} \quad (\text{for large } \gamma_b). \quad (2.54)$$

Error probability of ME-Coding in AWGN channel

The error probability of ME-coding has been expressed in [58]. The calculation is recalled here due to its importance for our work. On the other hand this calculation will be modified in the next section for the Rayleigh channel.

Denote P_{eS} and P_{eM} as the error probability of a high chip being received as a low chip and a low chip being received as a high chip, respectively, then for a coherent receiver and an AWGN channel, we have

$$P_{eS} = P_{eM} = \frac{1}{2} \operatorname{erfc} \left(\sqrt{\frac{E_c}{2N_0}} \right) \quad (2.55)$$

where E_c/N_0 is the average signal to noise ratio per chip.

These probabilities can also be expressed in terms of the bit energy E_b .

Assume that the duration and amplitude of the chip 1 are respectively T_c and A .

The average chip energy is:

$$E_c = \frac{A^2 \times T_c}{2} \quad (2.56)$$

The average symbol energy (n symbols with one chip and one all-zero symbol) is :

$$E_s = \frac{A^2 \times T_c \times n}{n + 1} \quad (2.57)$$

The average bit energy is

$$E_b = \frac{A^2 \times n \times T_c}{k(n + 1)} \quad (2.58)$$

Using (2.56), we can obtain the relation between E_b and E_c

$$E_c = \frac{k(n + 1)E_b}{2n} \quad (2.59)$$

So the two probabilities can be expressed in term of E_b

$$P_{eS} = P_{eM} = \frac{1}{2} \operatorname{erfc} \left(\sqrt{\frac{k(n + 1)E_b}{4nN_0}} \right) \quad (2.60)$$

Hard-decision decoding

Assuming that the source symbol S_i is transmitted using the code-word M_i , the receiver take a hard decision on each chip. The result can be (see figure 2.14):

- no error, the code word M_i is received decoded to the good source symbol S_i
- the wrong code word M_j is received resulting in the source symbol S_j . The number of bit errors is the Hamming distance d_{ij} between S_i and S_j .
- an illegal code word is received (two high chips for example), so a source symbol is taken randomly. In that case the bit error probability is

$$P_{mbe} = \frac{1}{n + 1} \sum_{j=0}^n \frac{d_{ij}}{k} = \frac{1}{2} \quad (2.61)$$

Now we have to distinguish the case where the original symbol S_i is all zero or not.

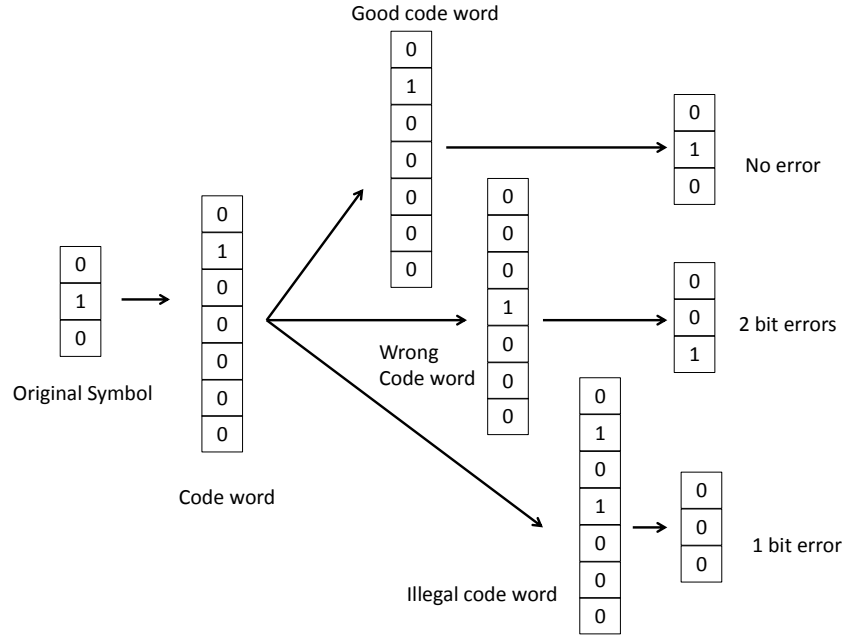


Figure 2.14: Example of hard decision process for ME-Coding

– S_i is the all-zero symbol.

The probability to get the good symbol S_i is

$$P_{m0} = (1 - P_{eS})^n \quad (2.62)$$

The probability to get another symbol S_j is

$$P_{0j} = P_{eS}(1 - P_{eS})^{n-1} \quad (2.63)$$

In that case, the bit error rate is $\frac{d_{0j}}{k}$.

The probability to get an illegal word is:

$$P_{mb} = 1 - P_{m0} - \sum_{j \neq 0} P_{0j} = 1 - (1 - P_{eS})^n - n \times P_{eS}(1 - P_{eS})^{n-1} \quad (2.64)$$

As written before the bit error rate is $1/2$.

Then the average bit error rate when the all-zero symbol is transmitted is :

$$P_{e/S_0} = P_{eS}(1 - P_{eS})^{n-1} \sum_{j=1}^n \frac{d_{0j}}{k} + \frac{1 - (1 - P_{eS})^n - n \times P_{eS}(1 - P_{eS})^{n-1}}{2} \quad (2.65)$$

- S_i is not the all-zero symbol.

The probability to get the good symbol S_i is

$$P_{mc} = (1 - P_{eM})(1 - P_{eS})^{n-1} \quad (2.66)$$

The probability to get another symbol S_j which is not the all-zero symbol is

$$P_{ij} = P_{eM}P_{eS}(1 - P_{eS})^{n-2} \quad (2.67)$$

In that case, the bit error rate is $\frac{d_{ij}}{k}$.

The probability to get the all-zero symbol S_0

$$P_{m0} = P_{eM}(1 - P_{eS})^{n-1} \quad (2.68)$$

In that case, the bit error rate is $\frac{d_{i0}}{k}$.

The probability to get an illegal word is :

$$P_{mb} = 1 - P_{m0} - P_{mc} - \sum_{j \neq 0, i} P_{ij} \quad (2.69)$$

and the bit error rate is $1/2$.

Then the average bit error rate when the all-zero symbol is transmitted is :

$$P_{e/S_i} = P_{m0} \frac{d_{i0}}{k} + \sum_{j \neq i} P_{ij} \frac{d_{ij}}{k} + \frac{P_{mb}}{2} \quad (2.70)$$

Finally, assuming a uniform distribution of source symbols, the total probability of error can be expressed as:

$$\begin{aligned} P_e &= \frac{1}{n+1} \left[\sum_{i=1}^n P_{e/S_i} + P_{e/S_0} \right] \\ &= \frac{1}{n+1} \left[\frac{n+1}{2} P_{eM} + \frac{n+3}{2} P_{eS} - P_{eM} P_{eS} \right. \\ &\quad \left. - P_{eS}^2 - \frac{1}{2} (n+1) \right] (1 - P_{eS})^{n-2} + \frac{1}{2} \end{aligned} \quad (2.71)$$

Soft-decision decoding

Since ME-coding with hard-decision decoding does not have any error recovery capability, the conception of soft decision decoding (code-by-code detection) is to improve the performance of ME-coding. Instead of chip by chip decision, the signal

amplitudes of all the n chips of the same code-word are compared with each other; the chip with the highest strength, if larger than a threshold s , is decoded as a "one" and the rest are decoded as "zero". If the largest chip is less than the threshold then the all-zero symbol is chosen. In this way we can form a legal code-word and decode it, eliminating the occurrence of an invalid code-word at the receiver.

We have also to distinguish the cases where the original symbol is or is not the all-zero symbol.

- When the original symbol is not all-zero.

P_{m0} is the probability that code-word M_i is received as M_0 ,

$$P_{m0} = P_{eM}(1 - P_{eS})^{n-1} \quad (2.72)$$

P_{ij} is the probability that code-word M_i is received as M_j .

We denote $c_k, 1 \leq k \leq n$ the n chips of the code word.

As we consider an AWGN channel, the probability density function of a chip is

$$p_1(x) = \frac{1}{\sqrt{2\pi\sigma^2}} e^{-\frac{(x-A)^2}{2\sigma^2}} \quad (2.73)$$

if 1 is transmitted with A the amplitude of the chip and σ^2 the noise variance

$$p_0(x) = \frac{1}{\sqrt{2\pi\sigma^2}} e^{-\frac{x^2}{2\sigma^2}} \quad (2.74)$$

if 0 is transmitted.

If x is the amplitude of the chip c_j , then the symbol S_j is chosen if:

- $c_k < x$ for all $k \neq i, j$. This is obtained with probability

$$\left[\int_{-\infty}^x p_0(r) dr \right]^{n-2} \quad (2.75)$$

- $c_i < x$ which is obtained with the probability

$$\int_x^{\infty} p_1(r) dr \quad (2.76)$$

- $c_j > s$

This last condition must be true for all the values of x , giving the following expression of P_{ij}

$$P_{ij} = \int_s^\infty p_0(x) \left[\int_{-\infty}^x p_0(r) dr \right]^{n-2} \int_x^\infty p_1(r) dr dx \quad (2.77)$$

Replacing the expression of the probabilities $p_0(x)$ and $p_1(x)$, we get:

$$P_{ij} = \int_s^\infty \frac{1}{\sigma\sqrt{2\pi}} \exp\left[-\frac{x^2}{2\sigma^2}\right] \left[\int_{-\infty}^x \frac{1}{\sigma\sqrt{2\pi}} \exp\left(-\frac{r^2}{2\sigma^2}\right) dr \right]^{n-2} \left[\int_{-\infty}^x \frac{1}{\sigma\sqrt{2\pi}} \exp\left[-(r-A)^2/2\sigma^2\right] dr \right] dx \quad (2.78)$$

The average bit error rate when transmitting S_i is :

$$P_{e,S_i} = P_{m0} \frac{d_{i0}}{k} + \sum_{j \neq i, j \neq 0} P_{ij} \frac{d_{ij}}{k} \quad (2.79)$$

– When the original source symbol is composed of only zeros.

The symbol S_j , $j \neq 0$ is obtained when the j^{th} chip which was transmitted as a 0 becomes larger than the threshold and is received as a 1. This is obtained with the probability :

$$P_{0j} = \int_s^\infty \left[\int_{-\infty}^y \frac{1}{\sigma\sqrt{2\pi}} \exp\left[-\frac{r^2}{2\sigma^2}\right] dr \right]^{n-1} \frac{1}{\sigma\sqrt{2\pi}} \exp\left[-y^2/2\sigma^2\right] dy \quad (2.80)$$

The average bit error rate when transmitting S_0 is :

$$P_{e,S_0} = \sum_{j=1} P_{0j} \frac{d_{0j}}{k} \quad (2.81)$$

Finally by averaging on all the transmitted symbols we get the average bit error probability:

$$P_e = \frac{1}{n+1} \left[\sum_{i=1}^n P_{e/S_i} + P_{e/S_0} \right] = \frac{1}{2} P_{m,0} + \frac{n}{2} P_{ij} + \frac{1}{2} P_{0,j} \quad (2.82)$$

$P_{m,0}$ is given by a close-form expression, but P_{ij} and $P_{0,j}$ must be numerically calculated to obtain the values of the bit error rate. This will be done further and the results will be compared to Monte-Carlo simulation but firstly we extend the calculation to the Rayleigh channel.

Error probability of ME-Coding OOK in Rayleigh channel

On the Rayleigh channel, for an ideal coherent receiver, denote respectively P_{eS} and P_{eM} the error probability of a high chip being received as a low chip and a low chip being received as a high chip. As seen in section 2.5.2, these probabilities can be written

$$P_{eS} = P_{eM} = \frac{1}{2} \left(1 - \sqrt{\gamma_c / (\gamma_c + 2)} \right) \quad (2.83)$$

where γ_c is the average signal to noise ratio per chip. To work with the bit energy we can use the same relation that in the previous section.

We propose to determine the performance of ME-coding in the Rayleigh channel for hard- decoding and soft decision decoding.

Hard-decision decoding

We can directly use the equation (2.71) and replace the probabilities P_{eS} and P_{eM} by the expression (2.83).

$$\begin{aligned} P_e &= \frac{1}{n+1} \left[\sum_{i=1}^n P_e \{S_i\} + P_e \{S_0\} \right] \\ &= \frac{1}{n+1} \left[\frac{n+1}{2} P_{eM} + \frac{n+3}{2} P_{eS} - P_{eM} P_{eS} \right. \\ &\quad \left. - P_{eS}^2 - \frac{1}{2} (n+1) \right] (1 - P_{eS})^{n-2} + \frac{1}{2} \end{aligned} \quad (2.84)$$

Soft-decision decoding

We can use the expression in equation (2.71), but we must reevaluate P_{m0} , P_{ij} and P_{m0} in the case of the Rayleigh channel.

The frequency-nonselective channel results in multiplicative distortion of the transmitted signal $s(t)$. Furthermore the condition that the channel fades slowly implies that the multiplicative process may be regarded as a constant during at least one signaling interval. Consequently, if the transmitted signal is $s(t)$, the received equivalent low-pass signal in one signaling interval is

$$y(t) = a e^{j\phi} s(t) + n(t) \quad (2.85)$$

where $n(t)$ represents the complex valued white Gaussian noise process corrupting the signal. Since a is Rayleigh distributed,

$$p(a) = \frac{a}{\sigma^2} e^{-a^2/(2\sigma^2)} \quad (2.86)$$

When the original symbol S_i is not all-zero P_{m0} is the probability that code-word M_i is received as M_0 ,

$$P_{m0} = P_{eM}(1 - P_{eS})^{n-1} \quad (2.87)$$

The probability P_{ij} that the symbol S_j is received, is given by

$$P_{ij} = \int_s^\infty \frac{1}{\sigma\sqrt{2\pi}} \exp\left[-\frac{x^2}{2\sigma^2}\right] \left[\int_{-\infty}^x \frac{1}{\sigma\sqrt{2\pi}} \exp\left(-\frac{r^2}{2\sigma^2}\right) dr \right]^{n-2} \left[\int_{-\infty}^x \frac{r}{\sigma^2} \exp[-r^2/2\sigma^2] dr \right] dx \quad (2.88)$$

When the original source symbol is composed of only zeros, the probability P_{m0} which is the probability that code-word M_0 is received as M_0 , can be written

$$P_{m0} = (1 - P_{eS})^n \quad (2.89)$$

The probability P_{0j} that S_j is received is given by

$$P_{0j} = \int_s^\infty \left[\int_{-\infty}^y \frac{1}{\sigma\sqrt{2\pi}} \exp[-r^2/2\sigma^2] dr \right]^{n-1} \frac{1}{\sigma\sqrt{2\pi}} \exp[-y^2/2\sigma^2] dy \quad (2.90)$$

As previously said, we can now get the total bit error rate for soft-decision decoding using the equation:

$$\begin{aligned} P_e &= \frac{1}{n+1} \left[\sum_{i=1}^n P_e \{S_i\} + P_e \{S_0\} \right] \\ &= \frac{1}{2} (P_{m0} + n P_{ij} + P_{0j}) \end{aligned} \quad (2.91)$$

The different probabilities can be evaluated by numerical calculations. It is also interesting to make a comparison with a Monte-Carlo simulation. This is the objective of the next section.

2.5.3 Simulation results versus theoretic results

The figures 2.15 provides the results obtained by the previous formulas (in solid lines) and Monte-Carlo simulation (different types of dots) for the AWGN channel. Results are given for BPSK, OOK, ME(7,3) and ME(63,6) with hard and soft decoding. From this curves, we can make the following comments:

- Firstly, we can notice a good concordance between the formulas and Monte-Carlo simulations which validates the proposed analysis.
- If we compare now the transmission methods, we can see the expected 3dB loss between BPSK and OOK.
- Minimum energy coding provides better results than OOK and the performance are better when the coding size is larger.
- The benefit of soft decision is important. For a BER equal to 10^{-3} , a power gain of 1 dB is obtained for ME(7,3) and 2 dB for ME(63,6).

From these results, we can conclude that for the AWGN channel, ME coding can be interesting in terms of transmit energy. Large coding sizes must be used to obtain an interesting gain in energy and, as seen for other transmission methods, the price to pay is the bandwidth efficiency.

We can also hope that the obtained gain will be more important if we consider the circuit power consumption due to the simplicity of the OOK transmitters and receivers.

The Fig. 2.16 shows the results obtained for the Rayleigh channel. We can also notice the good concordance between the analysis and the simulation. In term of performance the results are a bit disappointing. The performance of ME coding is always worse than BPSK and even OOK. From these remarks we can conclude that ME coding is not a good choice in the case of Rayleigh channel.

2.6 Summary

This chapter focuses on energy efficient transmission techniques. In the first part, the fundamental Shannon trade-off between energy efficiency and bandwidth efficiency has been recalled. We have shown also, using a simplified circuit model, that the circuit energy can largely change this trade-off. Then we focus on the transmit energy and we introduce some modulation schemes. We present the minimum energy coding that will be considered in a large part of this study.

The characteristics of the channel has a large influence on the performance of a link. We recalled the definition of the Additive White Gaussian Noise Channel and

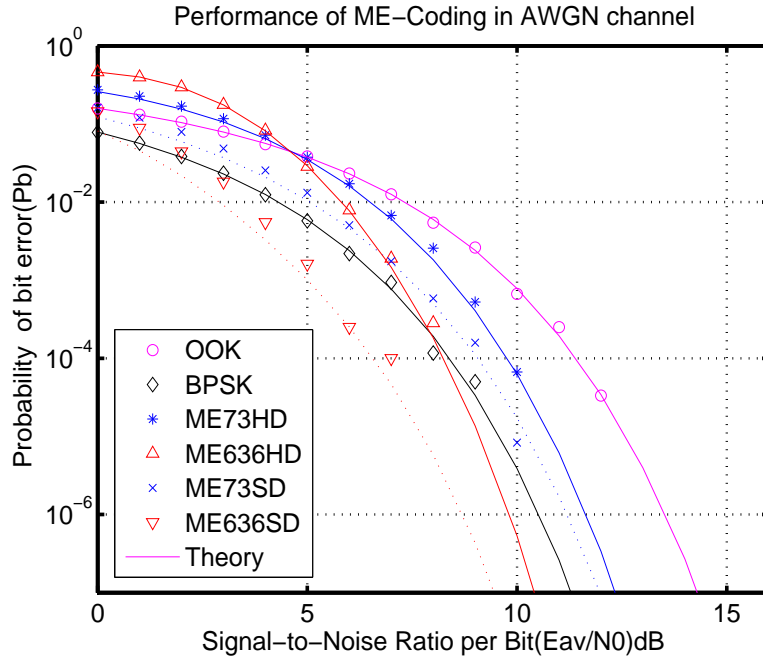


Figure 2.15: Performance of ME-coding in AWGN channel

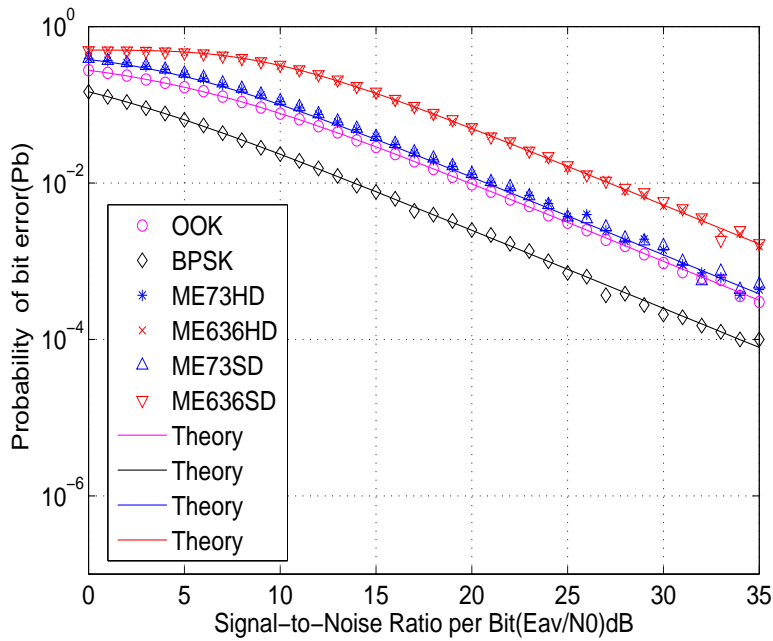


Figure 2.16: Performance of ME-coding in Rayleigh fading channel

Rayleigh fading channel. For these different channels, we gave the theoretical bit error probabilities of OOK, BPSK and ME-coding OOK. The theoretical results were compared to simulations. According to these results, we have shown that in AWGN, ME-coding based on OOK modulation can be interesting (better results than BPSK) in terms of bit energy for large coding rate, at the price of lower spectrum efficiency. However, this effect is not obtained for a Rayleigh fading channel.

These results are obtained considering only the transmit energy. As shown in the first part of this chapter, the circuit energy must also be considered to obtain realistic conclusions and perhaps better results. This aspect will be developed in the rest of this work. To begin this study, chapter 3 develops circuit energy models.

Energy consumption models

Previous studies consider only the transmit power (the transmit bit energy E_b/N_0) to analyze the transmission techniques. Taking into account the circuit energy can largely change the conclusions on the energy efficiency of a transmission scheme. So, it is necessary to use a circuit energy model.

Recent analyses of WSN energy efficiency have been widely based on a sensor node power consumption model [59, 60, 61]. For some models, the power consumption of the receiving circuitry is greater than the power consumption of the transmitting circuitry [60, 62, 63]. Similarly, the power consumption for baseband digital signal processing is comparable to the power consumption of the combined transmit and receive circuitry [63]. Furthermore, an accurate power consumption model should be able to accurately reflect the impact of recent advances in high efficiency power amplifiers for WSN applications [64, 65]. In this chapter, we try to develop a realistic power consumption model for WSN devices.

We will first focus on the architecture of a typical wireless sensor node to investigate the energy consumption of different components. Then, we present a general energy consumption model which is commonly admitted in studies of efficient transmission techniques between sensor nodes. However this commonly used model is not matched to OOK modulation. So we propose in the last part of the chapter new models matched to OOK modulation which will be used in our next studies.

3.1 The architecture of a typical wireless sensor node

This section presents the node-level architecture to compare the energy consumption of each part in the sensor node. Fig. 3.1 shows the architecture of a typical wireless sensor node, as usually assumed in the literature [66]. It consists of four main components: (i) a sensing subsystem including one or more sensors (with associated analog-to-digital converters) for data acquisition; (ii) a processing subsystem including a micro-controller and memory for local data processing; (iii) a power supply unit; and (iv) a radio subsystem for wireless data communication.

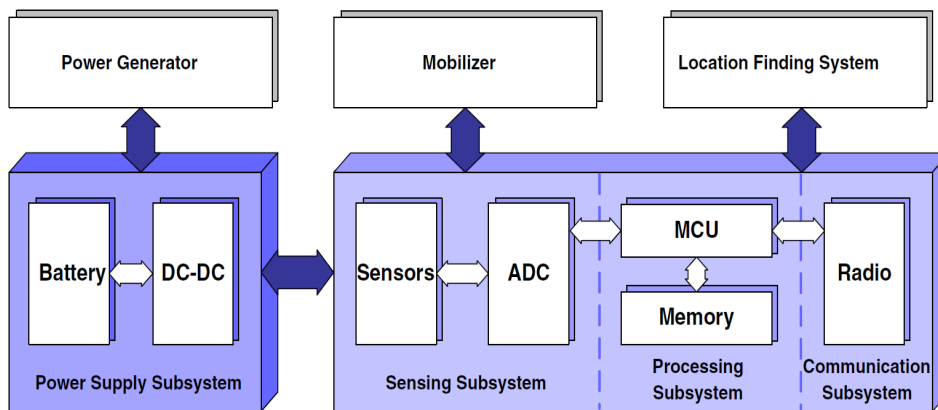


Figure 3.1: The architecture of a typical wireless sensor node.

In the sensing subsystem, sensors are literally used for sensing temperature, images, gas etc. The sensor unit is the medium to communicate between the physical world and the conceptual world of processing unit. It senses or detects the physical state and sends the data to processor. In reality a sensor acts as a transducer where energy is converted into analog signal or digital signal. Sensors can be distinguished based on what kind of energy they detect or transfer to the system.

Processing subsystem is a part of microcontroller unit which can read sensor data, perform some minimal computations and make a packet ready for transfer in the wireless communication channel. The local memory requirements will not be high and emphasis will be placed on the modes of operation to facilitate low-power operation. Basically the processor is built on the microcontroller which reads sensor data and makes the data ready for transfer.

In Power subsystem, base stations are more often connected to main power supply, whereas nodes in the network depend on batteries to supply power. Hence there is a

requirement to choose power efficient hardware and various efficient-operation modes to make the network more power efficient. Fig. 3.2 reflects power consumption of a typical wireless sensor node in various states [67].

The communication module/subsystem is typically an RF transceiver that should support the 802.15.4. This unit helps in collecting information and to exchange or control data acquisition. The maximum amount of energy is used in communication module when compared to the two other modules. Sharing information between sensor nodes will consume more amount of energy than implementing the calculation within individual node. The radio transmission and reception has proven to be the major energy consumer in the sensor network.

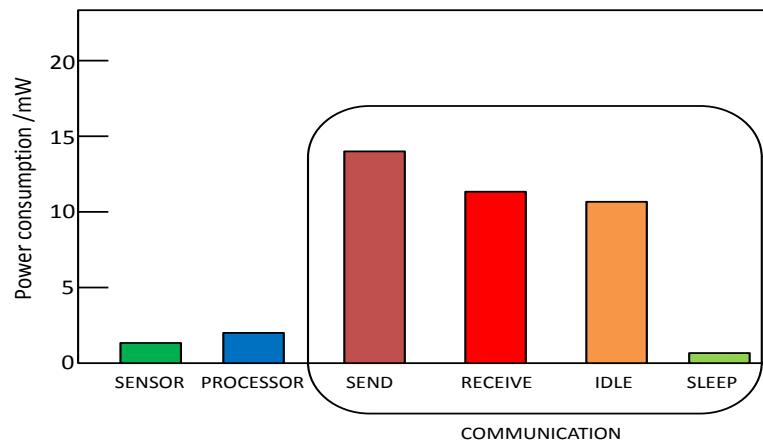


Figure 3.2: Power consumption of a typical wireless sensor node.

Obviously, the power breakdown heavily depends on the specific node. In [11] it is shown that the power characteristics of a Mote-class node are completely different from those of a Stargate node. However, the following remarks generally hold [11]. The communication subsystem has an energy consumption much higher than the computation subsystem. It has been shown that transmitting one bit may consume as much as executing a few thousands instructions [68]. Therefore, communication should be traded for computation. The radio energy consumption is of the same order of magnitude in the reception, transmission, and idle states, while the power consumption drops of at least one order of magnitude in the sleep state. Therefore, the radio should be put to sleep (or turned off) whenever possible.

Depending on the specific application, sensor nodes may also include additional components such as a location finding system to determine their position, a mobilizer to change their location or configuration, and so on. However, as the latter components are optional, and only occasionally used, we will not take them into account in the following discussion.

3.2 General energy consumption model

To facilitate subsequent analysis and comparisons, we introduce in this section two general system models for a single battery-driven node in transmit- or receive-mode and for the full function transceiver node. The diagram of a fully-functioning node [69] is shown in Fig. 3.3, which includes a transmitter, a receiver, a power supporting battery and a DC/DC converter to generate a desired and stable supply voltage for the transmitter or the receiver. The node works with half-duplex communication mode (alternately transmitting and receiving), which is commonly used in WSNs for power efficiency.

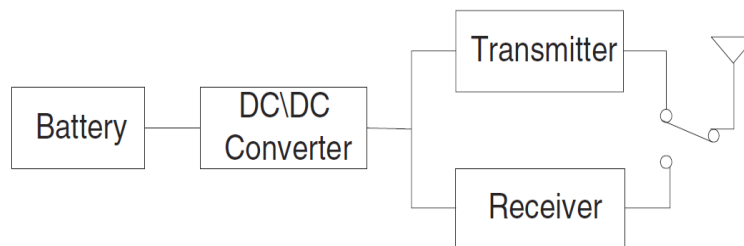


Figure 3.3: Block diagram of a fully-functioning node.

To explore the battery power consumption at the node, let us resort to a point-to-point link in the network. This link consists of a transmitting node and a receiving node [69], where only the transmitter in the former and the receiver in the later are switched on. Based on the link model shown in Fig. 3.4, it is possible to figure out the battery power consumptions in the transmitting node and receiving node respectively, then we can integrate them as the battery power consumption of the fully-functioning node.

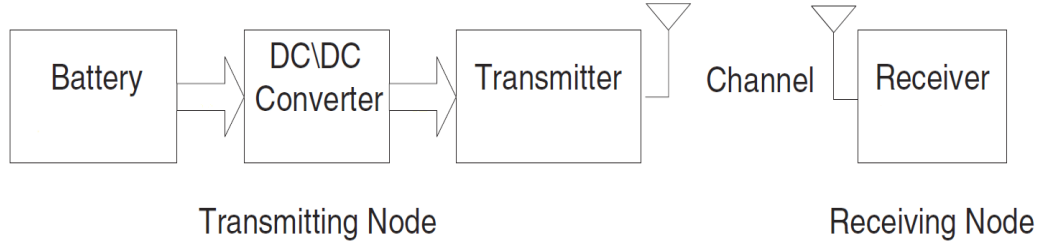


Figure 3.4: A link model.

3.2.1 General energy consumption model of fully-functioning node

For a wireless sensor fully-functioning node, the simple energy model for low power microsensors is shown in Fig. 3.5 [42]. It includes a sensor/DSP unit for data processing, D/A and A/D for digital-to-analog and analog-to-digital conversion, and a wireless transceiver for data communication. The sensor/DSP, D/A, and A/D operate at low frequency and consume less than $1mW$. This is over an order of magnitude less than the power consumption of the transceiver. Therefore, the energy model ignores the contributions from these components. The transceiver has three modes of operation: start-up, receive, and transmit. Each mode will be described and modeled.

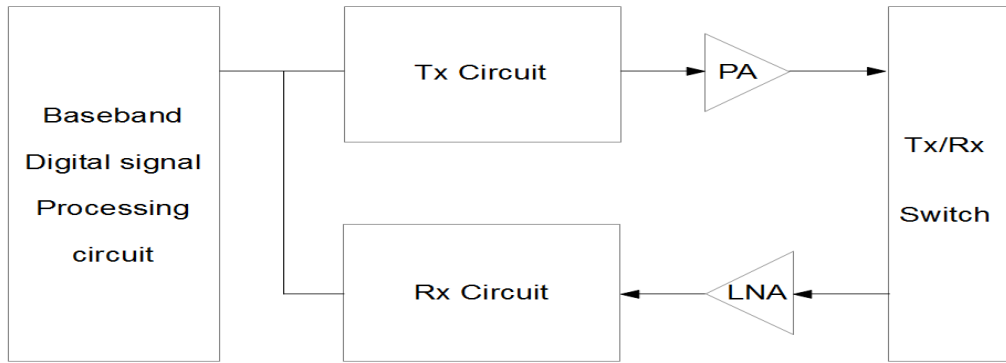


Figure 3.5: A model of the microsensor node.

According to the energy consumption model, the total energy consumption of the transceiver node is:

$$E_{total} = E_{start} + E_{rx} + E_{switch} + E_{tx} \quad (3.1)$$

where E_{start} is the start time for both the transmitter and receiver, E_{switch} is the switch energy consumption of the transceiver from the transmit state to the receive state, and

E_{rx} and E_{tx} represent respectively the energy consumption of the transmitter and the receiver.

A. Start-up Mode

When the transceiver is first turned on, it takes some time for the frequency synthesizer and the VCO to lock to the carrier frequency. The start-up energy can be modeled as follows:

$$E_{start} = P_{LO} \cdot t_{start} \quad (3.2)$$

where P_{LO} is the power consumption of the synthesizer and the VCO. The term t_{start} is the required settling time. RF building blocks including PA, LNA, and mixer have negligible start-up times and therefore can remain in the off-state during the start-up mode.

B. Receive Mode

The active components of the receiver include the low noise amplifier (LNA), mixer, frequency synthesizer, VCO, intermediate-frequency (IF) amplifier (amp), and demodulator (Demod). The receiver energy consumption can be modelled as follows:

$$E_{rx} = (P_{LO} + P_{RX}) \cdot t_{rx} \quad (3.3)$$

where P_{RX} includes the power consumption of the LNA, mixer, IF amplifier, and demodulator. The receiver power consumption is dictated by the carrier frequency and the noise and linearity requirements. The power consumption is dominated by the RF building blocks that operate at the carrier frequency. The IF demodulator power varies with data rate, but it can be made small by choosing a low IF.

C. Transmit Mode

The transmitter includes the modulator (Mod), frequency synthesizer and VCO (shared with the receiver), and power amplifier (PA). The data modulates the VCO and produces a radio frequency at the desired data rate and carrier frequency. A simple transmitter energy model is shown in Equation (3.4). The modulator consumes very little energy and therefore can be neglected.

$$E_{tx} = (P_{LO} + P_{PA}) \cdot t_{tx} \quad (3.4)$$

P_{LO} can be approximated as a constant. P_{PA} depends on the PA efficiency, the link-budget, and the sensitivity requirement.

In [42] the authors demonstrate how the above model can be used to estimate the battery life time of a Bluetooth transceiver. This is one of the lowest power 2.4GHz transceivers reported in literature. The following analysis focuses on the transmission of data in the physical layer and makes no assumptions about protocols used in the network layer and above. The energy consumption of the transceiver depends on how it operates. Assuming a 100-bit packet is received and a 100-bit packet is transmitted every 5ms, Fig. 3.6 shows a Bluetooth transceiver activity within one cycle of operation [42].

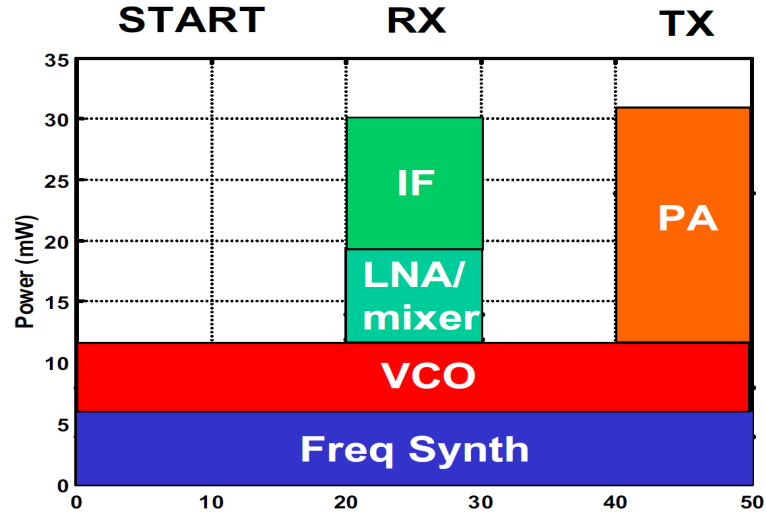


Figure 3.6: Burst receive/transmit cycle for Bluetooth Transceiver.

3.2.2 General power consumption model of communication link

We consider a general communication link connecting two wireless nodes, which can be MIMO, Multiple-Input Single-Output (MISO), Single-Input Multiple-Output (SIMO) or SISO. In order to consider the total energy consumption, all signal processing blocks at the transmitter and the receiver need to be included in the model. However, in order to keep the model from being over-complicated at this stage, baseband signal processing blocks (e.g., source coding, pulse-shaping, and digital modulation) are intentionally omitted. We also assume that the system is uncoded. Hence no Error Correction Code (ECC) blocks are included. The methodology used here can be ex-

tended to include those blocks in future research work. The resulting signal paths on the transmitter and receiver sides are shown in Fig. 3.7 and Fig. 3.8, respectively [70], where M_t and M_r are the numbers of transmitter and receiver antennas, respectively, and we assume that the frequency synthesizer (LO) is shared among all the antenna paths. For the SISO case, we have $M_t = M_r = 1$.

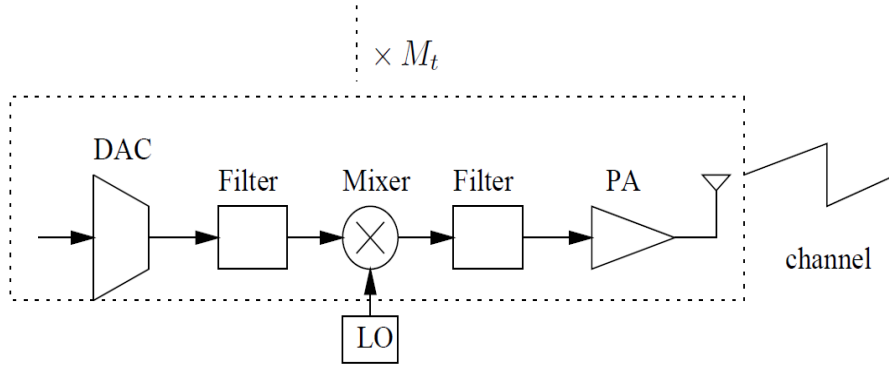


Figure 3.7: Transmitter Circuit Blocks (Analog).

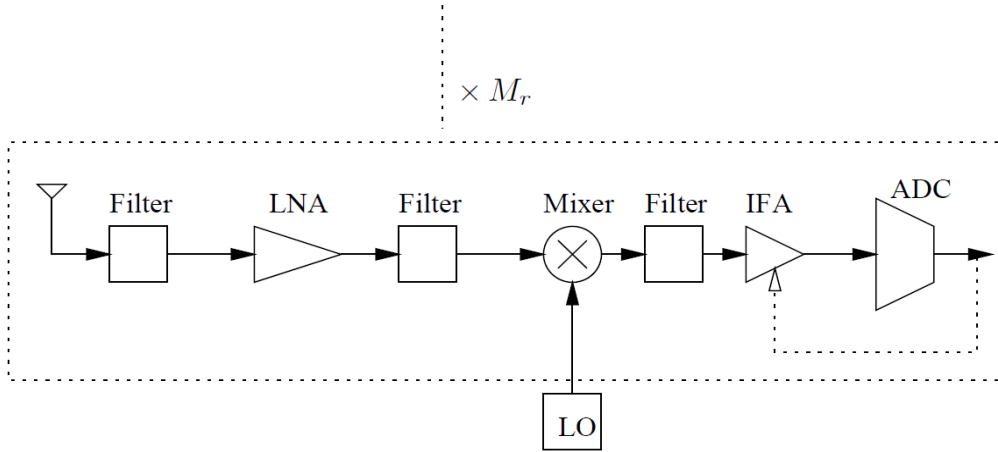


Figure 3.8: Receiver Circuit Blocks.

Similar to the SISO case discussed in [71, 67, 70], the total average power consumption along the signal path can be divided into two main components: the power consumption of all the power amplifiers P_{PA} and the power consumption of all other circuit blocks P_c . The first term P_{PA} is dependent on the transmit power P_{out} , which can be calculated according to the link budget relationship [46]. Specifically, when the channel only experiences a square-law path loss.

$$P_{out} = \bar{E}_b R_b \times \frac{(4\pi d)^2}{G_t G_r \lambda^2} M_l N_f \quad (3.5)$$

where \bar{E}_b is the required energy per bit at the receiver for a given BER requirement, R_b is the bit rate, d is the transmission distance, G_t is the transmitter antenna gain, G_r is the receiver antenna gain, λ is the carrier wavelength, M_l is the link margin compensating the hardware process variations and other additive background noise or interference and N_f is the receiver noise figure defined as $N_f = \frac{N_r}{N_0}$ with $N_0 = -171 \text{ dBm/Hz}$ the single-sided thermal noise Power Spectral Density (PSD) at room temperature and N_r is the PSD of the total effective noise at the receiver input.

The power consumption of the power amplifiers can be approximated as [70]

$$P_{PA} = (1 + \alpha) P_{out} \quad (3.6)$$

where $\alpha = \frac{\xi}{\eta} - 1$ with η the drain efficiency [46] of the RF power amplifier and ξ the Peak-to-Average Ratio (PAR) which is dependent on the modulation scheme and the associated constellation size [72]. The second term P_c in the total power consumption is given by

$$P_c \approx M_t (P_{DAC} + P_{mix} + P_{filt}) + 2P_{syn} + M_r (P_{LNA} + P_{mix} + P_{IFA} + P_{filr} + P_{ADC}) \quad (3.7)$$

where P_{DAC} , P_{mix} , P_{LNA} , P_{IFA} , P_{filt} , P_{filr} , P_{ADC} , and P_{syn} are the power consumption values for the DAC, the mixer, the Low Noise Amplifier (LNA), the Intermediate Frequency Amplifier (IFA), the active filters at the transmitter side, the active filters at the receiver side, the ADC, and the frequency synthesizer, respectively. To estimate the values of P_{DAC} , P_{ADC} and P_{IFA} , we use the model introduced in [72].

Finally, the total energy consumption per bit for a fixed-rate system can be obtained as

$$E_{bt} = (P_{PA} + P_c) / R_b \quad (3.8)$$

3.2.3 Application of the model to based OOK ME Coding

For the simulation, we assume a AWGN channel, i.e., the channel gain between each transmitter antenna and each receiver antenna is a scalar. In addition, the path loss is modeled as a power falloff proportional to the distance squared, as was shown in Equation (3.5). The related circuit and system parameters are defined in Table 3.1.

Table 3.1: System parameter

$f_c = 2.5GHz$	$\eta = 0.35$
$G_t G_r = 5dBi$	$\sigma^2 = \frac{N_0}{2} = -174dBm/Hz$
$B = 10KHz$	$\beta = 1$
$P_{mix} = 30.3mW$	$P_{syn} = 50.0mW$
$\bar{P}_b = 10^{-4}$	$T_s = \frac{1}{B}$
$P_{filt} = P_{filr} = 2.5mW$	$P_{LNA} = 20mW$
$N_f = 10dB$	$M_l = 40dB$

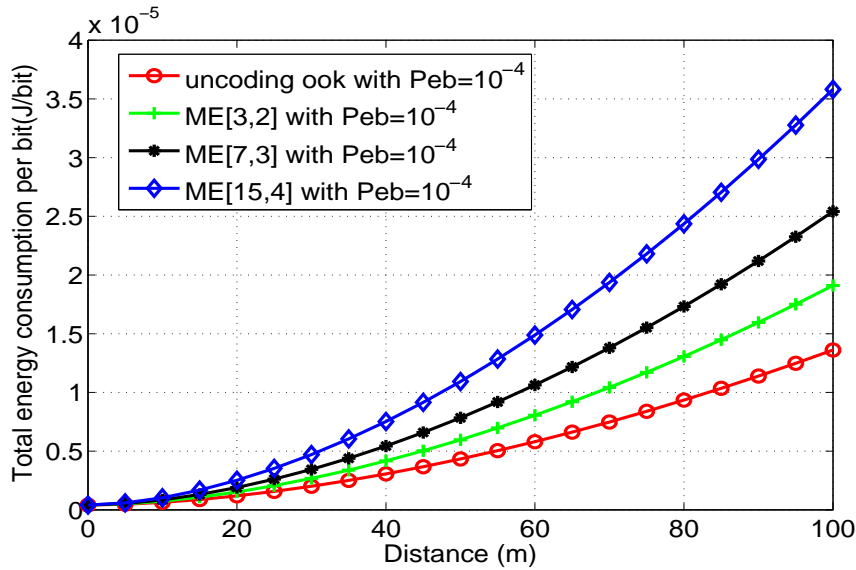


Figure 3.9: Energy consumption comparison

Fig. 3.9 compares the energy efficiency of ME-Coding schemes with OOK modulation. It is shown that the ME Coding is not energy efficient compared to the OOK modulation. The obtained results in the previous chapter are not confirmed when we consider the circuitry consumption. This can be explained by the fact that the presented general model is not matched to OOK modulation. Firstly, the circuit power consumption when transmitting a 0 is no different than when transmitting a 1 and secondly, the amplifier model is not adapted for a OOK modulation transmission.

To verify if the ME Coding schemes are energy efficient when the consumption of electronic circuits are considered, the next section proposes to introduce OOK matched energy consumption models.

3.3 OOK matched energy consumption models

OOK is a convenient modulation scheme for wireless communication because of its simplicity in implementation both at transmitter side and receiver side. Compared to other modulation schemes such as PSK, FSK and QAM, OOK can be easily implemented on top of the existing protocols such as 802.11, 802.16, GSM and CDMA. Minimum Energy coding can be implemented using OOK with the advantage that it can be expected that the circuit power consumption when transmitting a 0 will be lower than when transmitting a 1. We proposed an energy consumption model which is specially adapted to ME-Coding (energy efficient source coding method mentioned in chapter two) using OOK modulation. Besides, the originality of the proposed model is considering the energy consumption during the switch time from low bit to high bit or from high bit to low bit. It will further accurate the total energy consumption to show the real energy efficiency of ME-Coding.

Firstly we propose a normal mode which uses the circuit in nominal manner. Then, we define a more efficient model which shut down the circuit when transmitting a low bit.

3.3.1 Normal energy consumption model

We focus on the transmitter and the receiver described in figures 3.10 and 3.11 for which we consider only the analog parts.

The transmitter is composed of a local oscillator (LO) which generates the carrier wave. A switch transmits this signal through a filter to the power amplifier (PA) and the antenna if a high bit is sent. In case of low bit, no signal is transmitted.

The receiver is composed of a low noise amplifier (LNA), a frequency transposition associated to a local oscillator and a coherent or more often a non coherent detector.

We propose to evaluate E_{total} , the total energy consumption of the link when transmitting a message of L_{pkt} bits.

Assuming that :

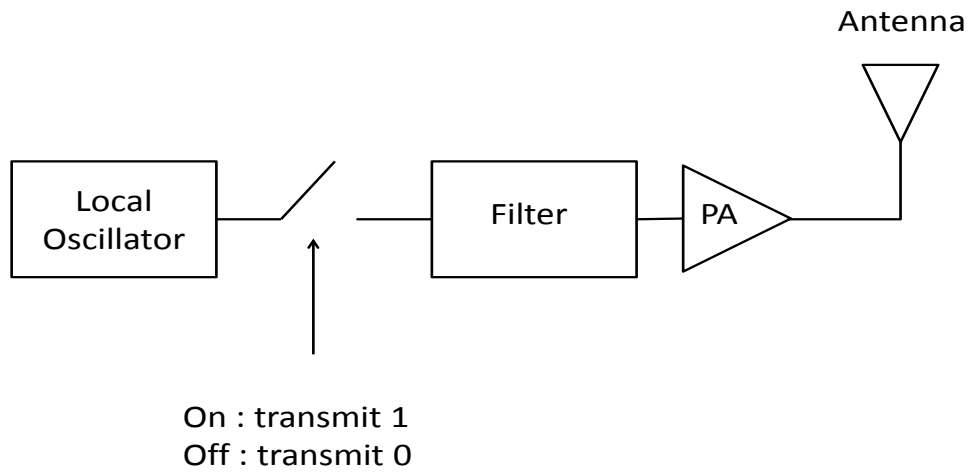


Figure 3.10: Transmitter circuit analog blocks

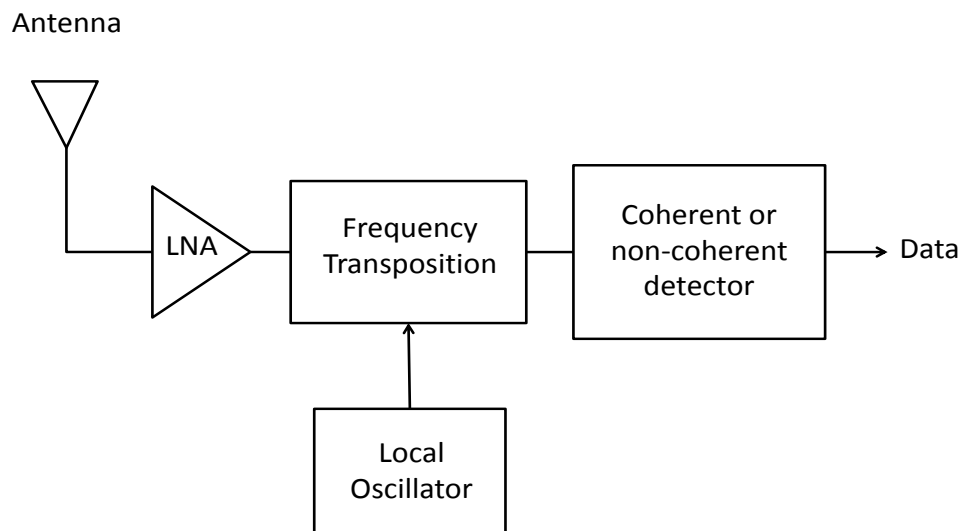


Figure 3.11: OOK Receiver circuit

- During the start time of the link t_{start} , the average power consumed by the transmitter and the receiver are respectively $P_{start_{tx}}$ and $P_{start_{rx}}$.
- The transmit time of a bit is t_b and the total transmit time (after the start time) is $t_{total} = t_b L_{pkt}$.
- The duty cycle of the bit frame (i.e. the number of high bits divided by the total number of bits) is r_d .

After the start time the power consumption of the transmitter depends on the transmitted bits :

- During the transmission of a low bit the power consumption is denoted P_{0tx} .
- During the transmission of a high bit, the power consumption can be expressed:

$$P_{1tx} + \frac{P_{out}}{\eta} \quad (3.9)$$

where P_{1tx} is a constant, η is the drain efficiency of the power amplifier and P_{out} is the output power (the power transmitted to the antenna).

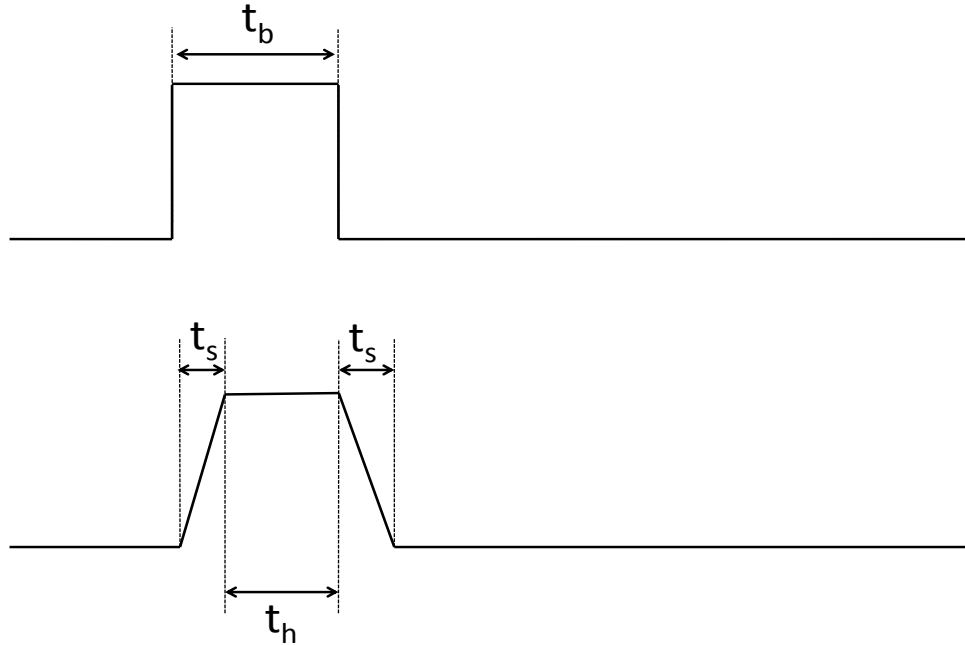


Figure 3.12: Definition of the switch time

In a real circuit, the transition from low bit to high bit is not instantaneous. We define the switch time t_s and the high bit duration t_h as shown in figure 3.12. The average power consumption during the switch time is denoted as $P_{switch_{tx}}$.

To express the average power during the transmission of a packet, we must know the high bit duty cycle but also the switch state frequency.

The assumed condition is that when transmitting L_{pkt} bits message, the duty cycle is r_d and the transmit time for one bit is t_b , the average switch number from high bit to low bit or from low bit to high bit, is $\overline{N}_s \in \{1, L_{pkt} - 1\}$.

The duty cycle r_d can be written:

$$r_d = \frac{N_H}{N_L + N_H} = \frac{N_H}{L_{pkt}} \quad (3.10)$$

where N_H and N_L are respectively the number of high and low bits in the packet.

The ratio of switch time on total transmit time r_s and the ratio of transmit high bit time on total transmit time r_h can be derived from the duty cycle r_d

$$r_s = \frac{t_s \times \overline{N}_s}{t_{total}} \quad (3.11)$$

$$\begin{aligned} r_h &= \frac{t_h \times N_H}{t_{total}} \\ &= \frac{t_b \times r_d \times L_{pkt} - \frac{1}{2} \times \overline{N}_s \times t_s}{t_{total}} \\ &= r_d - \frac{\overline{N}_s \times t_s}{2 \times t_{total}} \end{aligned} \quad (3.12)$$

When transmitting L_{pkt} bits message, the probability P_s to have N_s switches is

$$\begin{aligned} P_s(N_s) &= 2 \times \frac{(L_{pkt} - 1)!}{(L_{pkt} - 1 - N_s)! \times N_s! \times 2^{L_{pkt}}} \\ &= \frac{\binom{N_s}{L_{pkt} - 1}}{2^{L_{pkt} - 1}} \end{aligned} \quad (3.13)$$

When transmitting L_{pkt} bits message with a given duty cycle r_d , the average switch number \overline{N}_s can be obtained as follow

$$\begin{aligned} \overline{N}_s &= \frac{2 \times r_d \times L_{pkt} \times (L_{pkt} - r_d \times L_{pkt})}{L_{pkt}} \\ &= 2 \times r_d \times L_{pkt} \times (1 - r_d) \end{aligned} \quad (3.14)$$

Then the new functions of the two ratios r_s and r_h can be obtained

$$\begin{aligned} r_s &= \frac{2 \times t_s \times r_d \times L_{pkt} \times (1 - r_d)}{t_{total}} \\ &= \frac{2 \times t_s \times r_d \times (1 - r_d)}{t_b} \end{aligned} \quad (3.15)$$

$$\begin{aligned} r_h &= r_d - \frac{2 \times r_d \times L_{pkt} \times (1 - r_d) \times t_s}{2 \times t_{total}} \\ &= r_d - r_d \times (1 - r_d) \times \frac{t_s}{t_b} \end{aligned} \quad (3.16)$$

So the average power during the transmission is

$$P_{0tx} \times (1 - r_h - r_s) + (P_{1tx} + \frac{P_{out}}{\eta}) \times r_h + P_{switch_{tx}} \times r_s \quad (3.17)$$

We can deduce the energy consumed by the transmitter to send a packet of L_{pkt} bits:

$$E_{tx} = P_{start_{tx}} t_{start} + (P_{0tx} \times (1 - r_h - r_s) + (P_{1tx} + \frac{P_{out}}{\eta}) \times r_h + P_{switch_{tx}} \times r_s) \times t_{tx} \quad (3.18)$$

From this equation the transmitter energy per bit can be written:

$$E_{btx} = P_{start_{tx}} t_{start} / L_{pkt} + [P_{0tx} (1 - r_h - r_s) + (P_{1tx} + \frac{P_{out}}{\eta}) r_h + P_{switch_{tx}} r_s] / R \quad (3.19)$$

For large values of L_{pkt} , the influence of the start time is small, so :

$$E_{btx} \approx [P_{0tx} \times (1 - r_h - r_s) + (P_{1tx} + \frac{P_{out}}{\eta}) \times r_h + P_{switch_{tx}} \times r_s] / R \quad (3.20)$$

For the receiver, we assume that the power consumption does not depend on the transmitted bits. So a simple model is defined by

$$E_{rx} = P_{start_{rx}} t_{start} + P_{c_{rx}} t_{total} \quad (3.21)$$

where $P_{c_{rx}}$ is the power consumption during the processing of the bit frame.

From this expression, we can deduce the consumed Rx energy per bit which can be expressed as

$$E_{brx} = \frac{P_{start_{rx}} t_{start}}{L_{pkt}} + \frac{P_{c_{rx}} t_{total}}{L_{pkt}} \quad (3.22)$$

The total consumed energy per bit, for the link is the sum of E_{btx} and E_{brx} which yields :

$$E_{bT} = \frac{P_{start_{tx}} t_{start}}{L_{pkt}} + \frac{P_{0tx}(1 - r_h - r_s) + (P_{1tx} + \frac{P_{out}}{\eta})r_h + P_{switch_{tx}}r_s}{R} + \frac{P_{start_{rx}} t_{start}}{L_{pkt}} + \frac{P_{c_{rx}} t_{total}}{L_{pkt}} \quad (3.23)$$

If the start time is neglected we obtain

$$E_{bT} \approx \frac{P_{0tx}(1 - r_h - r_s) + (P_{1tx} + \frac{P_{out}}{\eta})r_h + P_{switch_{tx}}r_s}{R} + \frac{P_{c_{rx}} t_{total}}{L_{pkt}} \quad (3.24)$$

3.3.2 Condition and analysis of the proposed model

We consider the application of the proposed model to a realistic circuit. We consider the 400 MHz OOK transmitter MAX1472 which will be detailed in the next chapter. Figure 3.13 shows the power consumption of the circuit as the function of the output power, from 0 to 10 dBm, and for different input data duty cycle (rd).

As expected the consumed power increases with output power and decreases when the duty cycle is reduced.

In the first approach we consider a simplified model without considering the switch time ($t_s = 0$). So the power consumed by the transmitter is given by :

$$P_{0tx}(1 - r_h) + (P_{1tx} + \frac{P_{out}}{\eta})r_h \quad (3.25)$$

and we have $r_h = r_d$.

We can use the curve obtained for $r_d = 1$ in figure 3.13 to determine the parameters of the model. From the figure, we have :

$$\begin{aligned} (P_{1tx} + \frac{10}{\eta}) &= 24mW \\ (P_{1tx} + \frac{1}{\eta}) &= 12mW \end{aligned} \quad (3.26)$$

From these two equations, we can deduce $P_{1tx} = 10.66mW$ and $\eta = 0.75$.

Now, if we consider the curve for $r_d = 0.5$, we have for $P_{out} = 1mW$:

$$\frac{P_{0tx}}{2} + \frac{12}{2} = 8mW \quad (3.27)$$

and we obtain $P_{0tx} = 4mW$.

These parameters are presented in the Table 3.2.

Table 3.2: The simulation parameter

Parameter	Value	Unit
P_{0tx}	4	mW
P_{1tx}	10.66	mW
η	0.75	-

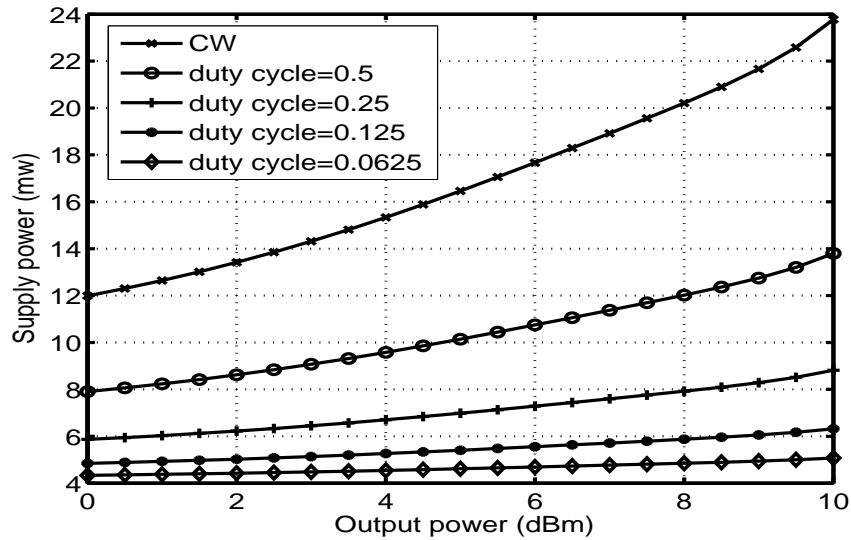


Figure 3.13: Total power consumption versus output power (circuit MAX1472, from datasheet)

Using the parameters from the Table 3.2, the total power consumption is plotted in Fig. 3.14. The results are very similar to the values deduced from the datasheet (Fig. 3.13) and we can conclude that this model can be used to verify the energy efficiency of ME-Coding in the following analysis.

We consider now the full model including the switch time. The figure 3.15, from the circuit data sheet, provides the demodulation of the output signal of the MAX1472 transmitter for a data rate equal to 100 kbit/s. From this figure, we can approximate the switch time by the raised time equal to about $0.5 \mu s$.

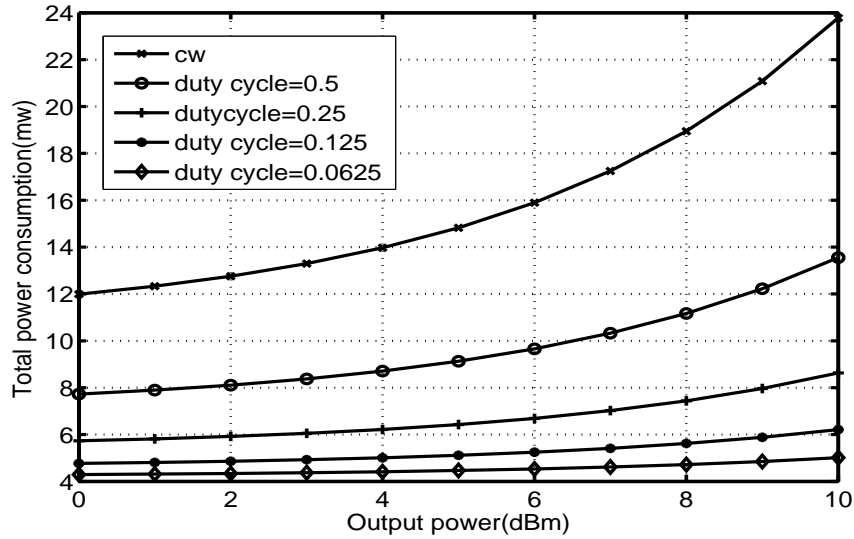


Figure 3.14: Total power consumption of the MAX1472 using the proposed model (without switch time)

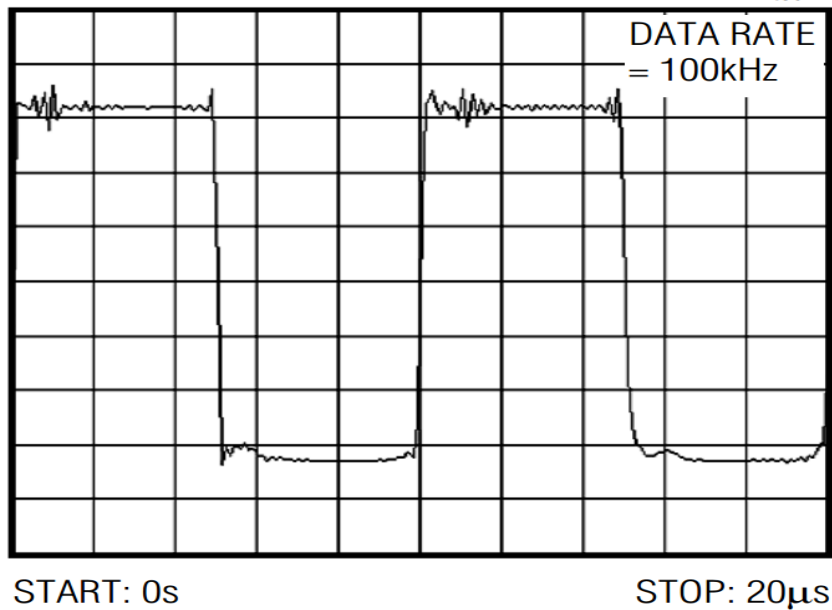


Figure 3.15: Demodulation of the output signal of the MAX1472 transmitter from circuit data sheet. Data rate = 100kbit/s

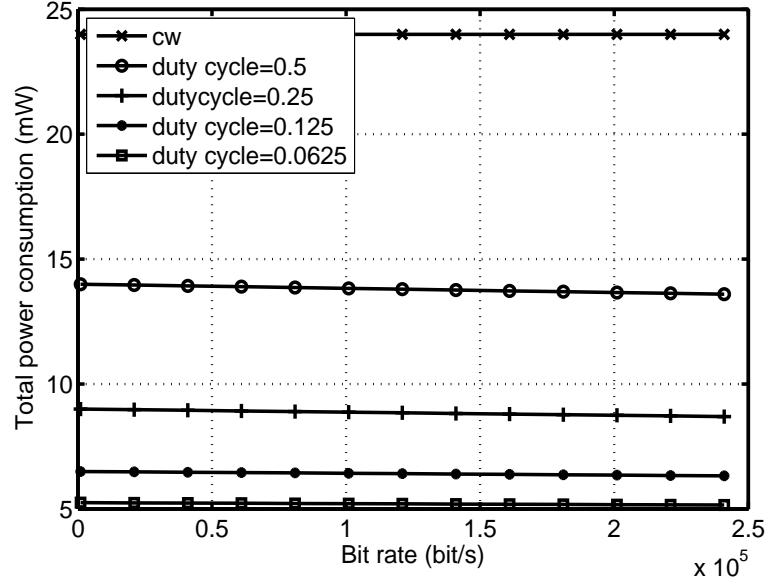


Figure 3.16: Total power consumption of the MAX1472 using the proposed model (with switch time= $0.5\mu s$)

The switch power depends also on the characteristics of circuit. For this first study we will assume that it is the average between the low bit power and the high bit power (without power amplifier):

$$P_{switch_{tx}} = \frac{P_{0tx} + P_{1tx}}{2} \quad (3.28)$$

The figure 3.16 shows the total power consumption versus the bit rate for different duty cycles r_d , considering a switch time $t_s = 0.5\mu s$ and for a maximum output power $P_{out} = 10mW$. We can notice that the total power consumption decreases with the bit rate for every duty cycle different from one. But the influence of the switch time on the power consumption decreases with the duty cycle (because the number of switches decreases) and is especially noticeable for $r_d = 0.5$. Even in that case the effect is small and for the considered circuit, it is probably not necessary to consider the switch time in the power consumption model.

3.3.3 Shutdown energy consumption model

In this section, a shutdown mode of transmitter is considered as described in figure 3.17. The whole circuit will shut down when transmitting a low bit.

It is expected that the transition time between low and high bit is increased due to

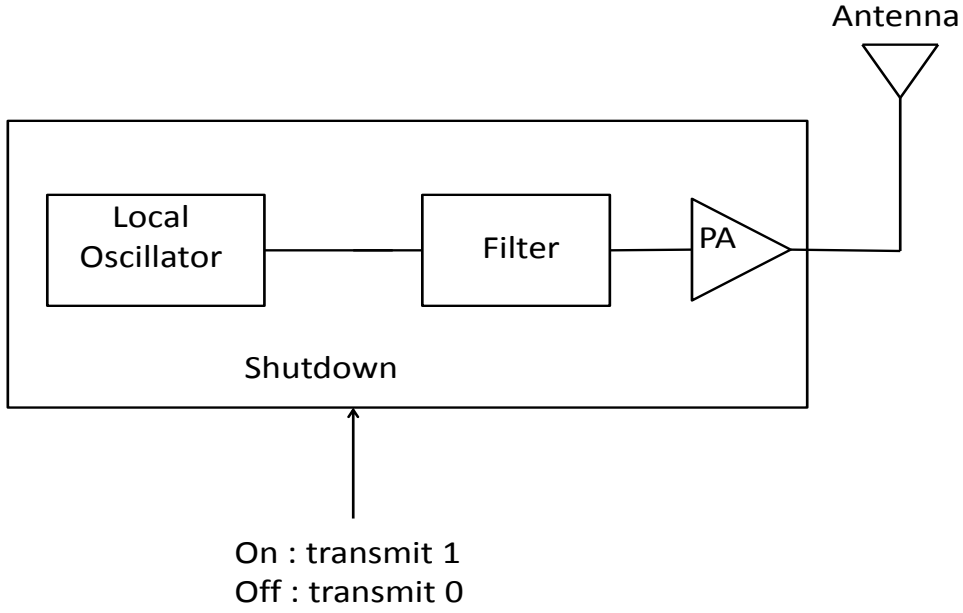


Figure 3.17: Transmitter circuit analog blocks - shutdown mode

the wake up of the circuit. This is illustrated in figure 3.18. Meanwhile, the wake up time is a limiting factor for the bit rate.

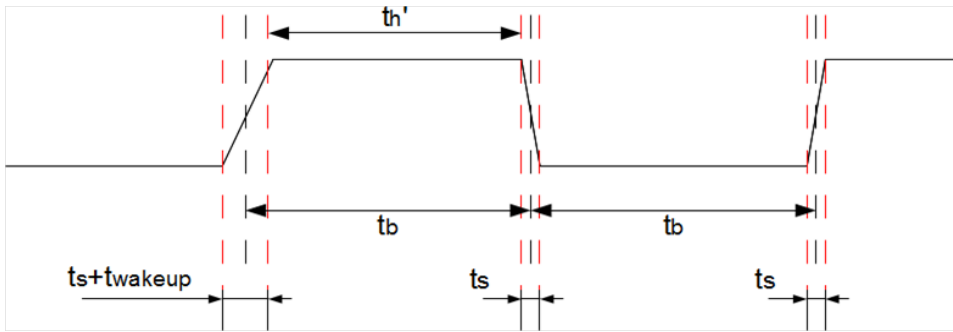


Figure 3.18: Transmit time of bit '1' and bit '0' in shutdown mode

We use the same assumptions as in the previous model. We consider the transmission of a L_{pkt} bit message. The duty cycle is r_d . The wake up time is t_{wakeup} and the transmit time for one bit is t_b .

The average switch number and each switch time, from bit '1' to bit '0', or from bit '0' to bit '1', are $\overline{N_s} \in \{1, L_{pkt} - 1\}$ and t_s .

Besides, $\overline{N_{s10}}$ and $\overline{N_{s01}}$ are the average switch number for switch from bit '1' to

bit'0' and for switch from bit'0' to bit'1', respectively.

$$\begin{aligned}\overline{N_{s_{10}}} &= \overline{N_{s_{01}}} = \frac{\overline{N_s}}{2} \\ t_s &< t_{wakeup} \ll t_b \\ t_{total} &= t_b \times L_{pkt}\end{aligned}\tag{3.29}$$

The ratio of switch time on total transmit time r'_s and the ratio of transmit high bit time on total transmit time r'_h can be derived from the duty cycle r_d .

$$r_d = \frac{N_H}{N_L + N_H} = \frac{N_H}{L_{pkt}}\tag{3.30}$$

$$\begin{aligned}r'_s &= \frac{t_s \times \overline{N_s} + t_{wakeup} \times \frac{\overline{N_s}}{2}}{t_{total}} \\ &= \frac{(t_s + \frac{t_{wakeup}}{2}) \times \overline{N_s}}{t_{total}} \\ &= \frac{(2 \times t_s + t_{wakeup}) \times r_d \times (1 - r_d)}{t_b}\end{aligned}\tag{3.31}$$

$$\begin{aligned}r'_h &= \frac{t'_h \times N_H}{t_{total}} \\ &= r_d - \frac{r'_s}{2} \\ &= r_d - \frac{(2 \times t_s + t_{wakeup}) \times r_d \times (1 - r_d)}{2 \times t_b}\end{aligned}\tag{3.32}$$

In real circuits the wakeup time is much bigger than the switch time. So we can assume that t_s is equal to zero. So we can neglect the power consumption during the switch time and consider only the wake up power consumption P_{wakeup} .

We will assume that the power consumption during the transmission of a low bit is zero because the circuit is in shutdown mode. So the average power consumption during the transmission of the bits is

$$P_{Tx} = (P_{1tx} + \frac{P_{out}}{\eta}) \times r'_h + P_{wakeup} \times r'_s\tag{3.33}$$

So the energy to transmit a packet of L_{pkt} bits is

$$E'_{tx} = \left((P_{1tx} + \frac{P_{out}}{\eta}) \times r'_h + P_{wakeup} \times r'_s \right) \times t_{tx} \quad (3.34)$$

The energy consumption per bit E'_{tx_b} can be derived from the above equations as below:

$$E'_{tx_b} = \left((P_{1tx} + \frac{P_{out}}{\eta}) \times r'_h + P_{wakeup} \times r'_s \right) / R \quad (3.35)$$

Then we analyze the influence considering the switch time. Some numerical simulation parameters are given in the Table 3.3. Here the parameters are also based on MAX1472.

Table 3.3: The simulation parameter

Parameter	Value	Unit
P_{1tx}	10.66	mW
P_{wakeup}	$(P_{1tx} + \frac{P_{out}}{\eta})$	mW
t_s	0.5	μs
t_{wakeup}	450	μs
η	0.75	

In the case of this circuit, the wake-up power is equal to the power during the transmission of a high bit. This is justified by the fact that the wake-up time is the time to stabilize the local oscillator. But all the circuits of the device are working in a nominal manner.

The numerical results, deduced from this new model, are given in figure 3.19.

We can notice that

- for a duty cycle equal to one the total power consumption is identical to the normal model. This result is obvious because the transmitter sends only high bits and there is no shutdown.
- for the other duty cycles, the power consumption is reduced. This is also demonstrated in figure 3.20 which represents the ratio of the total power consumption in shutdown mode to the total power consumption in normal mode. For output power of $2dBm$ and a duty cycle of $\frac{1}{4}$, energy saving by shutdown model is 40% compared with the normal model.

The shutdown mode is the more efficient in term of power consumption but it must be noticed that the wake up time is a limiting factor for the data rate. This will be detailed in the next chapter with the help of more efficient circuits.

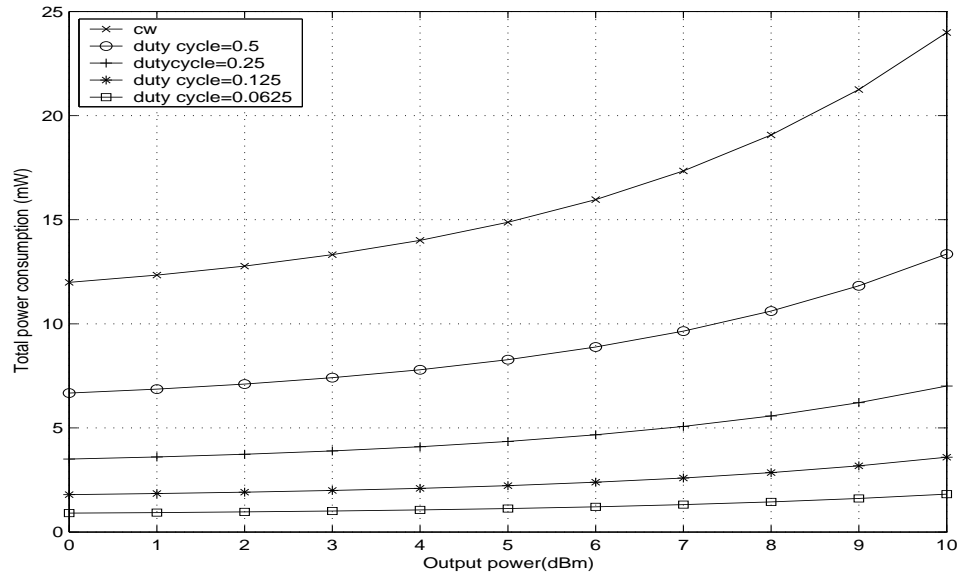


Figure 3.19: Total power consumption of the MAX1472 using the shutdown mode

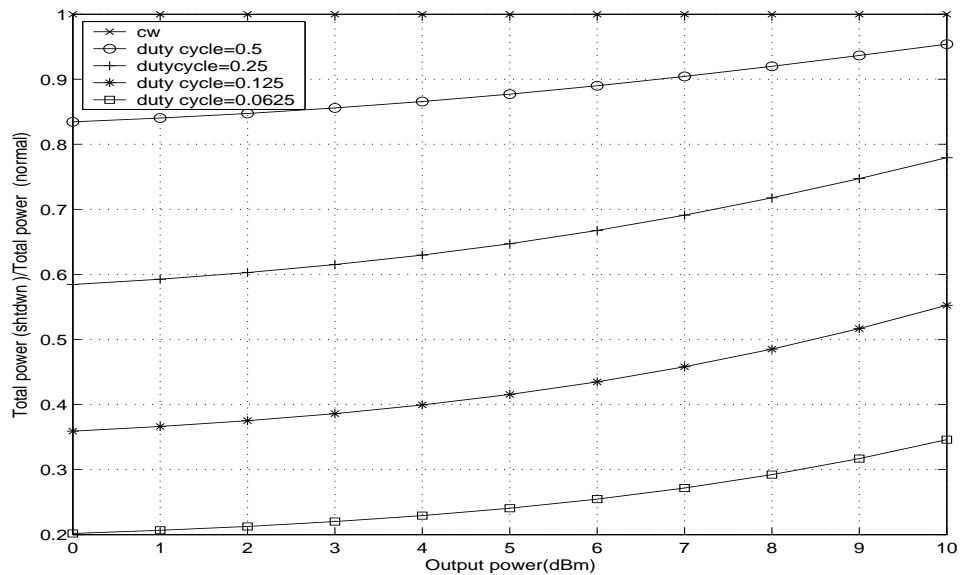


Figure 3.20: Comparison of the total power consumption of the MAX1472 using the shutdown mode and the normal mode

3.4 Conclusion

In this chapter, we consider the energy consumption models and give the overview of the energy consumption in wireless sensor nodes. Firstly, we introduce two general energy consumption models based on transceiver node and communication link respectively. Then, we present the energy consumption model we proposed which include the energy consumption during switch time between low bit and high bit. This model can be used to accurate the energy efficiency analysis of different energy efficient schemes (for example source coding method ME-Coding). Besides, we give the using condition of the proposed energy consumption models and the new model when the circuit is in shutdown mode. The last section shows the energy efficiency criterion.

These models will be used in the next chapter, to analyze the energy efficiency of Minimum Energy Coding, with different circuits.



4

Energy efficiency of Minimum Energy coding

Many coding or modulation schemes could be employed to operate with less SNR for a given bit error performance, but these are often complex and the circuit power consumption of the algorithms increases. For systems involving wireless sensors where the required bit rate is low, BPSK which consumes less power, seems to be a good choice. Simple digital modulation technique like OOK is usually not studied due to its bad performance. In AWGN channel, uncoded OOK requires two times more transmit power to obtain the same error performance as BPSK. Minimum Energy coding (ME-coding) based on On-Off Keying (OOK) is interesting to improve the error performance of OOK modulation and save transmit energy.

In the previous chapter, OOK matched energy consumption model is proposed. This model can be used to accurate the energy efficiency analysis of ME-Coding. In this chapter, our objective is to discuss the realistic energy consumption of the communication subsystem, the transceiver or the transmitter and the receiver. Several radio devices which are adjusted to use ME-coding OOK modulation for wireless transmission node are introduced. Then, we analyze the power efficiency of ME-coding using the proposed realistic energy consumption models which are based on different efficient OOK transmitters and receivers.

The remainder of this chapter is organized as follows. In section 4.1, we introduce

several devices in the application of WSNs and give descriptions of the device which we analyzed in this chapter. Section 4.2 analyzes the total energy consumption of the first transmitter and shows the maximum transmit bit rate limitation. Section 4.3 presents a new energy consumption model for a second energy efficient transmitter, which is derived from the general model described in chapter 3, then analyzes the energy consumption and provides the method for selecting optimal coding size. The last section shows the energy consumption of the receiver and of the combination of a transmitter and a receiver.

4.1 Description of the studied devices

According to the BER analysis presented in chapter 2, ME-Coding is known as an energy efficient coding scheme, when considering the transmit energy. However, the total energy consumption performance is worse than uncoded OOK when considering both the transmit energy and the circuit energy using the general energy consumption model in chapter 3. So it is necessary to find the devices and improve the energy consumption model, which are matched to ME-Coding. In order to keep low energy consumption, the low complexity OOK transmitter and receiver are better choices. Therefore, we investigate simple OOK transmitter MAX1472 and receiver MAX7033. Besides, an ultra low power transmitter is also discussed as it has the advantage of performance in energy consumption and has less limitation on the maximum transmit bit rate although it is not commercially available.

4.1.1 The first OOK transmitter

The first OOK transmitter is MAX1472, a crystal-referenced phase-locked loop (PLL) VHF/UHF transmitter designed to transmit OOK/ASK data in the 300 MHz to 450 MHz frequency range. The MAX1472 supports data rates up to 100kbps , and adjustable output power to more than $+10\text{dBm}$ into a 50Ω load. The crystal-based architecture of the MAX1472 eliminates many of the common problems with SAW transmitters by providing greater modulation depth, faster frequency settling, higher tolerance of the transmit frequency, and reduced temperature dependence. Combined, these improvements enable better overall receiver performance when using a super-heterodyne receiver such as the MAX1470 or MAX1473. This cheap transmitter has wild applications like remote keyless entry RF remote controls, tire pressure monitoring, security systems, radio-controlled toys, wireless game consoles, wireless com-

puter peripherals and wireless sensors.

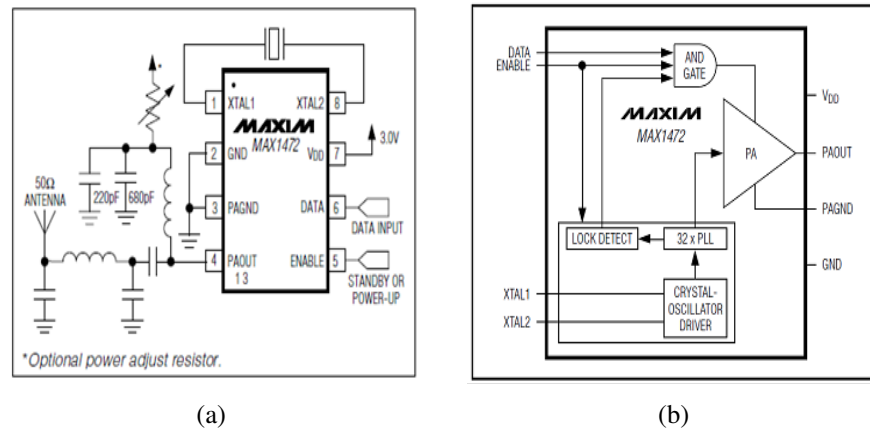


Figure 4.1: The analog block (a) Typical Application Circuit (b)Functional Diagram

Fig. 4.1 shows the block diagram of the first low energy consumption OOK transmitter. This device provides a shutdown mode. The ENABLE pin is internally pulled down with a $15 \mu A$ current source. If the pin is left unconnected or pulled low, the MAX1472 goes into shutdown mode, where the supply current drops to less than $5 nA$. When ENABLE is high, the IC is enabled and is ready for transmission after $220 \mu s$. The $220 \mu s$ turn-on time of the MAX1472 is mostly dominated by the crystal oscillator startup time. Once the oscillator is running, the $1.6 MHz$ PLL loop bandwidth allows fast-frequency recovery during power-amplifier toggling. This turn-on time will lead to a limitation of maximum bit rate for shutdown mode.

4.1.2 High performance OOK transmitter

To avoid the limitation, we try to search the second energy efficient OOK transmitter without this disadvantage. The transmitters in WSN/WBAN (wireless body area network)/WPAN (wireless personal area network) are characterized by energy efficiency which is the amount of energy consumed in transmitting a bit, usually expressed in nJ/bit . There have been lots of research work on WSN transceiver [73, 74, 75]. The fact that OOK transceiver is characterized by the simplicity of the circuitry, makes it an excellent solution for system miniaturization and energy optimization. The energy consumption of the OOK transmitters [73, 74] are $3.8 nJ/bit$ and $11.54 nJ/bit$ and are limited to bit rates less than $300 kb/s$. The authors in [75] proposed a speed-up circuitry accomplishing faster data rate up to $10 Mbps$. The OOK Tx is totally switched off when transmitting '0' to achieve lower energy consumption of $52 pJ/bit$.

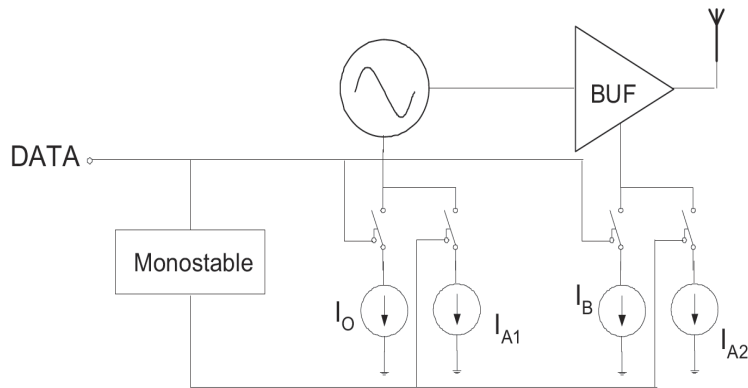


Figure 4.2: The block diagram of the second OOK transmitter

Fig. 4.2 shows the block diagram of the second low energy consumption OOK transmitter, where the oscillator and buffer are switched on and off when transmitting a "1" or "0" respectively. The data rate depends on how fast the output can be switched on and off. While the decay to "0" can be made fast by simultaneously shorting the output to ground and switching the supply or drain current off, the build-up to "1" is limited by the oscillator start-up. Two additional current sources (I_{A1} and I_{A2}) are introduced as supplementary bias currents to the oscillator and buffer, but they are only turned on for a short period of time during the build-up of the oscillation. While the current I_{A1} improves the build-up of the oscillator, I_{A2} helps to charge the reactive elements that form matching network of the buffer. This transmitter is not commercially available and we use data from the author paper for our study.

4.1.3 OOK receiver

Meanwhile, we study the energy consumption of the receiver as well. The MAX7033 fully integrated low-power CMOS superheterodyne receiver is ideal for receiving amplitude shift-keyed (ASK) data in the 300 MHz to 450 MHz frequency range. Therefore we can use it as a receiver in our circuit and combined with the OOK transmitter. This receiver can be used in the same applications as the MAX1472 transmitter.

Fig. 4.3 shows the functional diagram of the circuit. The MAX7033 CMOS super heterodyne receiver and a few external components provide the complete receive chain from the antenna to the digital output data. Depending on signal power and component selection, data rates as high as 33 kbps Manchester (66 kbps NRZ) can be achieved. The MAX7033 is designed to receive binary ASK data modulated in the 300 MHz to 450 MHz frequency range. ASK modulation uses a difference in amplitude of the

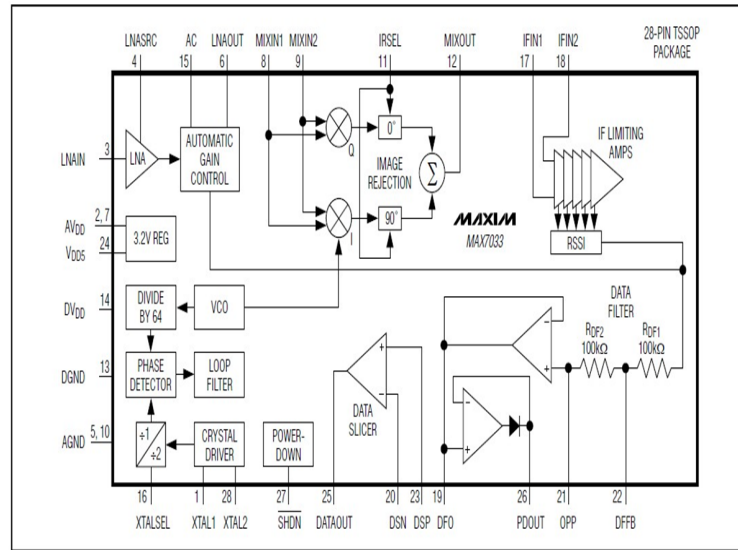


Figure 4.3: Functional diagram of MAX7033 receiver

carrier to represent logic 0 and logic 1 data.

As an illustration, the figure 4.4 presents an Arduino shield demonstrator of the OOK transmitter and receiver, based on the MAX1472 and MAX7033 which has been developed in the laboratory. This circuit is a transceiver which allows to make practical tests on these two devices. In particular, current measurements can be done using an Arduino card as an acquisition platform.

Based on these devices, we could realistically analyze the energy consumption of each radio device using the proposed energy model in chapter 3. But the energy consumption model should be modified according to the parameter of the practical device.

4.2 Energy consumption study of a realistic transmitter

This section presents realistic energy consumption models to evaluate the energy consumption including both the transmission energy and the circuit energy at the transmitter when using Minimum Energy coding On-Off Keying scheme. We consider a simple communication link between sensor nodes. We present two energy models for the specific circuit (the first transmitter MAX1472) and we consider also the limitations, introduced by a practical circuit, in terms of symbol bit rate and output power.

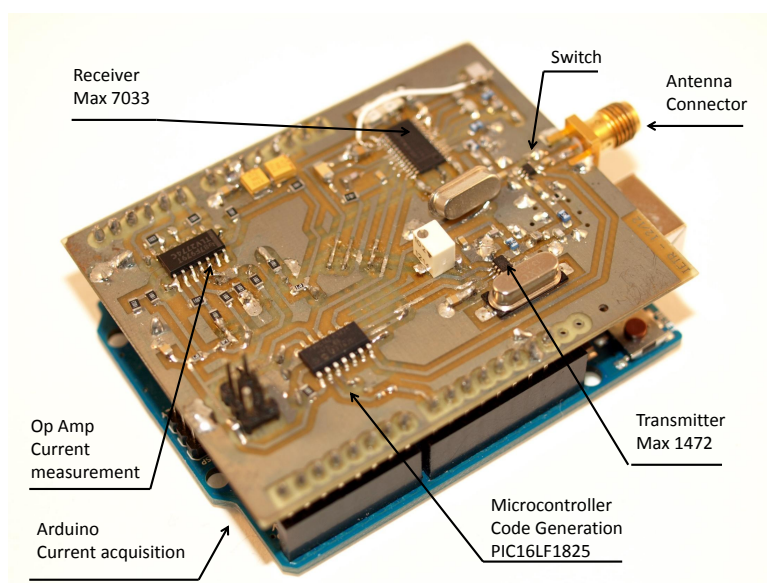


Figure 4.4: OOK transceiver developed in the laboratory

The results with the first model demonstrate that the total energy consumption of ME-Coding OOK is lower than that of the uncoded OOK, but the optimal choice of the code must take into account the limitations of the circuit. The second model with MAX1472 shutdown mode brings a reduction of the total energy consumption compared with the first model but is limited in the symbol rate.

The novelty is to evaluate the basic idea of minimum energy source coding scheme, including a circuit power consumption model matched to OOK modulation. Moreover, we consider the limitations of the practical circuit in terms of maximum output power and symbol bit rate and propose an optimized choice to reduce the total energy per bit.

Subsection 4.3.1 describes the minimum energy coding and provides a BER analysis. Subsection 4.3.2 presents the realistic energy consumption models and subsection 4.3.3 gives the analysis based on these models.

4.2.1 Minimum energy coding and BER analysis

ME-Coding optimizes energy by minimizing the number of ones which are present in the coded message as described in chapter 2 in detail. The basic idea involves mapping every k bits of a source bit-stream into an n - bit ($n = 2k - 1$) codeword (in standard form, $ME[n, k]$). In our case, all the source symbols are mapped into codewords within no more than one high bit. It reduces the transmission energy consumption but sacrifices bandwidth efficiency. Then by code-by-code detection process

(soft decision in [58]) we look at the bit with highest strength as $bit - 1$ and the rest is decided as $bit - 0$.

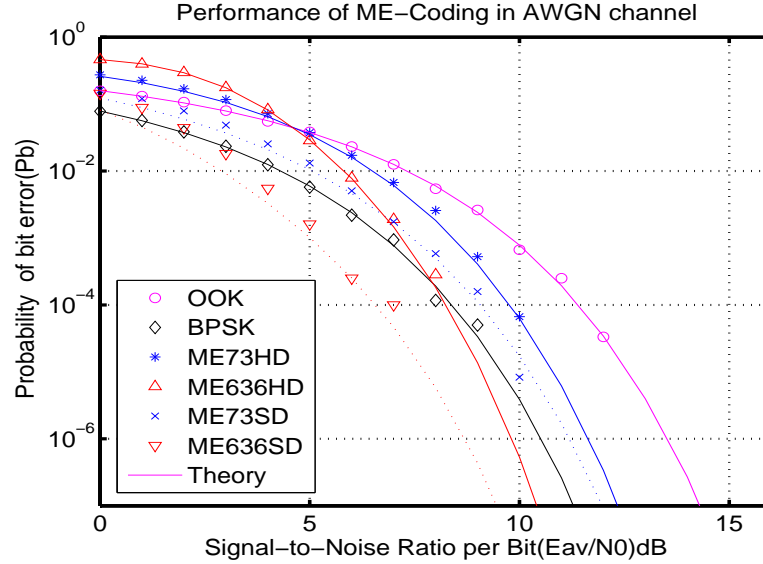


Figure 4.5: BER performance of ME-Coding

Assuming transmission over the AWGN channel, we could deduce bit error probabilities by using different source coding schemes. Fig. 4.5 recalls the improvement in the bit error performance using code-by-code detection [56]. Compared to uncoded OOK and for an error probability of 10^{-3} , about 3 dB and 5 dB improvement in SNR per bit are respectively obtained with ME[7,3] and ME[63,6] using soft decision. This gain can be used to reduce the transmit power in order to increase the energy efficiency. But the total energy budget we must also take into account the circuit power consumption.

4.2.2 Energy consumption model

Minimizing transmission energy is reasonable in traditional wireless links where the transmission distance is large ($> 100\text{m}$), so that the transmission energy is dominant in the total energy consumption. However, in many recently proposed wireless ad-hoc networks (e.g. sensor networks) the nodes are densely distributed, and the average distance between nodes is usually below 10m. In this scenario, the circuit energy consumption becomes comparable to or even larger than the transmission energy. Thus, in order to verify the energy optimization of the ME-Coding scheme, the overall energy consumption including both transmission and circuit energy needs to be

considered.

The system model with MAX1472(Simple OOK Model)

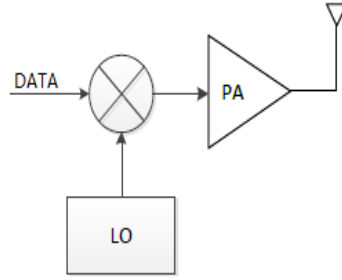


Figure 4.6: The equivalent analog block of the simple OOK model

We used MAX1472 which is a crystal-referenced phase-locked loop (PLL) VHF/UHF transmitter designed to transmit OOK/ASK data in the 300MHz to 450 MHz frequency range with a maximum bit rate R equal to 100kbit/s. The Equivalent analog block, given in Fig. 4.6, includes mainly a power amplifier and a frequency synthesizer. Energy consumption model can be deduced from the general model introduced in chapter 3 based on this diagram. The total power consumption per source bit of the analog blocks can be calculated from Equation (4.1):

$$P_{Total} = P_{tx} + P_{amp} + P_{anaT} \quad (4.1)$$

- P_{tx} is the transmitted power which depends on the antenna gain, the channel condition, the transmission distance, the carrier frequency, the requested BER and the modulation scheme. It can be calculated by the link budget equation for the considered modulation scheme as described in [46]:

$$P_{tx} = PL(d) \times M \times R \times k_B T_0 \times r_0 \quad (4.2)$$

- $PL(d)$ is the path loss, given by the following equation:

$$PL(d) = \left(\frac{4\pi d}{\lambda} \right)^2 \quad (4.3)$$

where λ is the carrier wavelength and d the distance between the transmitter and the receiver.

- The SNR per bit $r_0 = E_b/N_0$ depends on the requested BER. When considering the error control codes, it also depends on the applied specific code.
- R refers to the bit rate.
- M is the safety margin. We select it as $M_{dB} = 40\text{dB}$.
- The constant $k_B T_0$ is the typical value for the thermal noise power spectral density at the temperature T_0 and k_B is the Boltzmann's constant ($1.38 \times 10^{-23} \text{W} \cdot \text{S}/\text{K}$).
- P_{amp} is the additional power consumption of the amplifier (excluding the transmitted power).
- P_{ana_T} is the power consumed by the other transmitter circuits, including the frequency synthesizer.

In the following paragraphs, we define two power consumption models that can be used with the MAX 1472 circuit.

Power consumption of the simple OOK model

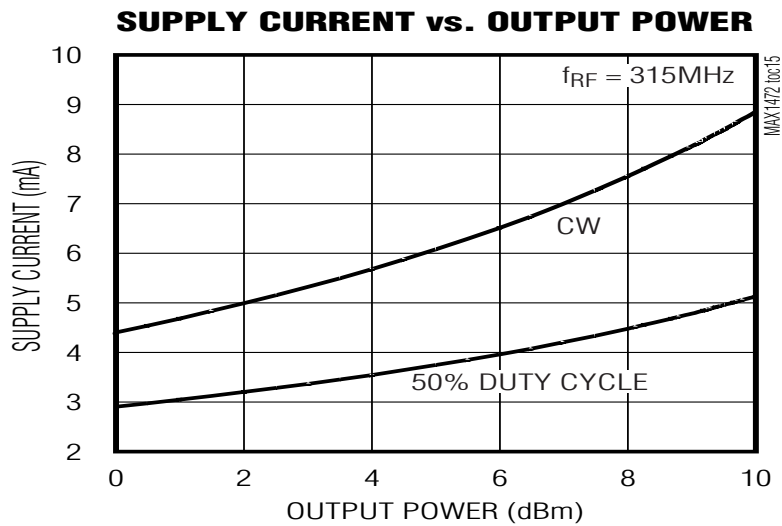
In this paragraph we define an accurate model of the MAX1472 transmitter. As shown in chapter 3, it is not necessary to take into account the switch time of the circuit which has small influence in energy consumption.

Fig. 4.7 (a) shows the relation of supply current versus output power given by the datasheet for $V_{DD} = 2.7\text{V}$ and $T_A = +25^\circ\text{C}$. In this curve, the output power is defined as the maximum output power (obtained for the transmission of a one). It must be noticed that it can only vary between 0 dBm and 10dBm. From these data we could get the function of supply current I versus output power by curve fitting. As the curves are not linear, the best fitting model is a cubic polynomial. The values obtained from this model are plotted in the Fig. 4.7 (b) and the curve with duty cycle= 0.5 is the same as that provided in the Fig. 4.7 (a).

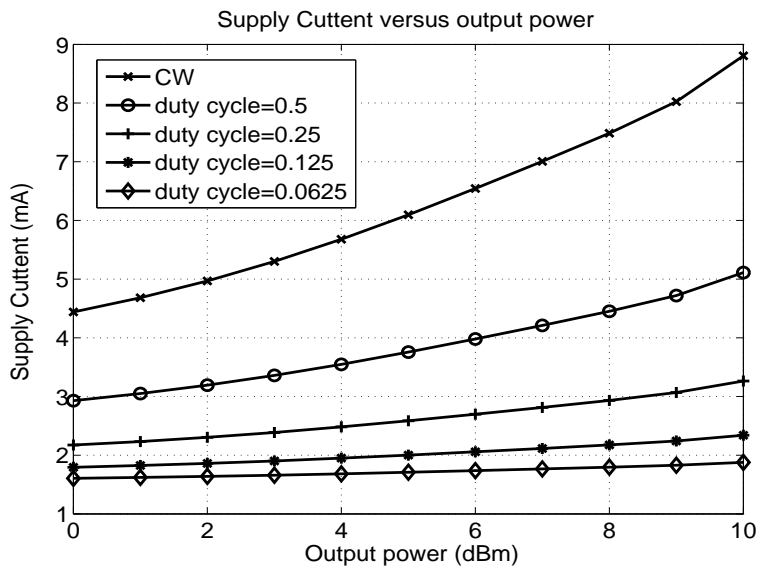
Then according to the equation $P_{Total} = V_{DD} \times I$, the model of the supply power versus output power is given by Equation (4.4):

$$P_{Total} = r_d \times (0.0147 \times P_{T(mW)}^3 - 0.3191 \times P_{T(mW)}^2 + 3.1887 \times P_{T(mW)} + 5.2794) + 3.825 \quad (4.4)$$

where r_d is the duty cycle.



(a)



(b)

Figure 4.7: Supply current vs. output power (a) CW and 0.5 duty cycle (b) Cubic polynomial curve fitting for different duty cycles

Modified model with shutdown mode (*SDOWN* model)

In the previous model the circuit is active even if a zero is transmitted. A better model can be introduced using the shutdown mode of the circuit. This modified model will be better matched to ME-coding OOK but is limited to lower symbol rate. Indeed, it must be noticed that the turn-on time of the device is $450\mu s$, so the symbol (or pulse) rate after coding must be reduced to less than 1 kchip/s.

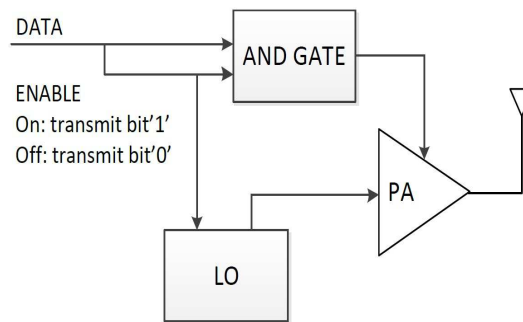


Figure 4.8: The equivalent analog block of *SDOWN* model

If the ENABLE pin is left unconnected or pulled low, the MAX1472 goes into shutdown mode, where the supply current drops to less than $I = 5nA$ at $V_{DD} = 2.7V$ and $T_A = +25^\circ C$. As it is shown in Fig. 4.8, the equivalent system model with the shutdown mode includes the power amplifier, the frequency synthesizer and the ENABLE on or off input, which is controlled by the transmission data.

According to this model, the total power consumption of the analog blocks can be calculated from Equation (4.5) and Equation (4.6)

When transmitting bit '1' :

$$P_{1tx} = P_{PA} + P_C \quad (4.5)$$

When transmitting bit '0' :

$$P_{0tx} = I \cdot V_{DD} = 2.7 \times 5 \times 10^{-9} = 1.35 \times 10^{-8} W \quad (4.6)$$

According to the equations in chapter 3 about the general model without considering the switch time ($t_s = 0$). The final Equation (4.7) can be deduced from Equation (4.5) and Equation (4.6) as follows :

$$P_{TotalSDOWN} = P_{0tx}(1 - r_h) + (P_{1tx} + \frac{P_{out}}{\eta})r_h \quad (4.7)$$

where r_h is the duty cycle of the coded message.

4.2.3 Energy Consumption Analysis

Total energy consumption analysis compared with the transmission energy

According to the total power consumption in Equation (4.7), the total energy consumption per bit is

$$E_{TotalSDOWN} = \frac{(1 - r_h) \times P_{analogL} + r_h \times P_{analogH}}{R} \quad (4.8)$$

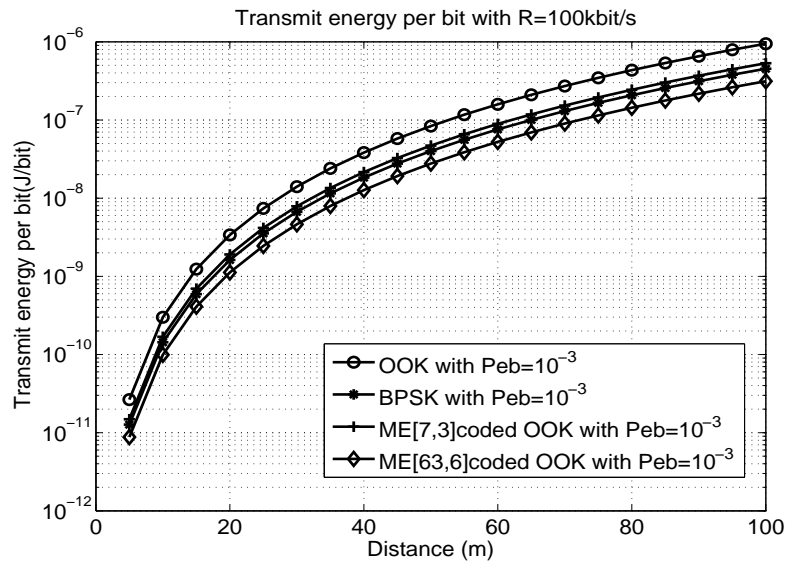
The transmit energy consumption per bit and the total energy consumption per bit of the simple OOK model are shown in Fig. 4.9. The bit rate is $R = 100$ kbit/s, and the distance ranges from 0 to 100 m.

When the average transmission energy is only considered, Fig. 4.9 (a) shows that the performance of the ME-coding OOK is better than the uncoded OOK. BPSK outperforms ME[7,3] a little bit, but the ME[63,6] wins back the lead as the source coding size k is increased. Even if BPSK can not used for the device, the transmit energy for BPSK modulation is given as a reference.

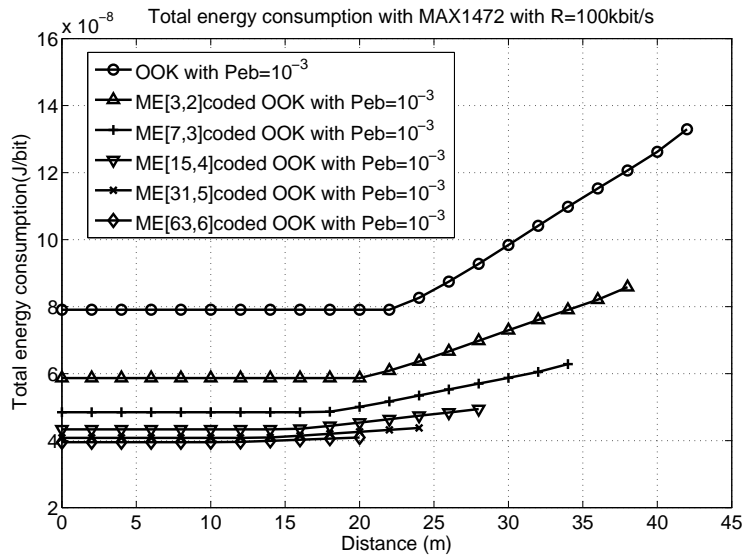
The total energy consumption is shown in Fig. 4.9 (b) in the condition that the maximum output power is between 0dBm and 10dBm due to the limitations of the circuit. When the needed maximum output power is less than 0dBm, the values obtained for 0 dBm are assumed. When the needed output power is larger than 10dBm, the required SNR is not achievable with the circuit.

As expected, the total energy consumption of the four methods are increased because the circuit energy is taken into account. When the transmission distance is less than 20 m, the total energy consumption per bit is very low, with a level of 10^{-8} J/bit. It increases dramatically when the distance exceeds 20 m. For short distance, the circuit energy is dominant and the transmission energy has little influence on the total energy consumption. As a result, the total energy consumption does not depend on the distance in this situation.

It is also clear in Fig. 4.9 (b) that the ME-coding OOK outperforms the uncoded OOK. Furthermore, the total energy consumption per bit is reduced when the ME-coding size k increases – ME[63,6] OOK performs the best. But as a result of the limitation of the maximum output power, the conclusion is untenable in all distances.



(a)



(b)

Figure 4.9: (a) Transmit energy per bit with R=100kb/s (b) Total energy consumption per bit with R = 100kb/s

For instance, if the transmission distance is smaller than $20m$, ME[63,6] is a good choice, while when the transmission distance is $30m$, the best choice is ME[7,3]. The reason is that the maximum output power for ME[63,6] can be higher than that of the ME[7,3] for the same distance (even if the required average power is lower).

It can be concluded that ME-coding is still the most energy efficient method with the simple energy model for wireless sensor network in short distance. The optimal coding can be determined as a function of the distance, taking into account the limitations of the circuit.

Results with the modified SDOWN model

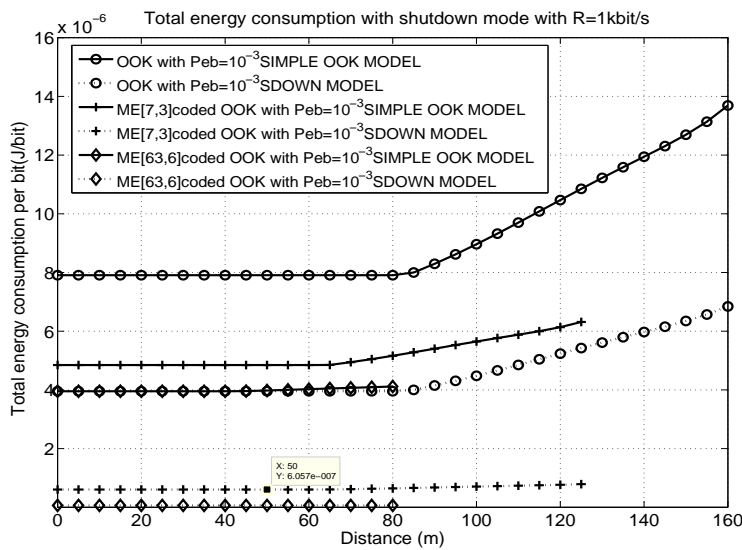


Figure 4.10: Total energy consumption per bit with MAX1472 with R=1 kbit/s

Fig. 4.10 gives the total energy per bit for the simple OOK model and the modified model with shutdown mode for a limited bit rate equal to 1 kbit/s. From this figure, the SDOWN model outperforms the simple OOK model. For instance, the energy consumption of ME[63,6] with modified model is almost just 6.1 nJ/bit which is much smaller than the value derived with the first energy model when the distance is 50m.

However, as the source bit rate for this model must be decreased to 1kbit/s, the total energy consumption is larger than that in Fig. 4.9(b). This effect will be detailed in the next section.

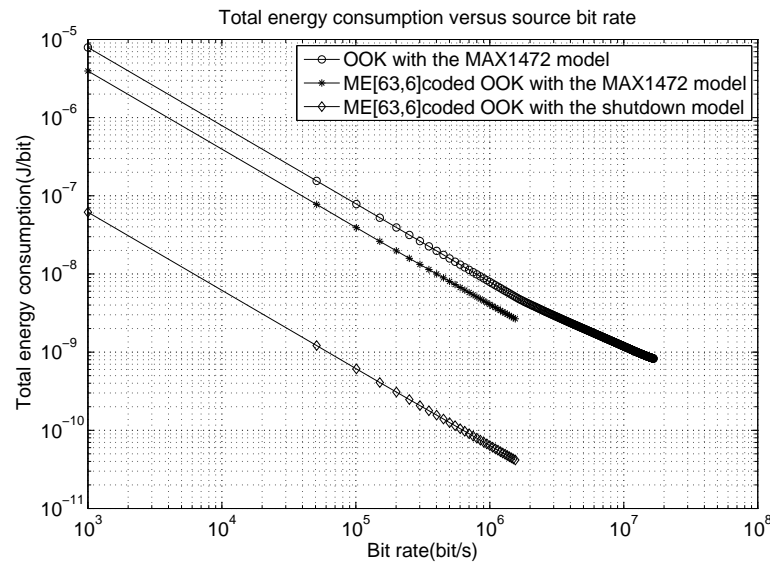


Figure 4.11: Relationship between energy consumption and bit rate, for $d = 10\text{m}$

Relationship between energy consumption and symbol bit rate

As shown in the Fig. 4.9 and Fig. 4.10, the energy consumption of the simple OOK model at 1kbit/s is larger than that at 100kbit/s. This is due to the fact that the energy consumption of the circuit is proportional to the bit duration. The relationship between energy consumption and symbol bit rate is shown in Fig. 4.11 for the distance $d = 10\text{m}$.

From these results, we could get an optimal source bit rate to obtain the lowest energy consumption. Unfortunately, the higher bit rate cannot be obtained with the MAX1472 which is limited to a chip rate equal to 100 kchip/s. So, in the case of this specific circuit we must chose the maximum bit rate that can be attainable for a given coding. For OOK, the maximum source bit rate is 100 kbit/s, while for ME[63,6] the value is just 1.58kbit/s.

4.2.4 Conclusion

In this section, we analyze the energy consumption of an OOK transmitter based on Minimum Energy coding. After the discussion on BER performance, we examine the energy consumption, including a realistic circuit energy model, based on a MAX1472. The limitations of this practical circuit in terms of maximum output power and symbol rate result in an optimal choice of ME coding for different ranges and performance. Then we propose a modified system model with shutdown mode which can be more

efficient but is limited to low bit rate (smaller than 1 kchip/s after coding). Taking into account the circuit energy, an optimal bit rate can be determined. Therefore, MAX1472 is a good choice for ME-coding OOK communication to get total energy optimization even if increasing its maximum bit rate specification and wake-up delay would be desirable.

4.3 Energy analysis of a high performance transmitter

This section proposes Minimum Energy (ME) coding to improve the energy efficiency using the second OOK transmitter with less limitation on the maximum transmit bit rate. Because the second device could completely switch off the transmitter during the transmission of '0' and has an energy efficiency of 52 pJ/bit , we can build a new power consumption model based on this real circuit.

4.3.1 Energy consumption model of the 52pJ/bit OOK transmitter

We consider the 433 MHz OOK transmitter described in [75, 76]. The circuit completely turns off the transmitter during the transmission of '0' and employs a speed up scheme to obtain high data rates and low wake up time. The data rate can be adjusted and adapted to the need of applications. The OOK transmitter has a measured output power $P_{out} = -12.7 \text{ dBm}$ with a dc power consumption of $560 \text{ }\mu\text{W}$ under a 1 V power supply, and when the speed-up circuitry is enabled, data rate increases to 10 Mb/s , with a dc power consumption of $518 \text{ }\mu\text{W}$ achieving an energy efficiency of 52 pJ/bit .

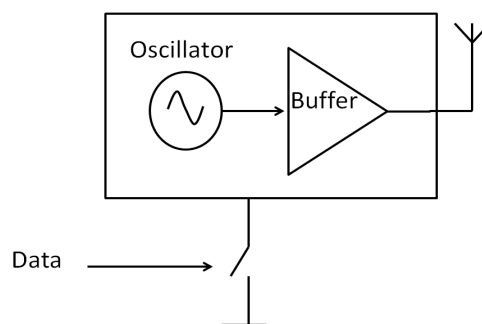


Figure 4.12: The block diagram of the ook transmitter

Fig. 4.12 shows the block diagram of the low energy consumption OOK transmit-

ter, where the oscillator and buffer are switched on and off when transmitting a "1" or "0" respectively. The data rate depends on how fast the output can be switched on and off. While the decay to "0" can be made fast by simultaneously shorting the output to ground and switching the supply or drain current off, the build-up time to "1" is limited by the start-up of the oscillator shown in Fig. 4.13.

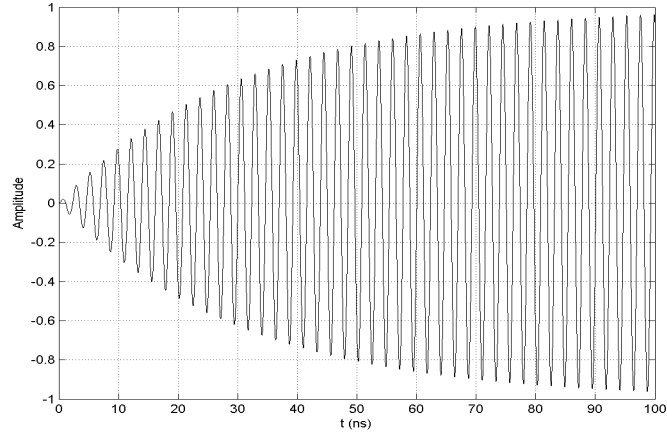


Figure 4.13: Oscillator output

When the oscillator is switched on, oscillation starts building up. An analysis of the equivalent circuit yields in Equation (4.9),

$$V_{out}(t) = K_1(1 - e^{-t/(2R_{eq}C_{eq})})\sin(2\pi f_0 t) \quad (4.9)$$

where, K_1 is the final amplitude of the oscillator output. The time constant for the envelope is $2R_{eq}C_{eq}$, and the time taken for the envelope to rise to 90 percent of its final value is 70 ns in speed-up mode. This rise time is important because it limits the maximum bit rate and as already seen the energy per bit decreases when the bit rate increases.

Table 4.1 from [75] summarizes the characteristics of the circuit. The output power P_{out} is -12.7 dBm. The dc current is the average current when the transmitter is modulated by equal probability of "0" and "1". At a data rate equal to 10 Mbit/s, the energy efficiency is 51.8 pJ/bit.

From the realistic parameters of the transmitter [75], the energy consumption per bit can be derived as follows. The energy consumption includes two parts: start up time period and constant period during transmitting of bit "1". So the power consumption can be written as :

Table 4.1: The parameter of the transmitter

PARAMETER	VALUE
Output Power	-12.7 dBm
DC Power	$1 \text{ V} \times 518 \text{ } \mu\text{A}$
	(when modulated with equal probability PRBS)
Data Rate	10 Mb/s
Energy Efficiency	51.8 pJ/bit
Rise Time	70 ns

$$P_{dc} = r_h \left(1 - \frac{t_{start}}{t_c}\right) P_h + r_h \frac{t_{start}}{t_c} P_{start} \quad (4.10)$$

where r_h is the duty cycle of the message, t_{start} is the start up time and t_c is the pulse duration. P_{start} and P_h are respectively the average powers during and after the start-up time. These parameters can be deduced from the data given in [75]. We have $t_c = 100 \text{ ns}$, $P_{dc} = 518 \text{ } \mu\text{W}$ for $r_d = 1/2$ (OOK), $t_{start} = 70 \text{ ns}$, so using equation (4.10), we can deduce $P_h = 1.121 \text{ mW}$ and $P_{start} = 1.06 \text{ mW}$.

Using the general energy consumption model in chapter 3, the energy consumption per source bit for ME-coding based on the second transmitter can be derived as follows. For ME[n,k], $t_c = k/(nR_s)$ where R_s is the source bit rate, and $r_d = 1/2^k$. So from Equation (4.10), we get:

$$E_{tx} = \frac{(k - nt_{start}R_s)P_h + n \cdot t_{start}R_sP_{start}}{k \cdot 2^k R_s} \quad (4.11)$$

Besides, as the start up time should be smaller than the chip duration $t_{start} < t_c$, there is a maximum chip rate. In our case, the maximum chip rate can be evaluated to 10 Mbps when the start up time t_{start} is 70 ns .

For a target Bit Error Rate (BER) performance, the transmit power P_{tx} depends on the antenna gain (assumed to be 1 in our case), the channel condition, the transmission distance and the carrier frequency. It can be calculated by the link budget equation as given by equation (4.2) which is recalled here:

$$P_{tx} = PL(d)MRk_BTr_0 \quad (4.12)$$

where r_0 is the required signal to noise ratio per bit. The other parameters of Equation (4.12) are given in the Table 4.2.

Table 4.2: The transmit parameter of the transmitter

PARAMETER	VALUE
The path loss	$PL(d) = \left(\frac{4\pi d}{\lambda}\right)^2$
The carrier frequency	433MHz
The safety margin	$M_{dB} = 30dB$
Boltzman's Constant	$k_B = 1.38 \times 10^{-23} \text{ Joules}/K$
Temperature	$T = 300K$, (room temperature)
Noise bandwidth	$R(Hz)$

The average output power P_{tx} is linked to the maximum output power P_{out} by $P_{tx} = r_h P_{out}$.

4.3.2 Energy consumption improvement

According to the energy consumption model of the low cost OOK transmitter shown in last part, we could analysis the energy consumption per bit by using the realistic OOK transmitter.

From the Equation (4.10), the power consumption per bit as the function of chip rate can be plotted in the following Fig.4.14 with different duty cycles.

As mentioned before the energy consumption is 1.212 mW for continuous wave, and 0.56 mW for OOK in the frequency 433 MHz and low transmit bit rate. When the transmit bit rate increases, the power consumption will decrease as the power consumption of the constant part P_h 1.212 mW is larger than the average power consumption of the rise up period P_{start} 1.06 mW. The power consumption influence of the bit rate is less and less as the duty cycle becomes small.

According to the energy consumption model of the Minimum Energy OOK transmitter shown in the previous part, we can analyze the total energy consumption per bit.

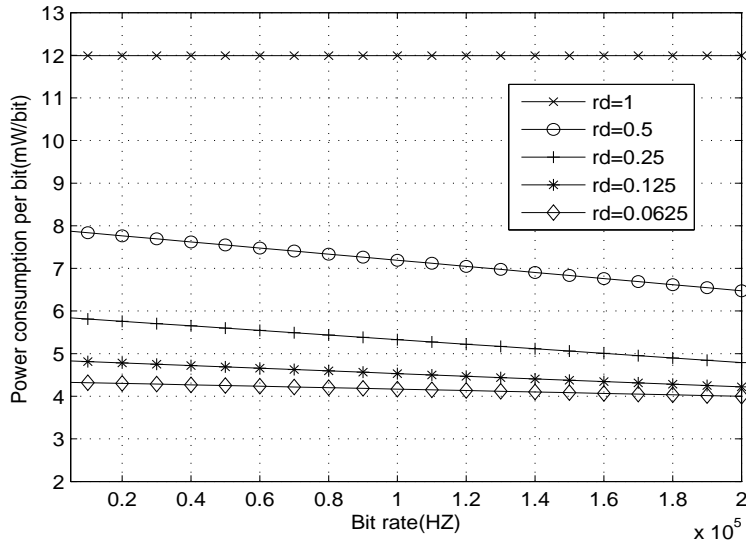


Figure 4.14: Total power consumption

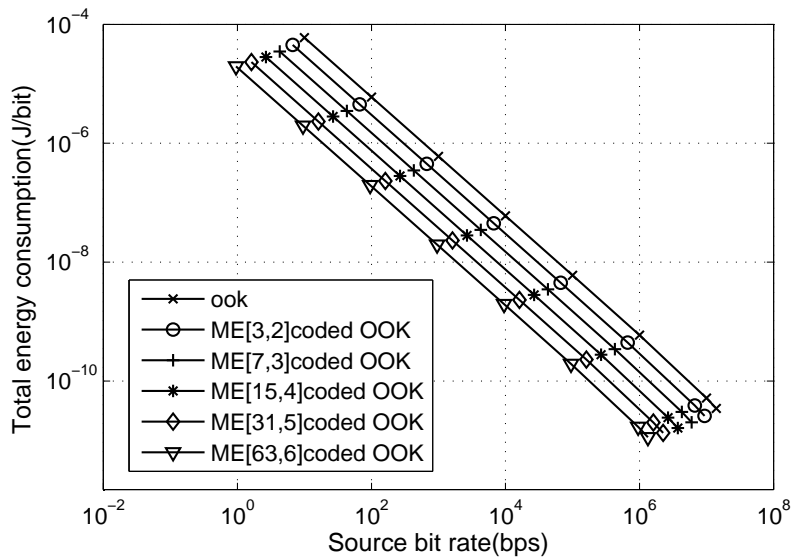


Figure 4.15: Total energy consumption per source bit

When the ME-coding scheme is used for this OOK transmitter (Equation (4.11)), the energy consumption per bit can be plotted in Fig. 4.15. Equation (4.11) is proved to be a monotonically decreasing function of the source bit rate R_s in Fig. 4.15. So increasing source bit rate can reduce the energy consumption per bit. For uncoded OOK, the energy consumption is near to a small value of 52 pJ/bit when the source bit rate is 10 MHz . More importantly, it is shown that ME-coding can be used to significantly reduce the energy per bit of this circuit. Furthermore, the improvement of energy consumption performance is more notable as k is larger.

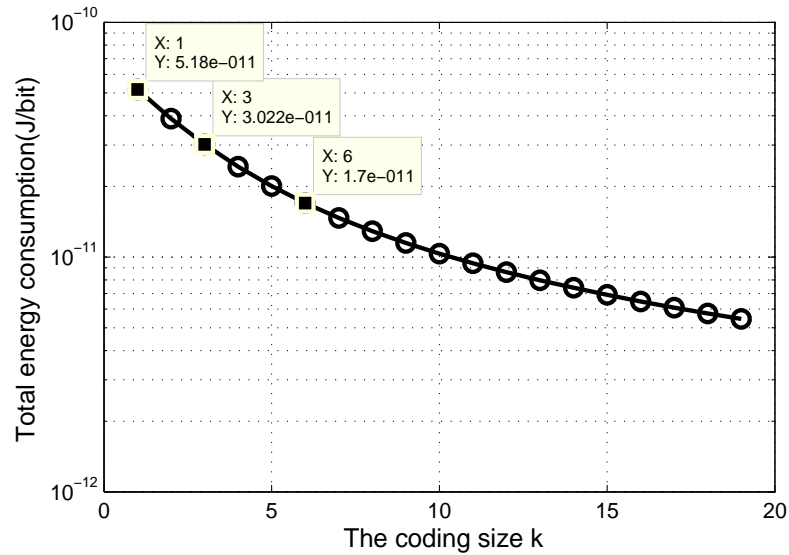


Figure 4.16: Total energy consumption as a function of k

We also analyze the choice of the coding size k for ME-coding as shown in Fig. 4.16, with the maximum chip rate of 10 Mbps . The total energy consumption is decreased when the coding size increases. So the optimal coding size k can be considered as large as possible. For instance, the energy consumption per source bit are 30 pJ/bit and 17 pJ/bit for a coding size $k = 3$ and $k = 6$ respectively, which is much smaller than the uncoded OOK ($k = 1$) 52 pJ/bit . However, the improvement is more important for $k < 10$ than for $k > 10$.

4.3.3 Optimization of the coding size

In a lot of applications, the area of transmission is limited and it can be interesting to optimize the circuit energy for a given transmit range. As the duty cycle is $r_d = 1/2^k$ for ME-coding size k , the transmit range can be deduced from Equation (4.12)

knowing that the output power is limited.

$$d = \frac{\lambda}{4\pi} \sqrt{\frac{P_{out}}{2^k M R k_B T_0 r_0}} \quad (4.13)$$

Because the output power of this circuit is fixed, increasing the coding size decreases not only the average transmitted energy per bit but also the range of the transmitter, according to Equation (4.11) and Equation (4.13). That means k should be as large as possible for more energy efficiency but as small as possible for large transmit range.

We assume an application where the range of the transmitter must be at least d_{min} and we want to find k that satisfies this constraint and minimizes the energy per bit consumed by the transmitter. This problem can be written as:

$$\text{Minimise } E_{tx}(k) \quad \text{s.t. } d \geq d_{min} \quad (4.14)$$

As the energy consumption and the transmission range are decreasing functions of the coding size k , the constraint is active. According to Equation (4.13), the solution of the optimization problem is to find k from the following equation:

$$2^k r_0(k) = \left(\frac{\lambda}{4\pi d_{min}} \right)^2 \frac{P_{out}}{M R k_B T_0} \quad (4.15)$$

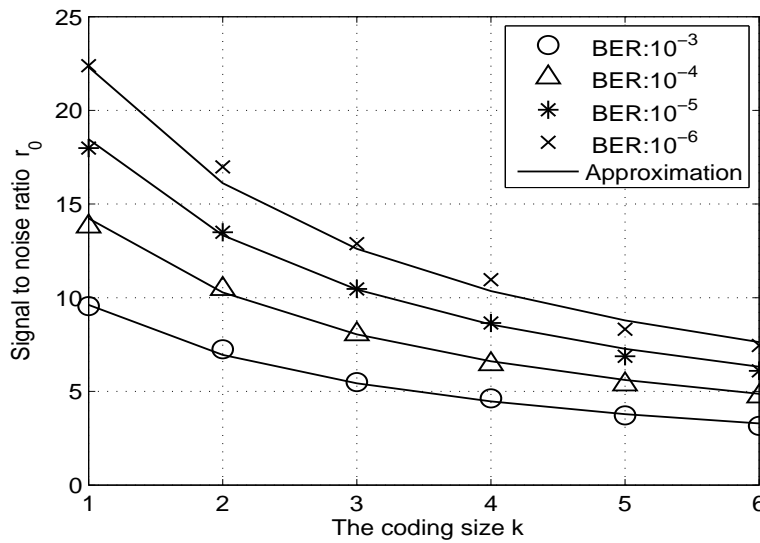


Figure 4.17: The signal to noise ratio r_0 versus coding size k

The bit Signal to Noise Ratio r_0 is a function of k . The chapter 2 [46] analyzes

BER performance of ME-coding OOK in detail. From our previous work [77], the true values of signal to noise ratio $SNR(dB)$ are recalled in Fig. 4.17 for different bit error rates. We propose to approximate these points by the following function:

$$r_0(k) = \frac{a}{k+b} \quad (4.16)$$

where a and b are given in Table 4.3 for different values of the BER. The approximation is also plotted in Fig. 4.17 through the true values. According to the approximation and equation (4.13), equation (4.15) can be written:

$$2^k \left(\frac{a}{k+b} \right) \leq \left(\frac{\lambda}{4\pi d_{min}} \right)^2 \frac{P_{out}}{MRk_B T_0} \quad (4.17)$$

which can be solved for k :

$$k \leq -\frac{1}{\ln 2} W_L \left(-\ln 2 a 2^{-b} \left(\frac{4\pi d_{min}}{\lambda} \right)^2 \frac{MRk_B T_0}{P_{out}} \right) - b \quad (4.18)$$

where $W_L(x)$ is the Lambert function (the demonstration is given in Appendix A).

Fig. 4.18 shows a comparison between the transmission ranges obtained by the true values of r_0 (mark points) and the approximations in Equation (4.16) (solid lines) respectively, for the given k . This figure indicates that the approximation gives correct results with the advantage of providing an analytic expression of the solution (Equation (4.18)).

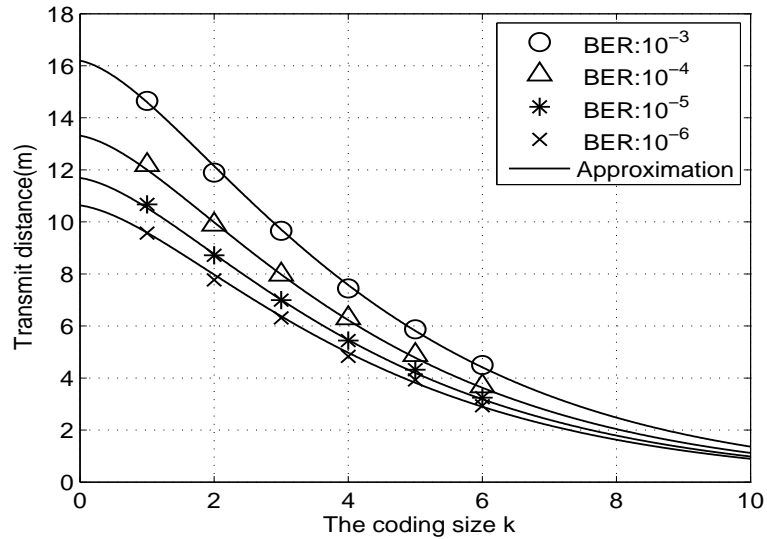


Figure 4.18: The transmit range versus coding size k

Table 4.3: The parameter of particular case

BER	a	b	$d_{min}(m)$	k_o	$E_{k_o}(pJ/bit)$	E_R
10^{-3}	25	1.6	3	7 (7.35)	14.68	0.28
			5	5 (5.60)	20.07	0.38
			10	2 (2.95)	38.85	0.75
10^{-4}	37	1.6	3	6 (6.67)	17.00	0.32
			5	4 (4.83)	24.28	0.46
			10	1 (1.99)	51.80	1.00
10^{-5}	48	1.6	3	6 (6.21)	17.00	0.32
			5	4 (4.34)	24.28	0.46
			10	1 (1.31)	51.80	1.00

For example in Table 4.3, assuming two given transmit distances d_{min} of 5 m and 10 m with $BER = 10^{-3}$, the coding size can be calculated by Equation (4.18), 5.6 and 2.95 respectively. Therefore the optimal coding sizes k_o could be figured out as 5 (ME[31,5]) and 2 (ME[3,2]). Besides, Table 4.3 also presents the energy consumption per bit E_{k_o} of the optimal coding size k_o and the energy reduction with respect to uncoded OOK: $E_R = E_{k_o}/E_1$. For small transmit ranges and large BER the coding size can be increased providing an important energy reduction.

4.3.4 Conclusion

This section studied the application of Minimum Energy coding to an efficient OOK circuit which completely switches off the transmitter during transmission of "0". For OOK, this circuit provides an energy efficiency of 52 pJ/bit and high data rate (10 Mbps). We define an energy model of the circuit and demonstrate that the energy per bit can be reduced to 30 pJ/bit using coding size $k = 3$. Moreover, the improvement will be more important as k increases.

Due to the fixed output power of the circuit, increasing the coding size reduces the transmit distance. A method is proposed to determine the optimal coding size for a given maximum range.

4.4 Receiver energy consumption

The MAX7033 is a fully integrated low-power CMOS superheterodyne receiver which is ideal for receiving amplitude shift-keyed (ASK) data in the 300MHz to 450MHz

frequency range. Therefore we can use it as a receiver in our circuit and combined with the OOK transmitter.

4.4.1 Energy consumption Model

When the supply voltage is $+3.3V$ and $f_{RF} = 433\text{ MHz}$, the supply current is $I_{DD} = 5.7mA$. For the same supply voltage, the shutdown supply current is $I_{SHDN} = 3.5\mu A$.

According to these data, when the supply voltage is $+3.3V$ and $f_{RF} = 433MHz$, the power consumption of the receiver is given below:

$$P_{RX_{DD}} = I_{DD} \times U = 3.3 \times 5.7 \times 10^{-3} = 18.81mW \quad (4.19)$$

So in this mode, the receiver power is constant and the total energy per bit is:

$$E_{RX} = P_{RX_{DD}} \times T_b \quad (4.20)$$

For the shutdown model,

$$P_{RX_{SHDN}} = I_{SHDN} \times U = 3.3 \times 3.5 \times 10^{-6} = 11.55\mu W \quad (4.21)$$

We propose to define a new scheme for the reception of ME-Coding OOK using the shutdown mode of the circuit.

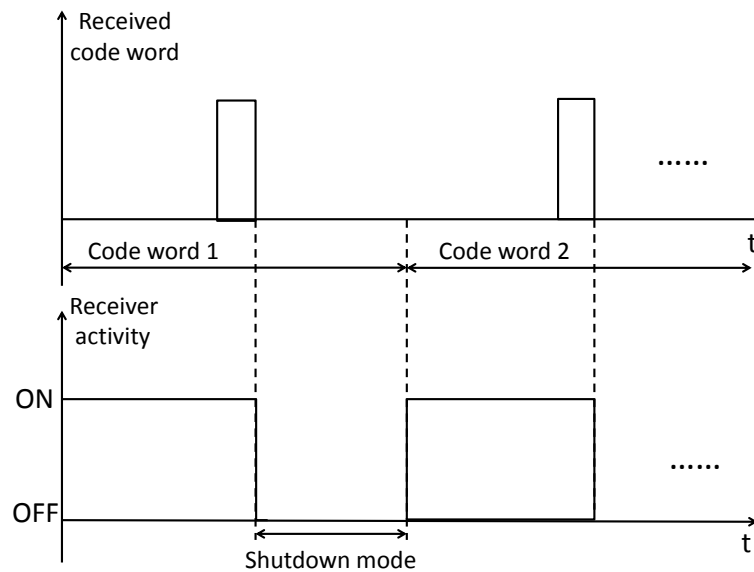


Figure 4.19: Activity of the receiver in shutdown mode

We know that the ME-Coding code-words have only one chip rate equal to 1. So when this chip is received, the receiver can switch in shutdown mode until the next code word (see figure 4.19). In that case the energy to power a code-word is function of the position of the chip one and given in table 4.4.

Table 4.4: Energy per codeword in shutdown mode

ME(n,k)	Energy of one codeword
00.....00	$P_{RX_{DD}} \times n \times T_c$
00.....01	$P_{RX_{DD}} \times n \times T_c$
00.....10	$P_{RX_{DD}} \times (n - 1) \times T_c + P_{RX_{SHDN}} \times T_c$
⋮	⋮
01.....00	$P_{RX_{DD}} \times 2 \times T_c + P_{RX_{SHDN}} \times (n - 2) \times T_c$
10.....00	$P_{RX_{DD}} \times T_c + P_{RX_{SHDN}} \times (n - 1) \times T_c$

The average energy of one codeword can be deduced as:

$$E_{RX_{codeword}} = \frac{1}{2^k} \times \left[2 \times n + \frac{(n \times (n - 1))}{2} \right] \times P_{RX_{DD}} + \frac{(n \times (n - 1))}{2 \times P_{RX_{SHDN}}} \times T_C \quad (4.22)$$

The average energy of one information bit is:

$$\begin{aligned} E_{RX_b} &= \frac{1}{(2^k \times k)} \times \left[2 \times n + \frac{(n \times (n - 1))}{2} \right] \times P_{RX_{DD}} + \frac{(n \times (n - 1))}{2} \times P_{RX_{SHDN}} \times T_C \\ &= \frac{1}{(2^{k+1})} \times [P_{RX_{DD}} \times (n + 3) + P_{RX_{SHDN}}] \times (n - 1) \times T_b \end{aligned} \quad (4.23)$$

Where T_C is the time per bit of coded message, $T_C = \frac{k}{n} \times T_b$, T_b is the time per bit of original message, $T_b = 1/R$ where R is the information bit rate.

4.4.2 Energy consumption of the receiver

According to the energy consumption model of the receiver shown in previous part, we could analyze the energy consumption per bit by using the realistic OOK receiver.

Fig. 4.20 and Fig. 4.21 give the numerical results of the energy consumption of the receiver in normal mode and shutdown mode, with the condition that the supply

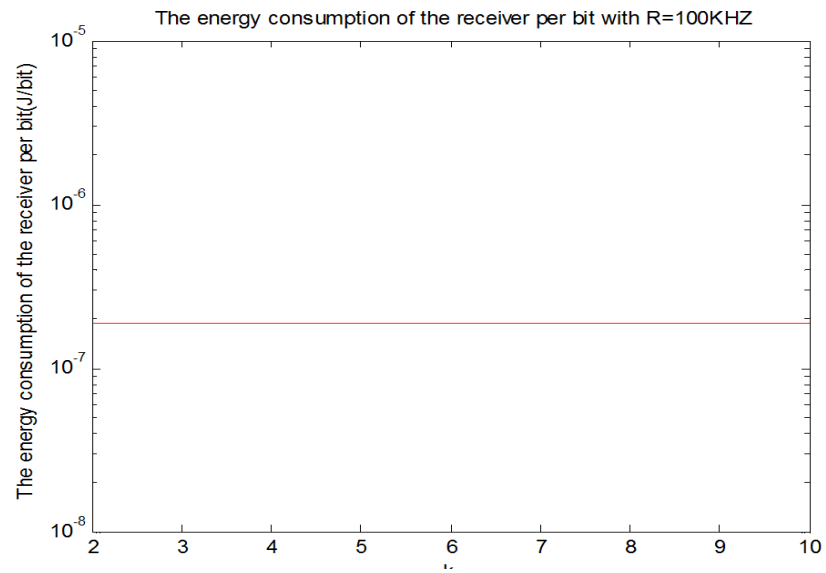


Figure 4.20: The energy consumption of the receiver in normal mode

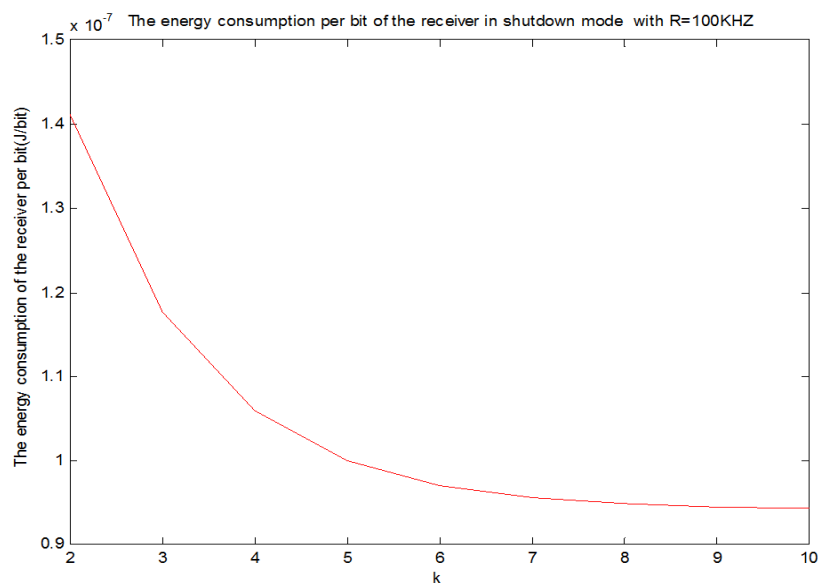


Figure 4.21: The energy consumption of the receiver in shutdown mode

voltage is $+3.3V$, source frequency is $433MHz$, and bit rate $R = 100kbit/s$. As the ME coding size k increased from 2 to 10, the energy consumption of receiver in Fig. 4.21 varied from $0.95 \times 10^{-7} J/bit$ to $1.4 \times 10^{-7} J/bit$ in shutdown mode which is just half of the normal mode $1.9 \times 10^{-7} J/bit$ in Fig. 4.20.

The following figures give the numerical results of the total energy consumption taking into account the transmitter part and the receiver part using the MAX1472 transmitter. With the condition that the bit error rate is 10^{-3} and the transmission distance is between 0m to 100m.

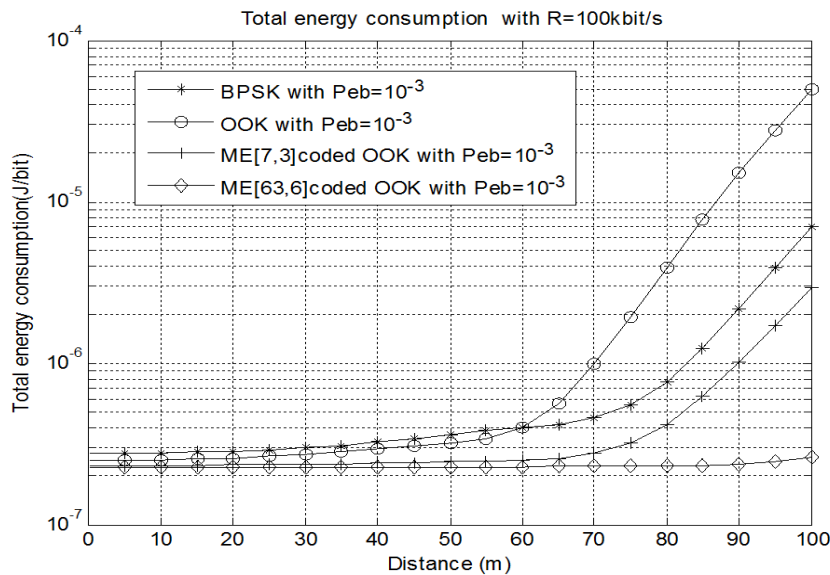


Figure 4.22: The energy consumption for $R = 100kbit/s$

Fig. 4.22 shows the total energy consumption of both the transmitter and the receiver in normal mode when the information bit rate is $100kbit/s$. The transmitter consumes most of the total energy, therefore the Fig. 4.22 has the same trend with as energy consumption of the transmitter.

Fig. 4.23 shows the total energy consumption from both the transmitter and the receiver in shutdown mode with on information bit rate equal to $100kbit/s$. Compared with the result in normal mode, the energy consumption decreased in different extent. For ME[7,3] and ME[63,6], the simulation result demonstrates the energy consumption is half of that in Fig. 4.22. But for uncoded OOK and BPSK, the shutdown mode works only in transmitter, so the variation is less than half.

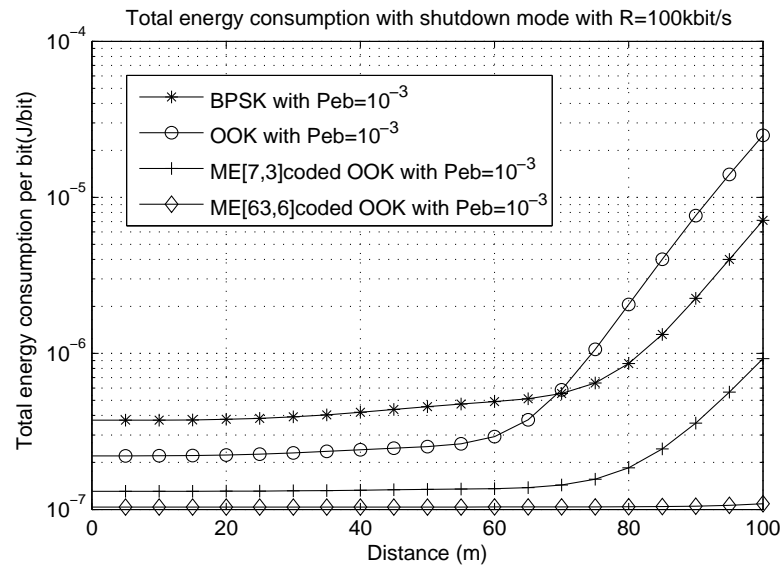


Figure 4.23: The energy consumption with shutdown mode for $R = 100kbit/s$

Fig. 4.24 shows the total energy consumption of both the transmitter and the receiver in shutdown mode with an information bit rate equal to $1kbit/s$. Fig. 4.25 shows the total energy consumption of both the transmitter and the receiver as a function of the symbol rate.

From Fig. 4.25, the energy consumption of the receiver decreases when symbol rate increases, and the energy consumption of the transmitter begins to increase and then decreases as the symbol rate is increasing due to the influence of the circuit energy consumption and the transmit energy consumption. Besides, it is possible to figure out the optimal transmit symbol rate to have the lowest total energy consumption, because the energy consumption of the receiver dominates in the total energy consumption when the symbol rate is smaller than the optimal value, while the energy consumption of the transmitter dominates in the total energy consumption when the symbol rate is larger than the optimal value.

4.5 Conclusion

This chapter focuses on the energy consumption analysis of ME-Coding based on the realistic energy models of several devices. ME-Coding using the classical sensor node energy model is worse than uncoded OOK. Devices adapted to ME-Coding are

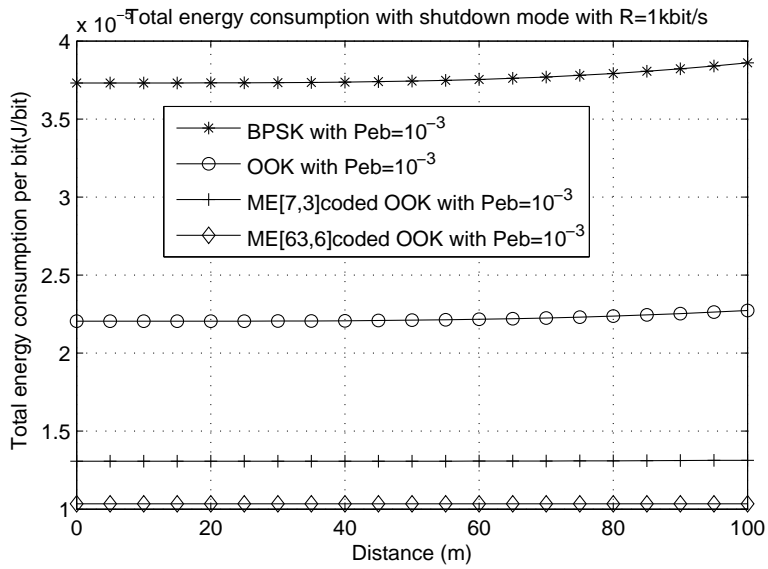


Figure 4.24: The energy consumption with shutdown mode for $R = 1kbit/s$

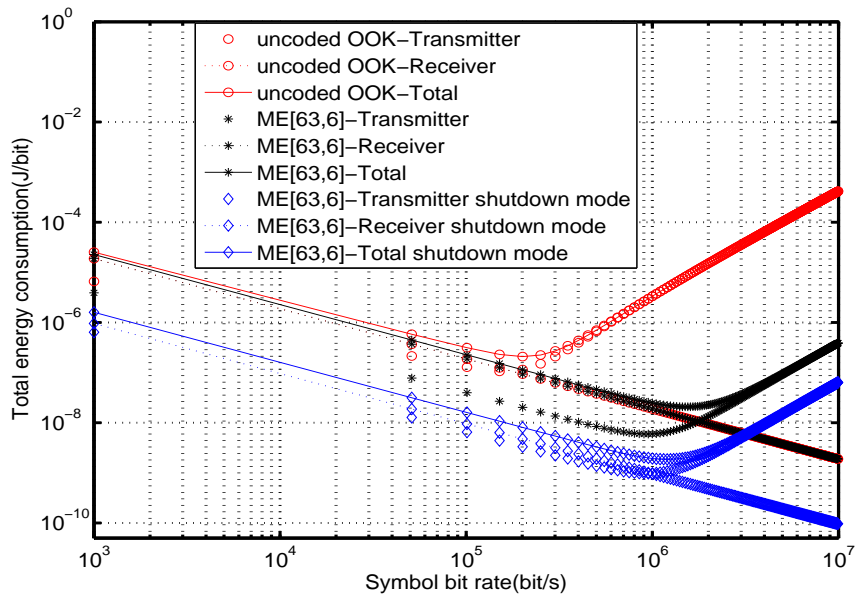


Figure 4.25: The total energy consumption VS the symbol rate

needed when considering both transmit energy and circuit energy. Two low complexity and low energy consumption transmitters are introduced. The first transmitter is also low cost for wide application and has the shutdown mode as well, but has a drawback in the limitation of maximum bit rate. So as to overcome the disadvantage and further reduce the energy consumption, the second transmitter is brought in with the energy consumption unit pJ/bit . Besides, the method of selecting the optimal coding size k is presented as well. The last section presents the energy consumption of a low cost receiver. The analysis of the energy consumption of the realistic transmitter and receiver proves the realization of energy efficiency of ME-Coding, even if the results could be improved by designing specific circuits for ME-Coding.

Error control schemes and Application

In chapter 4, we focus on the energy consumption analysis of ME-Coding based on the realistic energy models of several devices, and we consider a simple transmission between a transmitter and a receiver without considering error control. However, in wireless sensor networks, the information data are usually sensitive to transmission errors. Error control schemes, such as Error Control Codes (ECC) and Automatic Repeat reQuest (ARQ), could be utilized to provide reliable wireless communications. We present error control codes in chapter 2. They could provide better BER performance. However the error control schemes will introduce redundancy to the information data or lower bandwidth efficiency of the communication, these will cause extra energy consumption. When considering their implementation in wireless sensor networks, the energy efficiency should be investigated.

In this chapter, we consider the Basic ARQ error control protocol. It is assumed to be incorporated in SISO systems. In the protocol, a cyclic redundancy check sequence is used as error detection code to detect the transmission error on information data. To analyze the energy efficiency, we consider the total energy consumption using the energy consumption model described in chapter 3.

In the second part, we propose to increase the energy efficiency of an autonomous remote control and increasing the number of transmitted bits from a limited harvested energy. More importantly, we realize the real demonstrator to show that the proposed method can be implemented.

5.1 Error Control Protocols

Error control scheme that employs error control code and automatic repeat request is the typical way, which could be used at the data link layer, to provide reliable wireless communication with lower transmit power. As we discussed the error control code in chapter 2, we will introduce automatic repeat request and analyze the energy consumption performance in detail in this section.

5.1.1 Automatic repeat request Protocol

ARQ is an error control method for data transmission which makes use of acknowledgments and timeouts to achieve reliable data transmission. An acknowledgment is a message sent by the receiver to the transmitter to indicate that it has correctly received a data frame. Usually, when the transmitter does not receive the acknowledgment before the timeout occur or the acknowledge packet has indicated that there are errors in the preceding received packet; the transmitter will retransmit the frame. The retransmission will stop until the packet is either correctly received or the times of retransmission is beyond a predetermined maximum number of retransmissions.

Many different ARQ schemes have been proposed for packet retransmission. The simplest scheme is Wait-and-Go whereby the transmitter sends a packet and waits for its acknowledgment (ACK) before proceeding with the transmission of the next packet. A packet is retransmitted if its ACK is not received within a certain time-out interval which corresponds to the Round Trip Time (RTT).

More sophisticated is the Go-Back-N scheme, where the receiver keeps track of the sequence number of the next packet it expects to receive and sends that number with every ACK. If a packet from the transmitter does not reach the receiver, the receiver will stop acknowledging received frames. Once the transmitter has sent all of the packets in its window, it will detect that all of the packets since the first lost packet is outstanding. It will go back to sequence number of the last ACK it has received from the receiver and fill its window starting with that packet and continues the process

again.

Furthermore in a wireless link, advantage can be taken of the not sequential delivery. Retransmission begun as soon as a gap in the sequence of ACK packets is noticed. With such as Selective Acknowledgment (SACK), although a packet from the transmitter does not reach the receiver, the transmitter will continue to send subsequent packets until it has emptied its window, and the receiver will continue to fill its receiving window with the subsequent packets. The receiver keeps track of the sequence number of the earliest packet that it has not received and sends that number with every ACK it sends. Once the transmitter has sent all the frames in its window, it re-sends the packets number given by the ACKs, and then continues at the place where it left off.

The error control protocol that combines CRC and ARQ is specified in IEEE 802.16 standard at the MAC sublayer. In this protocol, the transmitter sends the packet with a request on the acknowledgment of successful reception. By checking the calculated checksum of CRC, the receiver sends an acknowledgment frame back to the transmitter if the packet is correctly received. Once this acknowledgment frame is received within the predefined duration, the transmission is considered successful and no further action regarding retransmission should be taken. On the other hand, if the packet is not correctly received, no acknowledgment frame will be sent back to the transmitter. Therefore, if an acknowledgment for the original transmission is not received within the acknowledgment waiting time and if the maximum retry times for the retransmission is not attained, original packet will be retransmitted again. Otherwise, the transmitter assumes that the transmission has failed.

To simplify, we assume that the CRC can detect all the transmission errors and allow infinite retries for the retransmission. Denoting the packet error probability to be P_{epkt} , the packet will be received intact during the first transmission with the probability of $(1 - P_{epkt})$. Otherwise, it will be received correctly after n times retransmissions with the probability of $P_{epkt}^n(1 - P_{epkt})$. Therefore, without the limits on retransmission tries, the mean times τ required for a successful reception is:

$$\begin{aligned}
 \tau &= (1 - P_{epkt}) + 2P_{epkt}(1 - P_{epkt}) + \dots + nP_{epkt}^n(1 - P_{epkt}) + \dots \\
 &= 1 + P_{epkt} + P_{epkt}^2 + P_{epkt}^3 + \dots + P_{epkt}^n + \dots \\
 &= \frac{1}{(1 - P_{epkt})}
 \end{aligned} \tag{5.1}$$

For short distance communications, AWGN channel among the nodes is practical

and SISO scheme is more appropriate. It is assumed that all errors in the packet could be detected at the receiver, although in practice, this may not be the case, particularly with only a checksum. However, because there is always a finite possibility of incorrect error detection, this assumption would make sense in most cases. We also assume that the event of unsuccessfully receive packet due to a damaged ACK is ignored, due to the fact that the length of the ACK packet is so small that it will not affect the performance estimation.

Suppose a packet with length of L bits is transmitted without coding, and thus the bit errors are independent, we will find the packet error probability to be:

$$P_{epkt} = 1 - (1 - P_e)^L \quad (5.2)$$

where P_e corresponds to the bit error probability.

The mean number of transmission required for successful reception is given by substituting this value of P_{epkt} into Equation 5.1 as follows:

$$\tau = \frac{1}{(1 - P_e)^L} \quad (5.3)$$

5.1.2 Energy consumption performance analysis

In this section, we investigate the ARQ schemes in AWGN channel. We propose a cross layer optimization strategy. Then we analyze the energy consumption performance based on the general energy consumption model in chapter 3.

In this section, we focus on minimizing the energy consumption of a node considering the transmitter and the receiver in Fig.5.1. So optimizing the transmit power to obtain the minimum transmit energy per information bit is our goal. We consider the following transmission model in Fig.5.2 with the following notations:

- L_{pkt} is the number of bits in the packet
- L_{start} is the preamble length of the packet
- t_{rx} is the maximum time for the reception of ACK (constant value)

In the simple considered scheme, the node sends a packet and wait during t_{rx} for the reception of acknowledgment.

If the ARQ is not good then a new transmission is realized. The transmitter is on during the transmission of the packet and the receiver is on during t_{rx} .

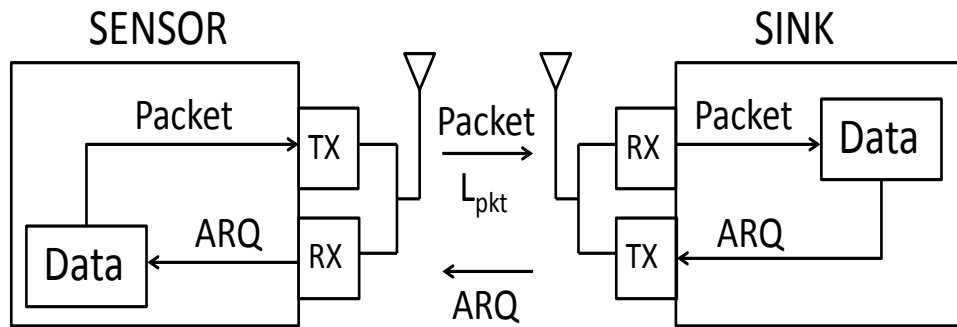


Figure 5.1: Transmission model

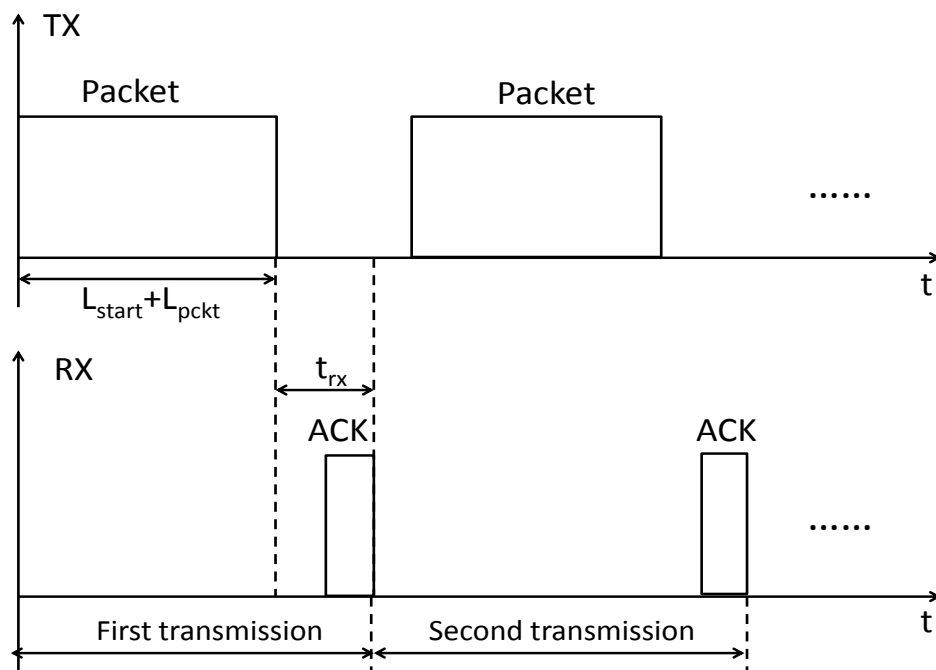


Figure 5.2: Illustration of the working of a simple ARQ protocol

Normally the communication units in the wireless sensor networks are not as complicated as the others, such as network cards in the PCs, and the messages which they monitor are more error-sensitive. So link level retransmission scheme should be used to achieve more reliability. Accordingly, the total energy needed per bit for successfully transmission will not be the same as the Equation (3.18) mentioned in chapter 3. It should also take the mean number of transmissions required for success into account.

Considering the basic ARQ protocol, the average time τ required for a successful reception can be determined by Equation (5.1). Then for an uncoded system, suppose a packet with length of L_{pkt} , then the total energy to transmit a packet with success can be derived from Equation (3.18), Equation (5.2) and Equation (5.3) to be:

$$E_{bpkt} = \tau \cdot \left\{ P_{starttx} t_{start} + \left(P_{0tx}(1 - r_h) + \left(P_{1tx} + \frac{P_{out}}{\eta} \right) r_h \right) \cdot L_{pkt} \cdot t_b \right. \\ \left. + P_{crx} t_{rx} \right\} \quad (5.4)$$

The energy to transmit a bit with success is:

$$E_{bT} = \frac{E_{bpkt}}{L_{pkt}} = \tau \cdot \left\{ \frac{P_{starttx} t_{start}}{L_{pkt}} + \frac{P_{0tx}(1 - r_h) + \left(P_{1tx} + \frac{P_{out}}{\eta} \right) r_h}{R} \right. \\ \left. + \frac{P_{crx} t_{rx}}{L_{pkt}} \right\} \quad (5.5)$$

For the numerical results, we assume $t_{rx} = 10$ $t_{start} = 10/R$

If the start time is neglected we obtain

$$E_{bT} = \tau \cdot \left\{ \frac{P_{0tx}(1 - r_h) + \left(P_{1tx} + \frac{P_{out}}{\eta} \right) r_h}{R} + \frac{P_{crx} t_{rx}}{L_{pkt}} \right\} \quad (5.6)$$

5.1.3 Numerical results

Firstly we focus on the average number of repetitions. We assume a coherent receiver and use the formulas for the bit error probability in AWGN channel which are given in chapter 2. For the channel we assume a free space path loss. In the link budget, we introduce a margin $F = 40dB$ including noise factor, other losses and receiver imperfections. The carrier frequency is 433 MHz. Using these assumptions, the E_b/N_o ratio can be expressed as:

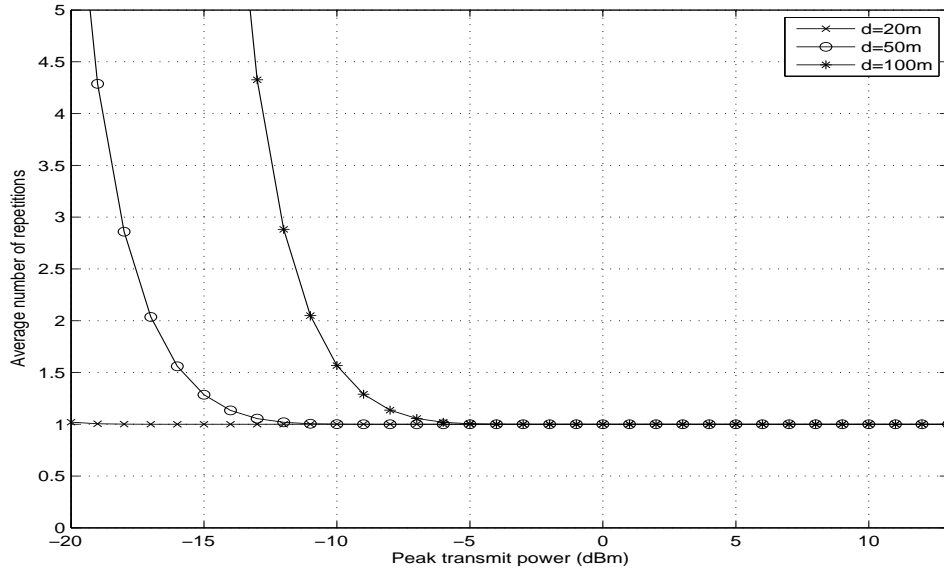


Figure 5.3: Average transmission times required for a successful reception as a function of the output power for sending a 1, using OOK

$$\frac{Eb}{No} = \frac{P_{out} r_h PL(d)}{R \times k_b \times T \times F} \quad (5.7)$$

where P_{out} is the output peak power (or output power to send a 1), $PL(d)$ is the path loss for a distance d , R is the bit rate, k_b is the Boltzmann constant, T is the temperature in Kelvin. For OOK $r_h = 1/2$ and for $ME(2^k - 1, k)$ $r_h = 1/2^k$.

The figure 5.3 provides the average number of repetitions using OOK modulation, a packet length L_{pkt} equal to 16 and for a bit rate $R = 100$ kbit/s. The results are given as a function of the peak output power, for different propagation distances. It can be shown that the average number of repetitions is equal to 1 for high output power and increases when the output power decreases. As expected, when the distance is increasing the output power must also be increased to maintain a low number of repetitions.

The figure 5.4 and 5.5 gives the same type of results using respectively $ME(7,3)$ and $ME(63,6)$. It can be shown that, to maintain an average number of repetitions equal to one, P_{out} must be increased. This result can be explained by the fact that even if the transmit energy can be reduced, the peak output power P_{out} must be increased to compensate the lower duty cycle obtained with minimum energy coding.

We can now investigate the total power consumption. The circuit model is the normal transmitter model given in chapter 3 whose parameters are recalled in the table 3.2. The power consumption of the receiver P_{crx} is also given in this table.

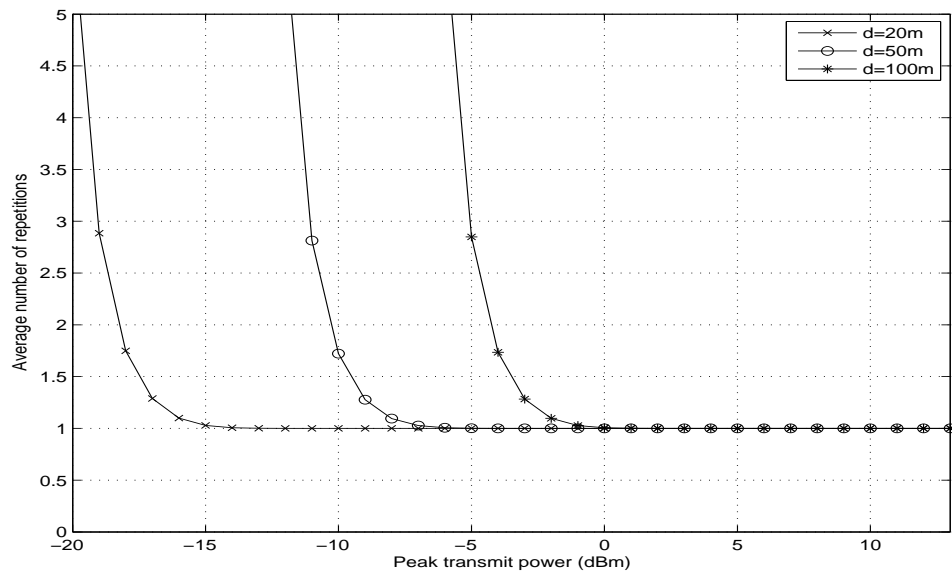


Figure 5.4: Average transmission times required for a successful reception as a function of the output power, using ME(7,3)

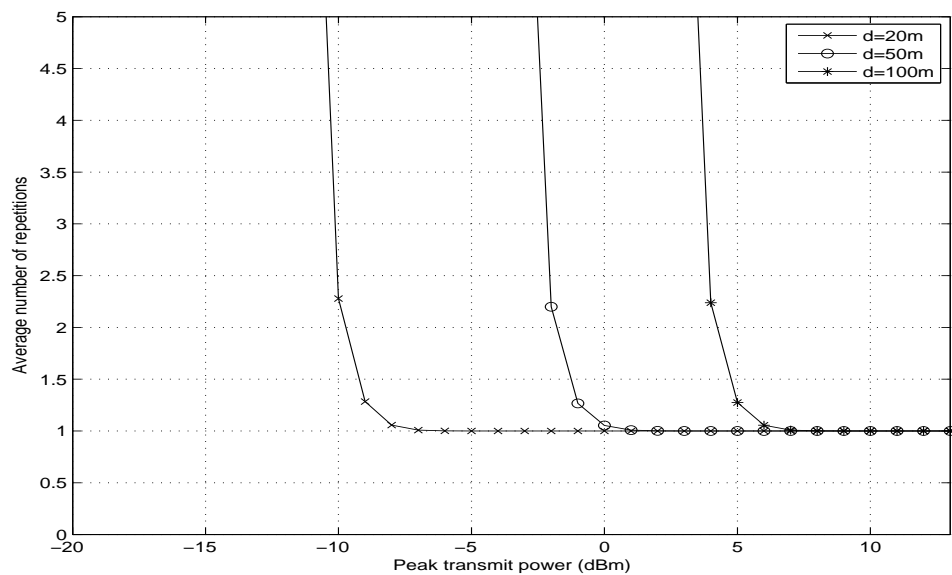


Figure 5.5: Average transmission times required for a successful reception as a function of the output power, using ME(63,6)

Table 5.1: The circuit parameters

Parameter	Value	Unit
P_{0tx}	4	mW
P_{1tx}	10.66	mW
η	0.75	-
P_{crx}	19	mW
t_{rx}	$10/R$	
R	100	kbit/s

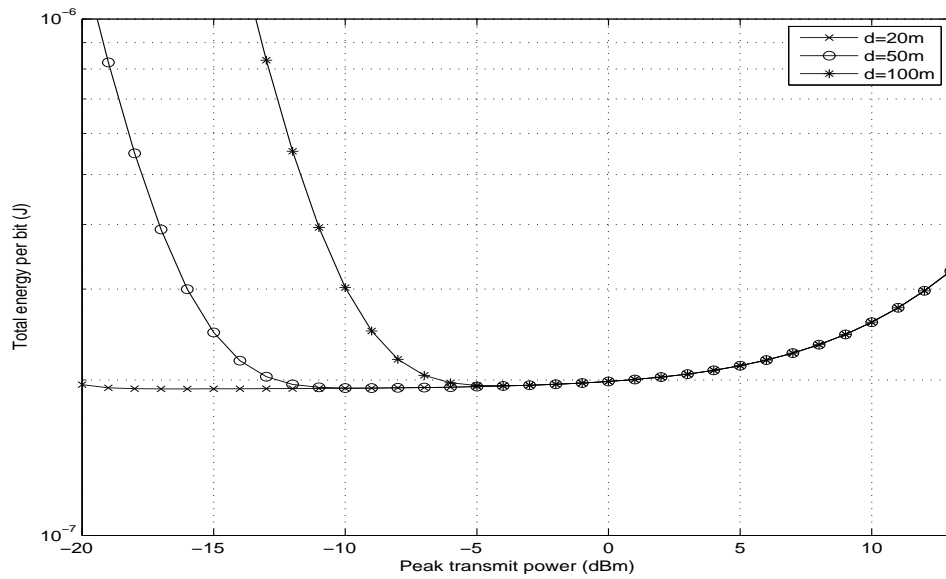


Figure 5.6: Average total energy per bit as a function of the output power, using OOK

The Figure 5.6 provides the average total energy per bit as a function of the output power for different propagation distances. It can be noticed that a minimum value can be observed. After this optimal value the energy increases due to the increase of the output power. Before this optimal value the energy increases also due to the average number of repetitions. When comparing these results to the previous figures, it can be noticed that the optimal value is obtained for the minimum peak output power allowing only an average of one transmission.

The figures 5.7 and 5.8 provide the total energy per bit for respectively ME(7,3) and ME(63,6). We can observe the same behavior with the difference that the increase in total energy after the minimum value is not so obvious. This is due to the fact that the effect of the peak output power on the circuit energy is a function of the duty cycle which is lower for ME coding.

Finally, it must be noticed that ME coding allows to reduce the total consumed

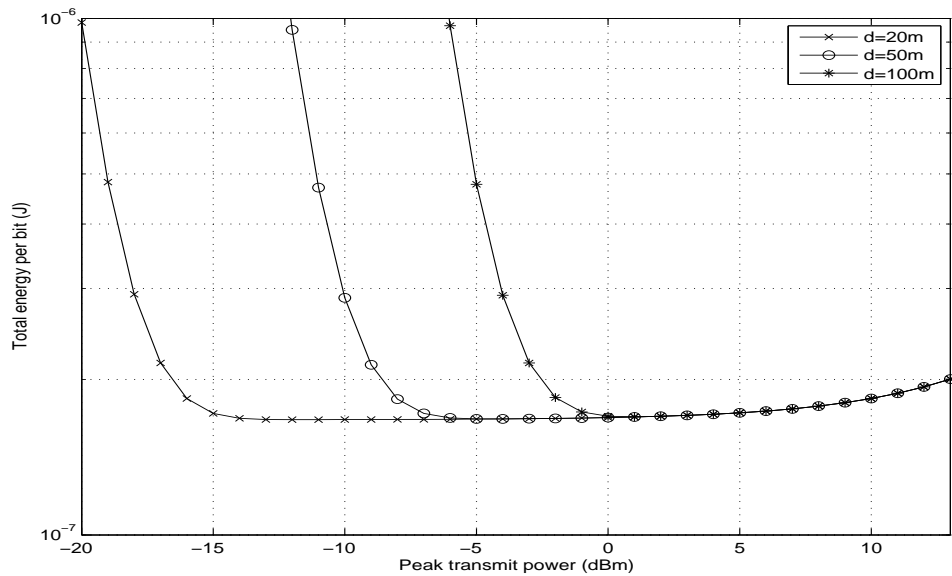


Figure 5.7: Average total energy per bit as a function of the output power, using ME(7,3)

energy.

5.1.4 Conclusion

In this section we have considered the energy efficiency of ME coding in the case of a simple automatic repeat request error control scheme. We considered the consumed energy of a node including the transmitter part for sending the packets and the receiver part for receiving the acknowledgments. We have shown that it is possible to find an optimum point for the total energy per bit and that ME coding provides an efficient solution in that context.

5.2 Self powered Energy Efficient OOK Transmitter

We propose to improve the energy efficiency of an autonomous remote control using OOK orthogonal modulation. We develop a power consumption model of an OOK transmitter and a micro-controller and show that we can increase the number of transmitted bits from a limited harvested energy. A real demonstrator has been realized and is presented at the end of this section.

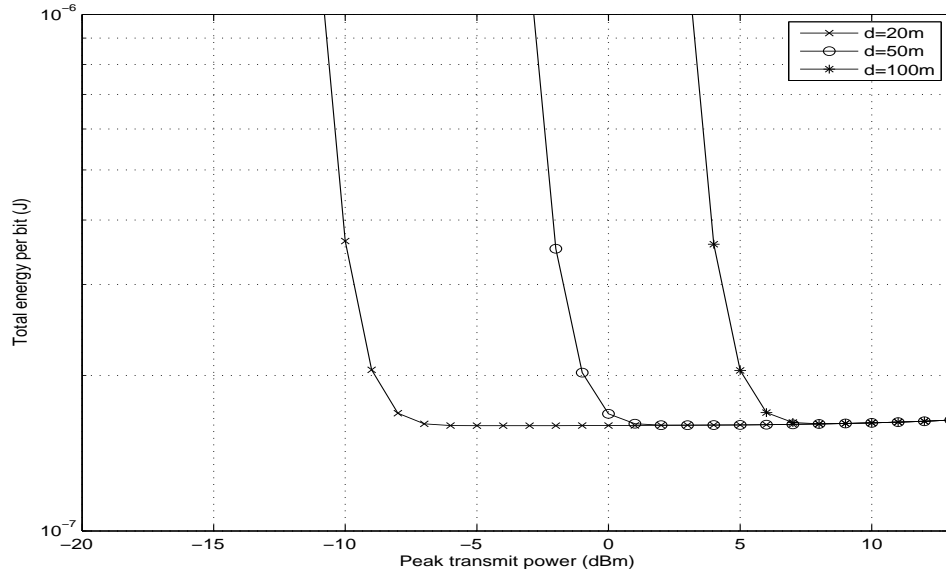


Figure 5.8: Average total energy per bit as a function of the output power, using ME(63,6)

5.2.1 Optimization of the autonomous transmitter

We focus on a device which has the functionality of a remote control. The user decides to send information by pushing a button. As shown in [78], the mechanical action of the user can be transformed in electrical energy using a piezoelectric element and triggers the transmission of information (i.e. identifier and/or data from a sensor). In [78] each action on the push button provides an energy of $68\mu J$ and using On Off Keying (OOK) modulation up to 36 bits can be transmitted. In our work we propose to increase the number of transmitted bits by using low duty cycle OOK modulation, in order to optimize the circuit power consumption. The figure 5.9 presents the block diagram of the autonomous transmitter. It is shown that, in this type of application, the circuit energy dominates the power consumption and that M orthogonal OOK modulations can dramatically decrease this power consumption.

Energy harvester

As proposed in [78] the energy harvester is composed of an ignition push button. The energy harvester is presented in figure 5.10. The equivalent model of the piezoelectric element is composed of a voltage source and a capacitor C_1 . When the button is pushed an AC voltage is generated by the source and must be rectified by a diode bridge. Then the energy is stored in the storage capacitor C_2 .

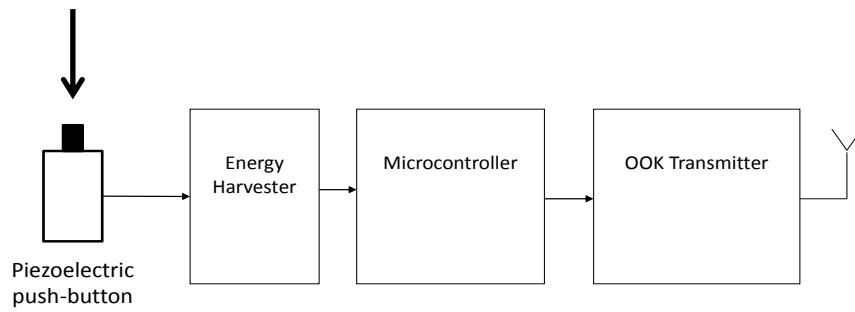


Figure 5.9: Block diagram of an autonomous transmitter

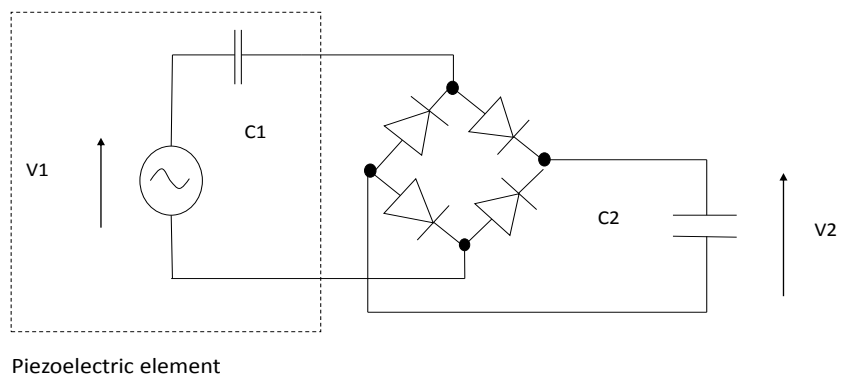


Figure 5.10: Block diagram of the piezoelectric harvester

The stored energy in the capacitor is:

$$E_{C_2} = \frac{1}{2}C_2V_2^2 \quad (5.8)$$

where V_2 is the voltage across C_2 .

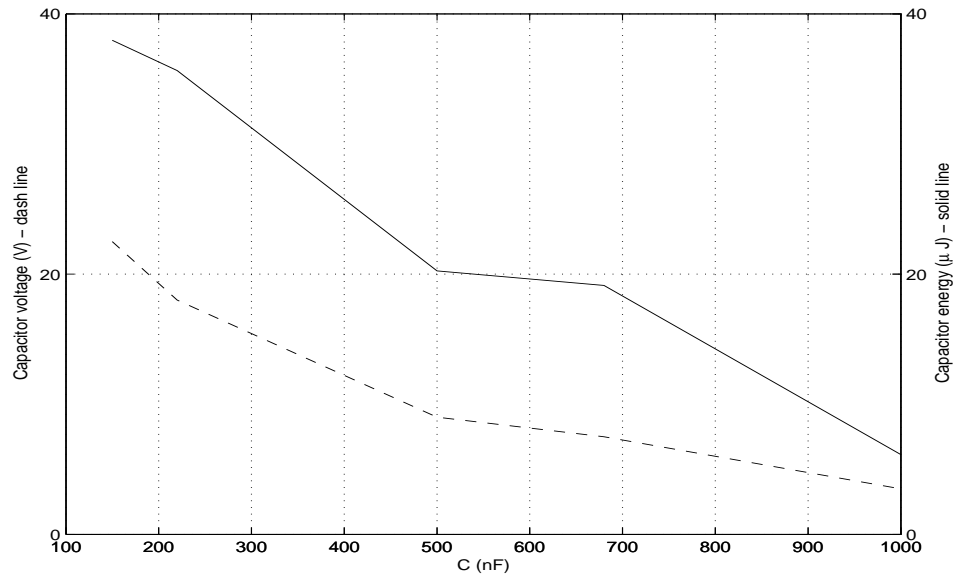


Figure 5.11: Capacitor voltage and stored energy

Figure 5.11 shows the measured capacity voltage and stored energy as the function of the capacity. Knowing that the voltage at the input of the regulator is limited to 20 V, measurements show that, each time the button is pressed, a maximum energy equal to about $38\mu J$ can be obtained. The storage capacity is connected to a voltage regulator (MAX666) in order to generate a DC output voltage to supply the other circuits. The efficiency of the voltage regulator is measured equal to 53%. So the available energy after the regulator is about $20\mu J$.

Circuit power consumption model

To determine the circuit power consumption model we must consider the micro-controller and the OOK transmitter.

The first device is a low power Microchip PIC12LF1501 8 bit micro-controller. The power consumption of this device is mainly a function of the supply voltage and the clock frequency. With the low energy internal oscillator at 31 kHz, the power consumption is given by Table 5.2. This frequency is low but is enough to implement the coding functions of the transmitter.

Table 5.2: *PIC12LF1501* power consumption as the function of the DC voltage using the low energy $31kHz$ internal oscillator

Dc Voltage (V)	Current μJ	Power μW
3.3	18.5	61
2.5	13	32.5
2	10	20
1.8	9	16.2

Table 5.3: RT40-433 power model parameters

P_{0tx}	0
P_{1tx}	0.71 mW
η	0.18

The transmitter is a RT40-433 SAW resonator Radio Transmitter Module from Telecontrolli, which is designed for low complexity applications as wireless security systems, remote gate controls and sensor reporting. We use this device in shutdown mode so that the binary frame to transmit is connected to the device supply voltage pin. So we can assume that no power is consumed during the transmission of a zero.

Using a model similar to the model proposed in chapter 3, the power consumption of the transmitter can be written:

$$P_{transmitter} = r_h \left(P_{1tx} + \frac{P_{out}}{\eta} \right) + (1 - r_h) P_{0tx} \quad (5.9)$$

where r_h is the duty cycle, P_{out} is the transmit power and P_{0tx} , P_{1tx} and η are parameters that can be determined using measurements. The value obtained for the RT40-433 circuit are given in Table 5.3.

The power consumption of the transmitter is much larger than the micro-controller. However the micro-controller must be taken into account especially for low duty cycle and low bit rate.

Total energy budget

We consider orthogonal modulations using OOK transmission, where the baseband symbol is defined by:

$$s_n(t) = 1_{[(n-1)\frac{T_s}{M}, n\frac{T_s}{M}]} \quad (5.10)$$

where M is the number of symbols. In that case the duty cycle is given by:

$$r_h = 1/M \quad (5.11)$$

where $M = 2^k$ and k is the number of bits per symbol.

The average power consumption is :

$$P_{CT} = \frac{1}{M} \times [P_{1tx} + \frac{P_{out}}{\eta} + (M - 1)P_{0tx}] \quad (5.12)$$

The transmit energy per bit is :

$$E_{Tb} = \frac{1}{k} (P_{out} \frac{T_s}{M}) \quad (5.13)$$

So P_{out} can be written as:

$$P_{out} = \frac{MkE_{Tb}}{T_s} = \frac{ME_{Tb}}{T_b} \quad (5.14)$$

and the total bit energy is:

$$E_{btot} = P_{CT}T_b = \frac{1}{M} (P_{1tx} + (M - 1)P_{0tx})T_b + \frac{E_{Tb}}{\eta} \quad (5.15)$$

To determine the required value of E_{Tb} , we consider the following path loss model:

$$PL(d) = \frac{g}{d^\alpha} \quad (5.16)$$

where d is the distance, g is the path loss at 1 meter, α is a coefficient which depends on the environment. Assuming a transmitting and receive antenna gain equal to one and free space attenuation, we have:

$$g = \left(\frac{\lambda}{4\pi}\right)^2 \quad (5.17)$$

where λ is the wavelength and $\alpha = 2$.

From the expressions given in chapter 2, we can deduce the SNR $r(M) = \frac{E_b}{N_0}$ to obtain a target bit error rate with M orthogonal modulations. Assuming that the power spectral density of the receiver noise is given by :

$$k_B \times T \times F \quad (5.18)$$

where k_B is the Boltzmann constant, T is the temperature in Kelvin and F is the margin

Table 5.4: Required $r(M)$ in dB for M orthogonal modulations

M	2 (OOK)	4	8	16	32	64	128	256
BER= 10^{-3}	9.8	7.3	6.1	5.3	4.7	4.3	3.9	3.7
BER= 10^{-6}	13.6	10.8	9.3	8.2	7.5	6.9	6.4	6.0

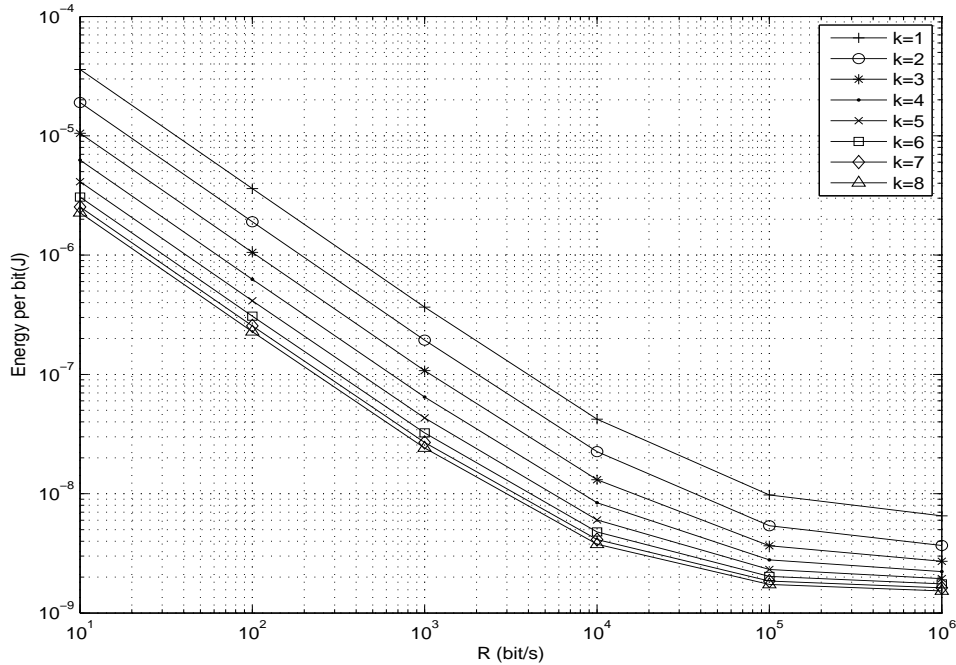
of the receiver, as defined previously. The transmit bit energy is :

$$E_{Tb} = \frac{r(M) \times k_b \times T \times F}{PL(d)} \quad (5.19)$$

Adding the transmit energy to the circuit energy, we get:

$$E_{btot} = \frac{T_b}{M} (P_{1tx} + (M - 1)P_{0tx}) + \frac{r(M) \times k_b \times T \times F}{\eta \times PL(d)} \quad (5.20)$$

The first part is proportional to T_b and can be minimized by increasing the bit rate and increasing M . The second part does not depend on the bit rate but depends on the order of the modulation. The required $r(M)$ is given in the table 5.4.

Figure 5.12: Energy per bit versus bit rate for different values of k , BER= 10^{-3}

The total energy per bit is given in figure 5.12 as a function of the bit rate for BER= 10^{-3} . The parameter P_{0tx} of the model is taken equal to the micro-controller

power. The other parameters are $T = 300K$, $F = 40dB$, $d = 100m$. From these curves, we can see that the total energy per bit decreases when the bit rate increases. The circuit energy is dominant until $R_b = 1Mbit/s$, and the influence of the transmit energy is negligible. After this bit rate, the saturation is due to the transmit energy.

The use of high order modulations allows decreasing dramatically the circuit energy.

These results show the behavior of the model but does not take into account the limitations of the specific circuit in terms of bit rate and transmit power.

The figure 5.13 shows the maximum transmit power P_{out} as a function of M and bit rate. As expected, we can see that the maximum transmit power must be increased for large values of M and bit rate. For our specific circuit the maximum output power is limited to 3.5 dBm and the bit rate to 9.6 kbit/s. However these curves show trends that can be used for the choice or design of a more efficient circuit.

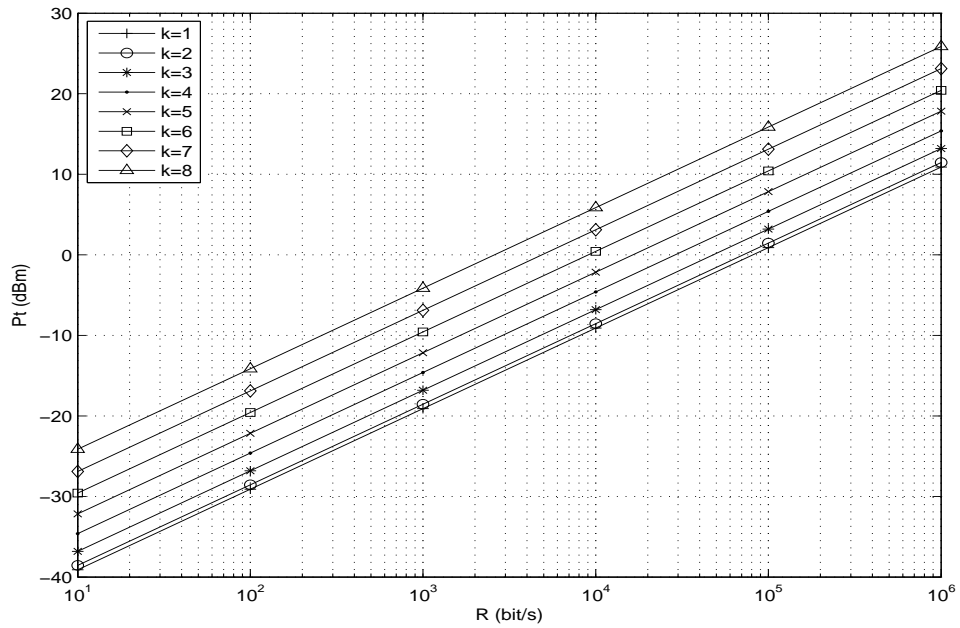


Figure 5.13: Maximum transmit power as a function of the bit rate for different values of k , $BER=10^{-3}$

How many bits can we transmit for a given harvested energy?

The total energy to transmit K bits is:

$$E_{btot} = K \times \left(\frac{T_b}{M} (P_{1tx} + (M-1)P_{0tx}) + \frac{r(M) \times k_b \times T \times F}{\eta \times PL(d)} \right) \quad (5.21)$$

So for a given harvested energy the number of bits that can be transmitted is:

$$K = \frac{E_{btot}}{\frac{T_b}{M}(P_{1tx} + (M-1)P_{0tx}) + \frac{r(M) \times k_b \times T \times F}{\eta \times PL(d)}} \quad (5.22)$$

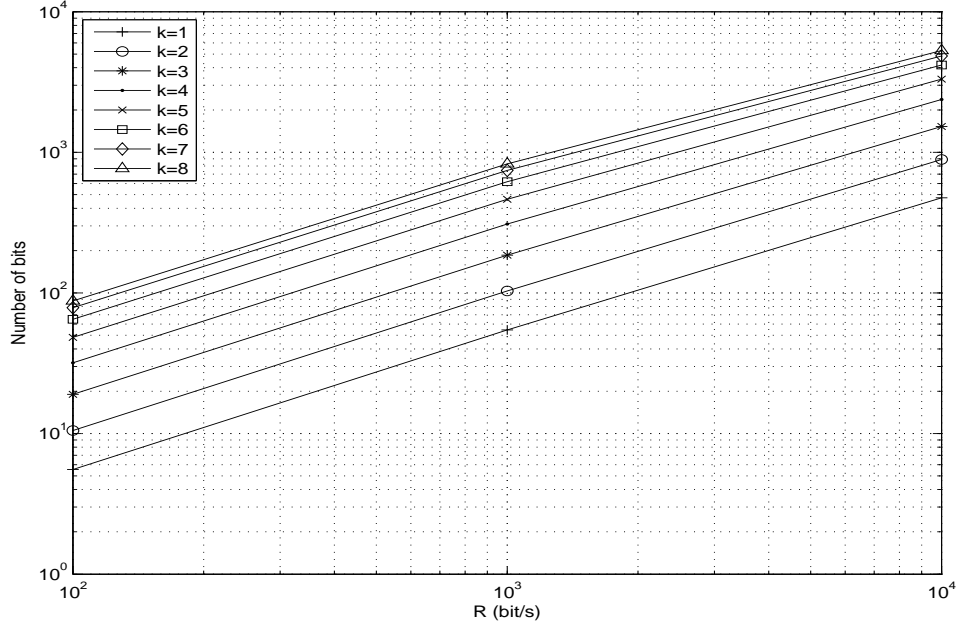


Figure 5.14: Number of bits versus bit rate for different values of k , $BER=10^{-3}$

This value is plotted in figure 5.14 with $E_{btot} = 20\mu J$. It can be shown that increasing the modulation order (M) and the bit rate allows to increase the number of transmitted bits. For example, from OOK to orthogonal modulation with $k = 5$ the number of transmitted bits can be multiplied by 10.

Chip rate constraint

From the previous results, it is shown that the bit rate must be maximized to minimize the energy per bit. But real circuits have limitation in modulation rate. The objective of this paragraph is to optimize the energy per bit with a chip rate constraint.

For a given bit rate, the chip rate is increased when number of bit per symbol k is increased:

$$T_b = \frac{T_s}{k} = \frac{M \times T_c}{k} \quad (5.23)$$

So:

$$T_c = \frac{k \times T_b}{2^k} \quad (5.24)$$

The maximum modulation rate of the RT40-433 transmitter circuit is 9600Hz . Taking the minimum chip duration of the device $T_{cmax} = 1/9600\text{s}$, the total energy per bit can be written for $k > 1$

$$E_{btot} = \frac{T_{cmax}}{k} (P_{1tx} + (2^k - 1)P_{0tx}) + \frac{r(M) \times k_b \times T \times F}{\eta \times PL(d)} \quad (5.25)$$

and for OOK

$$E_{btot} = \frac{T_{cmax}}{2} (P_{1tx} + P_{0tx}) + \frac{r(M) \times k_b \times T \times F}{\eta \times PL(d)} \quad (5.26)$$

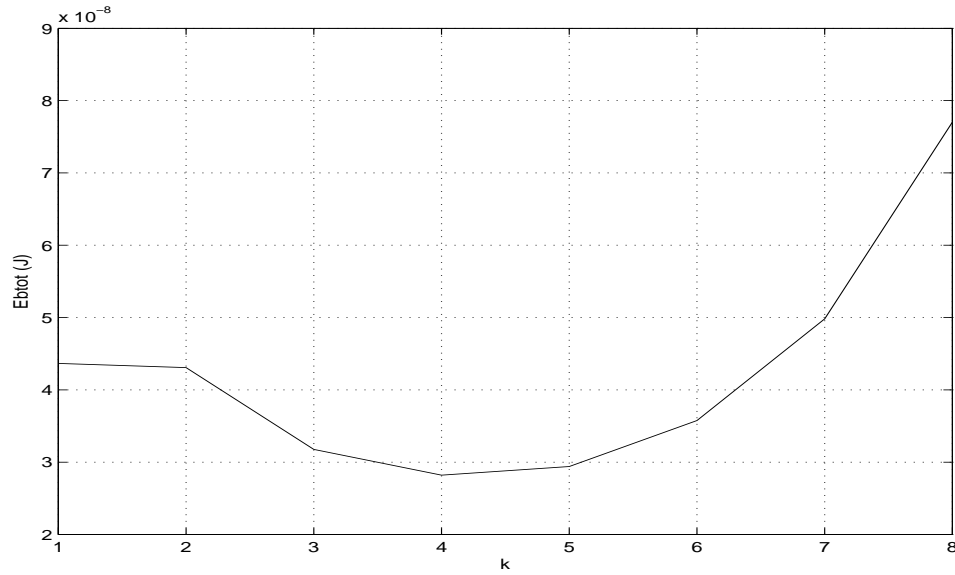


Figure 5.15: Total energy per bit versus k for a fixed chip rate equal to 9600 kHz , $k = 1$ is OOK, $k > 1$ is 2^k orthogonal modulation

The figure 5.15 shows the total energy per bit as a function of k for a fixed chip rate. An optimal value $k = 4$ can be obtained. For lower value of k , when k increases, the total energy per bit is decreased but for larger values of k , the bit rate must be decreased, due to the chip rate constraint and the energy is increased.

Experimental demonstrator

The demonstrator is composed of a self powered energy efficient OOK transmitter (figure 5.16) as described in the previous subsection and a receiver associated to a led

lamp (figure 5.17).

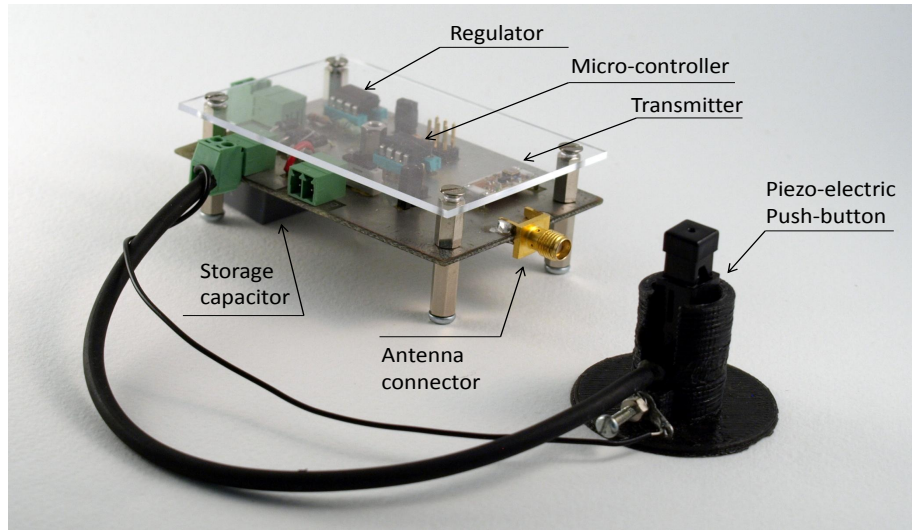


Figure 5.16: Piezo-electric transmitter

Each time the piezoelectric button is pushed, the $20 \mu J$ energy is used to send an identifier using orthogonal OOK modulation. A start impulse is also generated to be used as a time reference by the receiver (figure 5.18).

The receiver is based on an OOK receiver associated to a micro-controller (AT-Tiny85) programmed using the Arduino software. The microcontroller makes measurements of the pulse positions (using the reference pulse) and realizes the symbol to bit decoding. If the identifier is correct, the led lamp is switched on or off.

This type of device can be used in a large range of application with the advantage that no battery is needed.

5.3 Summary

In this chapter, we consider the energy efficiency of the error control protocol in wireless sensor networks. We have shown that ME-Coding can be used to improve the energy efficiency of a simple ARQ protocol.

Then, we propose to improve the energy efficiency of an autonomous remote control using OOK orthogonal modulation. We develop a power consumption model of an OOK transmitter and a micro-controller and show that we can increase the number of

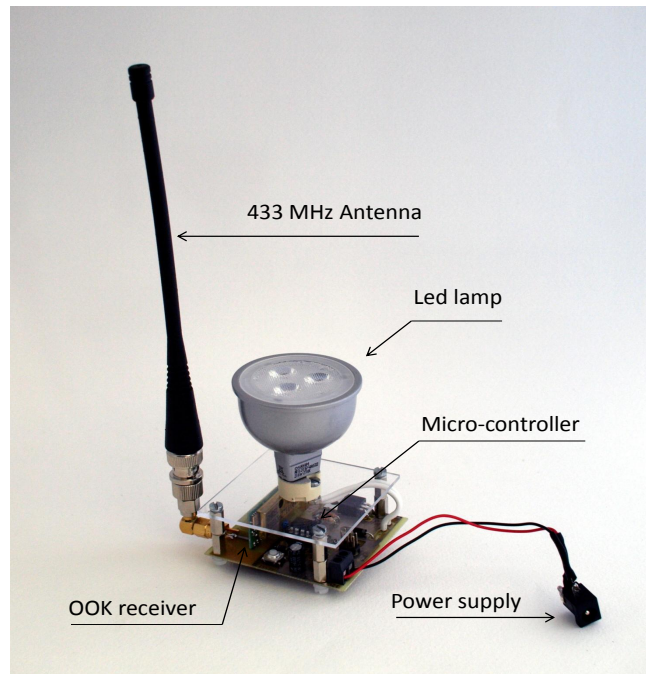


Figure 5.17: Led lamp receiver

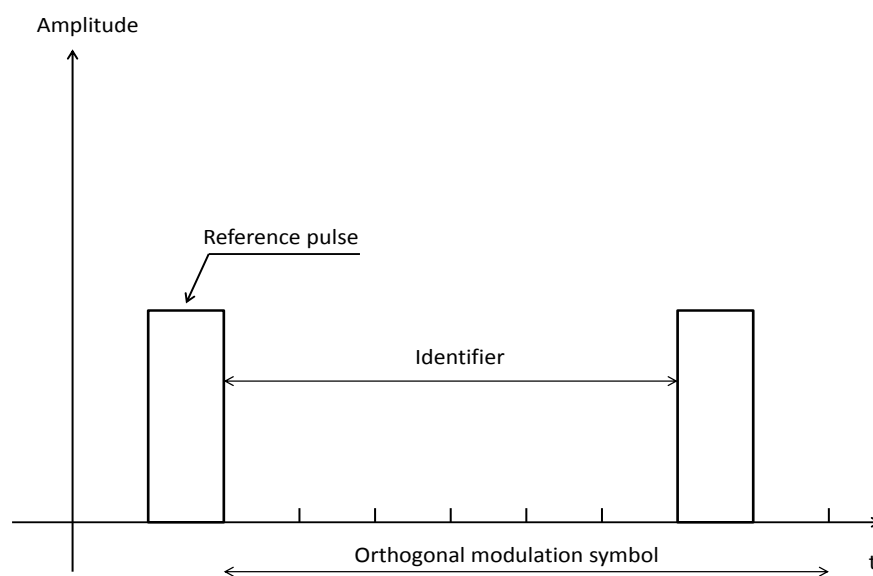


Figure 5.18: Waveform received after OOK demodulation. The identifier is the time position of the second pulse.

transmitted bits from a limited harvested energy. Finally, a real demonstrator has been realized.



6

Conclusion and future works

6.1 Conclusion

The aim of this thesis was to explore energy efficient transmission methods. We focused on the energy efficiency and low complex implementation of source coding method (ME-Coding), based on realistic energy consumption models of devices matched with these modulations.

Firstly, many energy efficient transmission techniques were discussed and the fundamental Shannon trade-off between energy and spectrum efficiency was also recalled. Using a simplified circuit model, we showed that taking into account the circuit energy can largely change this trade-off. Then we focused on the transmit energy and introduced some modulation schemes: On-Off Keying modulation and orthogonal modulation. Besides, we presented the Minimum Energy Coding which is the main subject of our study. In radio transmission, a large part of the transmitted energy is lost in the propagation channel. The characteristics of the channel has a large influence on the performance of a link. We recalled the definition of the Additive White Gaussian Noise channel and Rayleigh fading channel. For these different channels, we gave the theoretical bit error probabilities of OOK, BPSK and ME-coding OOK. The theoretical results were compared to simulations. According to these results, we have shown that in AWGN channel, ME-coding based on OOK modulation can be interesting (better

results than BPSK) in terms of bit energy for large code length, hence at the price of lower bandwidth efficiency. However, this effect is not obtained for a Rayleigh channel. These results were obtained considering only the transmit energy.

As classical studies consider only the transmit power or the transmit bit energy (or the SNR E_b/N_0) to compare the transmission techniques, we have seen that taking into account the circuit energy can largely change the conclusions on the energy efficiency of a transmission scheme. For this type of study, it is necessary to use a circuit energy model. Different models exist in the literature. We firstly considered a classical model which is frequently used for wireless sensor networks. The architecture of a typical wireless sensor node was presented to investigate the energy consumption of different components. However this commonly used model is not matched to OOK modulation. As the total energy consumption of ME-Coding using the classical energy model is worse than uncoded OOK, the devices adapted to ME-Coding are needed when considering both transmit energy and circuit energy. So we proposed new models using the characteristics of realistic circuits, based on the energy consumption analysis of the sensor node. Then, we presented a new energy consumption model which includes the energy consumption during switch time between low bit and high bit. Besides, we gave the using condition of this model and proposed a new approach based on the circuit shutdown mode. These generic models can be used to analyze the energy efficiency of Minimum Energy Coding, with different circuits.

As the data rate is usually low, spectral efficiency is traded off for power efficiency so that simple modulation schemes, such as OOK and FSK, can be used. We focused on minimizing the total energy consumption of wireless sensor networks by using low energy coding scheme. In order to improve the energy efficiency performance, we considered Minimum Energy coding based on On-Off Keying (OOK). So we could use this coding scheme to improve the error performance of OOK modulation. Because we want to discuss the realistic energy consumption of the communication subsystem, we introduced several radio devices of wireless transmission node which are adjusted to use ME-coding OOK modulation. Then, we analyzed the power efficiency of ME-coding OOK using the proposed realistic energy consumption models based on two efficient OOK transmitters and one receiver. Two low complexity and low energy consumption transmitters were introduced. The first transmitter is also low cost for a wide range of applications and has the shutdown mode as well, but with an important limitation on the maximum bit rate. So as to overcome the disadvantage and further reduce

the energy consumption, the second transmitter is brought in with energy consumption in the pJ/bit domain. Besides, the method of selecting the optimal coding size k was presented as well. At last, the work is completed with the energy consumption of a low cost receiver. The analysis of the energy consumption of a realistic transmitter and receiver prove the energy efficiency of ME-Coding.

Finally we proposed more complex applications of the proposed energy transmission techniques. Firstly, we investigated a basic ARQ error control protocol which can be used in wireless sensor applications to improve the reliability of the transmission. We analyzed this protocol and, using the developed power consumption models, we showed that ME coding can be an interesting option in that context. The second application is a practical simple communicating device supplied by limited energy harvesting, for which a real demonstrator was developed. We presented a power model of this device, including the micro-controller and the transmitter and showed that low duty cycle modulation (orthogonal modulations) can largely reduce the power consumption and increase the number of information bits that can be transmitted with a small amount of energy.

6.2 Future works

At this point of the work, we can mention different ideas for further research.

More investigation on low duty cycle modulations

We have shown the interest of low duty cycle modulation (ME coding and orthogonal modulations) in term of transmit energy and mainly in circuit energy. More investigation can be done on channel coding associated to these modulations in order to find the trade-off between the complexity increase and the consumed energy. If now we consider a multiple access channel, it can be interesting to evaluate the contribution of these modulations to the reduction of the multi-user interference. Indeed, using these modulations, the activity of one user on the channel is less so we can expect a reduction of its contribution to the interference. This work has already been proposed in the case of CDMA but this subject can be addressed more deeply for different access methods or multiple access control protocols. Finally, there are lot of similarities between low duty cycle modulation and ultra wide band modulations. This aspect must

be more investigated.

MAC layer consideration

Energy efficient communication require the coordination among the involved sensor nodes. Medium Access Control (MAC) synchronizes the channel access in an environment where numerous nodes access a shared communication medium. The MAC layer has a major role in making the network more power-efficient. A large amount of energy can be saved at this layer. Therefore, an efficient MAC layer protocol is interesting to be explored for the application of the proposed transmission methods.

Hardware implementation

A number of research works have theoretically proven the advantages of ME-Coding scheme and we have shown results of energy efficiency analysis using energy models derived the realistic radio devices. We have used circuits which are available for OOK modulations but not specifically designed for ME coding. We have shown the limitations of these devices, especially in the shutdown mode, for the bit rate and peak power. From our study, we can propose specifications for new efficient circuits matched to ME-coding. Using these circuits new prototypes could be developed for applications in a wide range of domains, from smart home to safety, health-care etc...



Index of value definition

Value	Definition
E_b	Energy per bit
k	Number of source bits/Coding size
n	Number of chips
P_e	Error rate
P_{eb}	Bit error rate
γ_s	Symbol SNR
γ_b	Bit SNR
E_s	Symbol energy
E_b	Bit energy
P_{eS}	Error probability of high chip
P_{eM}	Error probability of low chip
E_{start}	Start up energy
E_{tx}	Energy consumption of transmitter
E_{rx}	Energy consumption of receiver

Value	Definition
t_{start}	Start up time
t_{tx}	Time duration of transmitter
t_{rx}	Time duration of receiver
P_{out}	Output power
P_c	Circuit power
r_d	Duty cycle
r_s	Ratio of switch time on total time
r_h	Ratio of high chip duration on total time
N_s	Switch number
d	Distance
K	Number of information bit



B

Optimization of the coding size

In mathematics, the Lambert W function [79, 80, 81], also called the omega function or product logarithm, is a set of functions, namely the branches of the inverse relation of the function $f(z) = ze^z$ where e^z is the exponential function and z is any complex number. In other words

$$z = f^{-1}(ze^z) = W(ze^z) \quad (\text{B.1})$$

By substituting $z = W(z)$ in the above equation, we get the defining equation for the W function (and for the W relation in general:

$$z = W(z)e^{W(z)} \quad (\text{B.2})$$

for any complex number z .

Diagram of the real branches of the Lambert W function is shown in Fig.B.1.

Many equations involving exponentials can be solved using the W function. The general strategy is to move all instances of the unknown to one side of the equation and make it look like $Y = Xe^X$ at which point the W function provides the value of the variable in X .

In other words :

$$Y = Xe^X \iff X = W_L(Y) \quad (\text{B.3})$$

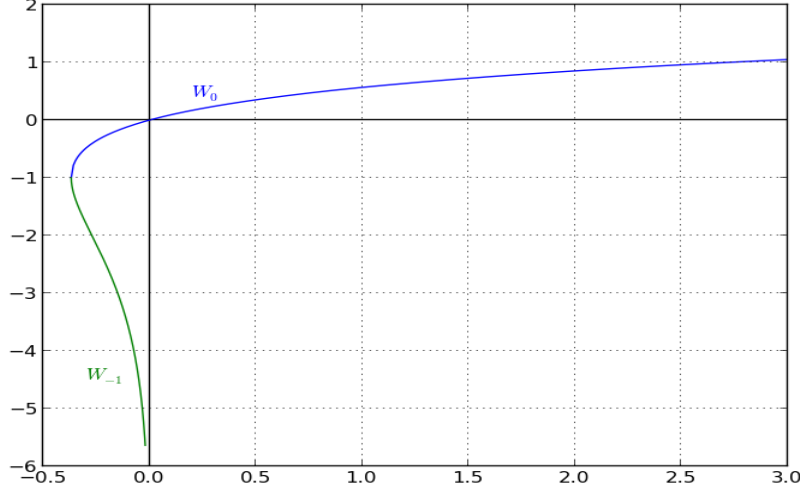


Figure B.1: Diagram of the real branches of the Lambert W function

Generally, for the equation

$$p^{mx+n} = cx + d \quad (\text{B.4})$$

where $p > 0$ and $c, a \neq 0$

can be transformed via the substitution

$$-t = mx + \frac{md}{c} \quad (\text{B.5})$$

into

$$tp^t = R = -\frac{m}{c} p^{n - \frac{md}{c}} \quad (\text{B.6})$$

giving

$$t = \frac{W_L(R \ln p)}{\ln p} \quad (\text{B.7})$$

which yields the final solution

$$x = -\frac{W_L\left(-\frac{m \ln p}{c} p^{n - \frac{md}{c}}\right)}{m \ln p} - \frac{d}{c} \quad (\text{B.8})$$

So from Equation (4.17) in section 4.4 as follow

$$2^k \left(\frac{a}{k+b}\right) \leq \left(\frac{\lambda}{4\pi d_{min}}\right)^2 \frac{P_{out}}{MRk_B T_0} \quad (\text{B.9})$$

can be rewritten as

$$2^k \leq \frac{N}{a} (k + b) = \frac{N}{a} k + \frac{Nb}{a} \quad (\text{B.10})$$

where $N = \left(\frac{\lambda}{4\pi d_{min}}\right)^2 \frac{P_{out}}{MRk_B T_0}$

Let $p = 2, m = 1, n = 0, c = \frac{N}{a}, d = \frac{Nb}{a}$.

Equation (B.9) can be solved for k :

$$k \leq -\frac{1}{\ln 2} W_L\left(-\ln 2 a 2^{-b} \left(\frac{4\pi d_{min}}{\lambda}\right)^2 \frac{MRk_B T_0}{P_{out}}\right) - b \quad (\text{B.11})$$

where $W_L(x)$ is the Lambert function.



Résumé étendu (French extended abstract)

Introduction

Les progrès technologiques ont permis le développement d'applications de capteurs sans fil. Les capteurs densément distribués, généralement utilisés pour la collecte des données, la surveillance environnementale, l'automatisation industrielle ou la sécurité, impliquent le plus souvent de faibles débits de données et de faibles portées de transmission. Malgré les avancées technologiques logicielles et matérielles, l'efficacité énergétique demeure une contrainte importante pour la conception des réseaux de capteurs sans fil. Pour ces applications, les nœuds sont généralement déployés avec des ressources énergétiques réduites et le remplacement d'une batterie peut s'avérer coûteux. Plusieurs méthodes peuvent être utilisées pour minimiser la consommation d'énergie dans les réseaux de capteurs sans fil. Dans cette thèse, nous nous concentrons sur la couche physique et sur la réduction de la consommation d'énergie des méthodes de transmission en utilisant des modulations à faible énergie et faible rapport cyclique. Cette solution pour améliorer l'efficacité énergétique d'un nœud se fait au détriment de l'efficacité spectrale.

Efficacité énergétique des méthodes de transmission

Dans un premier temps, nous nous intéressons à l'efficacité énergétique des méthodes de transmission. Shannon a montré qu'il existe un compromis entre l'efficacité énergétique et l'efficacité spectrale pour des communications fiables. En effet, considérant uniquement l'énergie transmise, la réduction de l'énergie par bit est obtenue au détriment de l'efficacité spectrale. Parmi les différentes modulations, la modulation BPSK (Binary Phase Shift Keying) est préférée pour les applications nécessitant de faibles débits de données et ayant des contraintes énergétiques, de part sa simplicité et son efficacité énergétique. Une modulation simple comme l'OOK (On-Off Keying) ne semble pas intéressante à cause de ses mauvaises performances en termes de taux d'erreur. Cependant, le codage à minimum d'énergie (codage ME) permet de réduire la consommation lorsqu'il est employé avec une modulation OOK. Le principe est de coder les bits sources (0 ou 1) par des mots de code comportant le moins possible de 1.

Le codage ME propose de réduire la consommation en générant des mots de code possédant au maximum un 1. La distance entre ces mots ne permet donc pas de détecter ou de corriger systématiquement des erreurs. Mais, en utilisant une détection sur l'ensemble du code en réception, il est possible d'obtenir certaines corrections d'erreurs. Cette correction reste cependant limitée et il est possible de combiner le codage ME avec un schéma de correction d'erreurs comme un codage convolutif ou un codage par bloc. Malheureusement, l'utilisation supplémentaire d'un code correcteur d'erreurs ajoute de la complexité dans les circuits, augmente la longueur des mots de code et ajoute des 1 dans les mots émis, ce qui va à l'encontre de la réduction de consommation recherchée.

A l'aide de résultats théoriques, confortés par des simulations, nous montrons que, dans le cas d'un canal BBAG (Bruit Blanc Additif Gaussien), le codage ME permet d'améliorer les performances obtenues pour une modulation OOK. Pour un taux de codage suffisamment grand, le codage ME donne de meilleurs résultats en termes d'énergie par bit que la modulation BPSK, au prix, cependant, d'une plus faible efficacité spectrale. Ces résultats ne se retrouvent pas dans le cas d'un canal de Rayleigh.

Modèles de consommation énergétique

Les résultats précédents sont obtenus en considérant seulement l'énergie émise. L'énergie consommée par les circuits électroniques n'est pas prise en compte, ce qui ne nous permet pas d'obtenir des conclusions quant à la consommation du capteur

(nœud). Nous introduisons donc des modèles de consommation énergétique. En se basant sur l'architecture d'un capteur typique, nous présentons un modèle de consommation énergétique général pour un capteur fonctionnant en mode émission/réception et un modèle de consommation énergétique pour un lien de communication comportant un émetteur et un récepteur. Malheureusement, les modèles de consommation classiques ne sont pas adaptés à la modulation OOK et les résultats de simulation obtenus ne mettent pas en évidence l'efficacité du codage ME.

Nous proposons donc un modèle de consommation énergétique pour lequel la consommation des circuits lors de l'émission d'un 0 est plus faible que lors de l'émission d'un 1. Pour être plus précis dans ce modèle, nous considérons en plus l'énergie consommée lors de la transition d'un état bas à un état haut et réciproquement. Le rapport cyclique est également introduit dans ce modèle, ce qui permettra facilement de passer de la modulation OOK au codage ME pour n'importe quel taux de codage. Ce modèle est validé par comparaison avec circuit réel : l'émetteur OOK MAX1472. La puissance consommée par l'émetteur est similaire à celle obtenue par notre modèle quelque soit la puissance d'émission et quelque soit le rapport cyclique du signal émis. Les résultats montrent également que l'énergie consommée lors de la transition d'un état vers un autre est négligeable et peut donc être ignorée.

Pour rendre le codage ME encore plus performant, un modèle de consommation énergétique "shutdown" est proposé. Ce modèle consiste à éteindre (mettre en veille) les circuits électroniques lors de l'émission d'un 0 et de les réalimenter pour l'émission d'un 1. Pour ce modèle, outre l'énergie consommée lors des transitions et le rapport cyclique, le temps de réveil des circuits électroniques est également pris en compte. Toujours en considérant l'émetteur OOK MAX1472, nous remarquons que bien que la puissance consommée soit réduite lors de l'utilisation du mode "shutdown", le temps de réveil des circuits est un facteur limitant quant au débit des données à transmettre.

Analyse de l'efficacité énergétique pour le codage à minimum d'énergie

Une fois le modèle de consommation énergétique posé et validé, nous pouvons analyser l'efficacité énergétique du codage ME pour de véritables circuits adaptés à la modulation OOK. Pour ce faire, nous considérons un émetteur OOK à faible complexité qui est le circuit MAX1472 et un récepteur associé le MAX7033 ainsi qu'un émetteur OOK très faible puissance qui a l'avantage d'être plus performant en consommation d'énergie et d'autoriser des débits plus élevés.

Le circuit MAX1472 est un émetteur OOK fonctionnant dans la bande de fréquence

allant de 300 MHz à 450 MHz et supportant des débits allant jusqu'à 100 kbit/s. Sa puissance de sortie maximale est de +10 dBm. Il est composé principalement d'un amplificateur de puissance et d'un synthétiseur de fréquences. À l'aide des modèles validés dans le chapitre précédent, nous établissons un modèle pour une émission OOK simple et un modèle pour le mode d'émission "shutdown". Les résultats obtenus pour une émission OOK simple montrent que lorsque nous considérons uniquement l'énergie émise, le codage ME est plus performant que la modulation OOK. À partir d'un certain taux de codage, ses performances deviennent meilleures que celles obtenues pour la modulation BPSK. Lorsque la consommation d'énergie totale est considérée, le codage ME est également plus performant que la modulation OOK et l'énergie consommée par bit décroît au fur et à mesure que le taux de codage diminue. Cependant, la limitation de puissance d'émission du circuit impose un taux de codage limite pour une distance d'émission donnée. Pour le mode d'émission "shutdown", le codage ME est encore plus performant mais est limité à de plus faibles débits à cause du temps de réveil des composants électroniques (220 μ s). Finalement, en prenant en compte l'énergie des circuits, un débit optimal peut être déterminé.

Pour passer outre la limitation de débit du circuit et le temps de réveil assez conséquent, nous nous sommes intéressés à un second émetteur OOK très faible puissance. Il fonctionne à la fréquence de 433 MHz pour un débit allant jusqu'à 10 Mbit/s et une puissance de sortie équivalente à -12,7 dBm. Il permet d'atteindre une efficacité énergétique de 52 pJ/bit en modulation OOK. Le temps de réveil avoisinant les 70 ns, ce circuit permet d'atteindre des débits plus élevés en mode "shutdown". Une fois le modèle de consommation énergétique établi, l'efficacité du codage ME est démontrée. Plus le taux de codage est faible, plus l'efficacité énergétique est grande et plus la distance de transmission est réduite puisque le circuit fonctionne à puissance d'émission fixe. Pour une distance de transmission donnée et une qualité de service fixée, il est possible de déduire un taux de codage optimal permettant de minimiser l'énergie par bit consommée.

Le dernier circuit étudié est le récepteur MAX7033 fonctionnant dans la bande de fréquence allant de 300 MHz à 450 MHz. Il peut être associé à un émetteur OOK. Tout comme précédemment, nous pouvons trouver un modèle pour une réception OOK simple et un modèle pour un mode de réception "shutdown". Dans ce dernier cas, les circuits électroniques sont éteints (mis en veille) dès la réception d'un 1. La réception en mode "shutdown" permet d'économiser près de la moitié de la consommation énergétique du récepteur. Si nous examinons la consommation globale de l'ensemble du lien de communication (émetteur plus récepteur) pour un débit de 100 kbit/s, nous re-

marquons que l'énergie consommée par le récepteur est très faible et que les résultats sont similaires à ceux obtenus pour l'émetteur seul. Une étude de la consommation énergétique totale de l'ensemble (émetteur plus récepteur) en fonction du débit montre qu'il est possible de déterminer un débit optimal minimisant l'énergie consommée totale. Pour un débit plus petit que cette valeur optimale, la consommation du récepteur est dominante alors que pour un débit plus grand, c'est la consommation de l'émetteur qui domine.

Protocoles de contrôle d'erreurs et application

Le codage ME permet de réduire la consommation énergétique. Le combiner avec un protocole de contrôle d'erreurs permet d'améliorer les performances en termes de taux d'erreurs au détriment d'une surconsommation énergétique due à la redondance d'information introduite. Dans certains cas de figure, cela pourrait être avantageux. Nous proposons donc d'étudier l'intégration d'une méthode simple : le protocole ARQ (Automatic Repeat reQuest). La combinaison du CRC (Cyclic Redundancy Check) et de l'ARQ est spécifiée dans le standard IEEE 802.16. Par soucis de simplification, nous considérons que le CRC peut détecter toutes les erreurs de transmission et que le nombre de retransmission n'est pas limité. Un modèle de consommation énergétique se basant sur ces hypothèses est présenté. Nous observons que pour le modèle de consommation considéré, le nombre moyen optimal de répétitions est égal à 1. Bien que la puissance crête soit plus importante dans le cas du codage ME que dans le cas de la modulation OOK, l'énergie totale moyenne par bit nécessaire reste inférieure. Le codage ME reste donc une solution efficace dans ce contexte.

Pour montrer que la méthode proposée peut être implémentée dans un environnement réel, la dernière partie de la thèse présente un émetteur OOK efficace en énergie autoalimenté. Cet émetteur est une télécommande basée sur un élément piézoélectrique. Après avoir établi le modèle de consommation de l'émetteur accompagné du microcontrôleur, l'énergie totale par bit est évaluée dans le cas d'une modulation OOK orthogonale. Cette énergie décroît lorsque le débit augmente et lorsque l'ordre de la modulation orthogonale augmente, ce qui permet d'accroître le nombre de bits pouvant être transmis pour une énergie disponible donnée. Finalement, un démonstrateur expérimental réalisé au sein du laboratoire est présenté.

Conclusion et perspectives

Dans cette thèse, nous nous sommes concentrés sur la couche physique et sur la réduction de la consommation d'énergie des méthodes d'émission en utilisant des modulations à faible énergie. Une première étude a permis de déduire que pour un canal BBAG, le codage à minimum d'énergie basé sur la modulation OOK est efficace énergétiquement, mais au prix d'une efficacité spectrale réduite. Seule la puissance de transmission a été considérée et la consommation des circuits électroniques n'a pas été prise en compte. Ensuite, des modèles de consommation d'énergie différents ont été introduits afin d'obtenir une analyse de l'efficacité énergétique d'émetteurs réalistes. Le fait que le codage à minimum d'énergie améliore l'efficacité énergétique a été confirmé et les limites des circuits électroniques pratiques ont été mises en évidence. Enfin, le protocole réseau a été abordé par l'introduction du protocole de contrôle d'erreurs ARQ. Finalement, l'efficacité énergétique d'une télécommande autonome a été améliorée en utilisant la modulation orthogonale OOK et un véritable démonstrateur a été présenté.

La combinaison avec un codage de canal, la capacité de réduction de l'interférence multi-utilisateur des modulations à faible rapport cyclique, la prise en compte de la couche MAC (Medium Access Control) et l'implémentation matérielle sont trois des perspectives envisageables pour ce travail.



Research and Published Papers

Journal Papers

1. Yue Peng, Duolong Wu, Guillaume Andrieux, Jean-François Diouris, *Research on Energy-efficiency in Wireless Sensor Networks Based on Minimum Energy Coding*, Journal of Guangdong University of Technology, Guangzhou, Chine, 2014,V31(1): 86-89.
2. Yue Peng, Guillaume Andrieux, Jean-François Diouris, *Energy Consumption Improvement of an Efficient OOK Transmitter Based on Minimum Energy Coding*, to be submitted.
3. Yue Peng, Guillaume Andrieux, Jean-François Diouris, *Energy-Efficient Transmission for Low Data Rate Communication*, to be submitted.

Conference Papers

1. Yue Peng, Guillaume Andrieux, Jean-François Diouris, *Energy consumption models for OOK transmitter based on minimum energy coding*, (SIFWICT 2013), 3-4 June 2013, Guangzhou, Chine
2. Yue Peng, Guillaume Andrieux, Jean-François Diouris, *Realistic Energy Consumption Model for On-Off Keying Based Minimum Energy Coding*, Vehicular Technology Conference (VTC Spring), 2014 IEEE 79th , vol, no, pp.1,5,18-21 may 2014

3. Yue Peng, Guillaume Andrieux, Jean-François Diouris, *Energy Consumption Improvement of OOK Transmitter Based on Minimum Energy Coding*, (SIFWICT 2015), 12 June 2015, Nantes, France

Bibliography

- [1] SCHWIEBERT, L.; GUPTA, S.K.S.; AUNER, P.S.G.; ABRAMS, G.; IEZZI, R.; MCALLISTER, P.. **A biomedical smart sensor for the visually impaired.** *IEEE Sensors*, **1(9)**:693 – 698, Feb. 2002. [15](#)
- [2] BOO-HO YANG. **A twenty-four hour tele-nursing system using a ring sensor.** *Robotics and Automation, IEEE International Conference on*, **1(9)**:387– 392, May 1998. [15](#)
- [3] LE QUANG VINH TRAN; BERDER, O.; SENTIEYS, O.. **RIC-MAC: A MAC protocol for low-power cooperative wireless sensor networks.** *in Wireless Communications and Networking Conference (WCNC), 2014 IEEE*. pages 1944–1949, 2014. [15](#)
- [4] TRONG NHAN LE; PEGATOQUET, A.; SENTIEYS, O.; BERDER, O.; BELLEUDY, C.. **Duty-cycle power manager for thermal-powered Wireless Sensor Networks.** *Personal Indoor and Mobile Radio Communications (PIMRC), 2013 IEEE 24th International Symposium on*, pages 1645–1649, 2013. [15](#)
- [5] YOUNIS, M.; GHUMMAN, K.; ELTOWEISSY, M.. **Location-Aware Combinatorial Key Management Scheme for Clustered Sensor Networks.** *Parallel and Distributed Systems, IEEE Transactions on*, **17(8)**:865–882, Aug 2006. [16](#)
- [6] RUIZ, L.B.; NOGUEIRA, J.M.; LOUREIRO, A.A.F.. **MANNA: a management architecture for wireless sensor networks.** *Communications Magazine, IEEE*, **41(2)**:116–125, Feb 2003. [16](#)
- [7] SEAH, W.K.G.; ZHI ANG EU; TAN, H.. **Wireless sensor networks powered by ambient energy harvesting (WSN-HEAP) - Survey and challenges.** *Wireless Communication, Vehicular Technology, Information Theory and Aerospace Electronic Systems Technology, 2009. Wireless VITAE 2009. 1st International Conference on*, pages 1–5, May 2009. [16](#)

- [8] CASTAGNETTI, A.; PEGATOQUET, A.; TRONG NHAN LE; AUGUIN, M.. **A Joint Duty-Cycle and Transmission Power Management for Energy Harvesting WSN.** *Industrial Informatics, IEEE Transactions on*, **10**(2):928–936, May 2014. [16](#), [18](#)
- [9] BRASCHE, G.. **Trends and Challenges of Wireless Sensor Networks.** *Applications and Services in Wireless Networks, 2008. ASWN '08. Eighth International Workshop on*, pages 7–7, 2008. [16](#)
- [10] SIMJEE, F.; CHOU, P.H.. **Everlast: Long-life, Supercapacitor-operated Wireless Sensor Node.** *Low Power Electronics and Design, 2006. ISLPED'06. Proceedings of the 2006 International Symposium on*, pages 197–202, Oct 2006. [16](#)
- [11] RAGHUNATHAN, V.; SCHURGERS, C.; SUNG PARK; SRIVASTAVA, M.B.. **Energy-aware Wireless Microsensor Networks.** *Signal Processing Magazine, IEEE*, pages 40–50, March 2002. [16](#), [61](#)
- [12] CHULSUNG PARK; CHOU, P.H.. **AmbiMax: Autonomous Energy Harvesting Platform for Multi-Supply Wireless Sensor Nodes.** *Sensor and Ad Hoc Communications and Networks, 2006. SECON '06. 2006 3rd Annual IEEE Communications Society on*, **1**:168–177, Sept 2006. [16](#)
- [13] WRIGHT P.K.; ROUNDY S.; RABAEY J.M.. **Energy Scavenging for Wireless Sensor Networks.** *Springer-Verlag, New York, LLC*, 2004. [16](#)
- [14] RAHIMI, M.; SHAH, H.; SUKHATME, G.; HEIDEMAN, J.; ESTRIN, D.. **Studying the feasibility of energy harvesting in a mobile sensor network.** *Robotics and Automation, 2003. Proceedings. ICRA '03. IEEE International Conference on*, **1**:19–24 vol.1, 2003. [16](#)
- [15] KANSAL, A.; SRIVASTAVA, M.B.. **An environmental energy harvesting framework for sensor networks.** *Low Power Electronics and Design, 2003. ISLPED '03. Proceedings of the 2003 International Symposium on*, pages 481–486, 2003. [16](#)
- [16] LIU SHAOQIANG; HONG DANLONG; CHEN LEI; FAN XIAOPING. **Energy saving scheme for data acquisition of WSN node.** *in Computer Science and Information Technology (ICCSIT), 2010 3rd IEEE International Conference on*, **4**:518–522, July 2010. [16](#)
- [17] JENNIFER YICK; BISWANATH MUKHERJEE; DIPAK GHOSAL . **Wireless sensor network survey.** *Computer Networks*, pages 2292–2330, 2008. [16](#)

- [18] BO JIANG; RAVINDRAN, B.; HYEONJOONG CHO **Probability-Based Prediction and Sleep Scheduling for Energy-Efficient Target Tracking in Sensor Networks**. *IEEE Transactions on Mobile Computing*, **12**(4):735–747, 2013. 18
- [19] PEI HUANG; LI XIAO; SOLTANI, S.; MUTKA, M.W.; NING XI. **The Evolution of MAC Protocols in Wireless Sensor Networks: A Survey**. *Communications Surveys Tutorials, IEEE*, **15**(1):101–120, 2013. 18
- [20] SUBRAMANIAN, G.; AMUTHA, R.. **Efficient and secure routing protocol for wireless sensor networks using mine detection An extension of triple umpiring system for WSN**. *Computing Technology and Information Management (ICCM), 2012 8th International Conference on*, 18
1:141–145, April 2012.
- [21] YUNUS, F.; ISMAIL, N.-S.N.; ARIFFIN, S.H.S.; SHAHIDAN, A.A.; FISAL, N.; SYED-YUSOF, S.K.. **Proposed transport protocol for reliable data transfer in wireless sensor network (WSN)**. Modeling, Simulation and Applied Optimization (ICMSAO), 2011 4th International Conference on *in Modeling, Simulation and Applied Optimization (ICMSAO), 2011 4th International Conference on*, pages 1–7, April 2011. 18
- [22] AL-FARES, M.S.; ZHILI SUN; CRUICKSHANK, H.. **A Reliable Multi-hop Hierarchical Routing Protocol in Wireless Sensor Network (WSN)**. *Information Technology: New Generations, 2009. ITNG '09. Sixth International Conference on*, pages 1604–1605, April 2009. 18
- [23] STANOJEV, I.; SIMEONE, O.; BAR-NESS, Y.; DONG HO KIM **Energy efficiency of non-collaborative and collaborative Hybrid-ARQ protocols**. *IEEE Transactions on Wireless Communications*, **8**(1):326–335, 2009. 18
- [24] YANWEI WU, XIANG-YANG LI, YUNHAO LIU, AND WEI LOU. **Energy-Efficient Wake-Up Scheduling for Data Collection and Aggregation**. *Parallel and Distributed Systems, IEEE Transactions on*, **21**(2):275–287, Feb 2010. 18
- [25] LIU XIANG; JUN LUO; ROSENBERG, C.. **Compressed Data Aggregation: Energy-Efficient and High-Fidelity Data Collection**. *Networking, IEEE/ACM Transactions on*, **21**(6):1722–1735, Dec 2013. 18
- [26] QIANG GAO; YI ZUO; JUN ZHANG; PENG, XIAO-HONG. **Improving Energy Efficiency in a Wireless Sensor Network by Combining Cooperative MIMO With Data Aggregation**. *Vehicular Technology, IEEE Transactions on*, **59**(8):3956–3965, 2010. 18

- [27] FENG, YUNXIA; TANG, SHAOJIE; DAI, GUOJUN. **Fault tolerant data aggregation scheduling with local information in wireless sensor networks.** *Tsinghua Science and Technology*, **16**(5):451–463, Oct 2011. [18](#)
- [28] THARINI, C.; RANJAN, P.V.; DEEPAN, R.; SELVAKUMAR, S.; SYED. **Distributed data compression for energy efficiency in wireless sensor networks.** *International Conference on Electronic Design.*, pages 1–5, 2008. [18](#)
- [29] HUSSIAN, S.I.; JAVED, H.; UR REHMAN, W.; KHALIL, F.N.. **CoXoH: Low cost energy efficient data compression for wireless sensor nodes using data encoding.** *Computer Networks and Information Technology (ICCNIT), 2011 International Conference on*, pages 149–152, July 2011. [18](#)
- [30] CAPO-CHICHI, M.E.P.; FRIEDT, J.-M.; GUYENNET, H.. **Using Data Compression for Delay Constrained Applications in Wireless Sensor Networks.** *Sensor Technologies and Applications (SENSORCOMM), 2010 Fourth International Conference on*, pages 101–107, July 2010. [18](#)
- [31] RAZA, U.; CAMERRA, A.; MURPHY, A.L.; PALPANAS, T.; PICCO, G.P.. **Practical Data Prediction for Real-World Wireless Sensor Networks.** *Knowledge and Data Engineering, IEEE Transactions on*, **27**(8):2231–2244, Aug 2015. [18](#)
- [32] HONGBO JIANG; SHUDONG JIN; CHONGGANG WANG. **Prediction or Not? An Energy-Efficient Framework for Clustering-Based Data Collection in Wireless Sensor Networks.** *IEEE Transactions on Parallel and Distributed Systems*, **22**(22):1064 – 1071, 2011. [18](#)
- [33] CHU DU; ZHANGBING ZHOU; LEI SHU. **An efficient technique of scheduling mobile sinks in hybrid WSN.** *Industrial Electronics Society, IECON 2014 - 40th Annual Conference of the IEEE*, pages 3885–3891, Oct 2014. [18](#)
- [34] DE, D.; SEN, A.; GUPTA, M.D.. **Cluster Based Energy Efficient Lifetime Improvement Mechanism for WSN with Multiple Mobile Sink and Single Static Sink.** *Computer and Communication Technology (ICCCT), 2012 Third International Conference on*, pages 197–199, Nov 2012. [18](#)
- [35] SHUAI GAO; HONGKE ZHANG; DAS, S.. **Efficient Data Collection in Wireless Sensor Networks with Path-Constrained Mobile Sinks.** *IEEE Transactions on Mobile Computing*, **10**(4):592–608, 2011. [18](#)
- [36] LIU, F.; CHENG, X.; RIVERA, M.J.M.. **Location-aware key establishment in wireless sensor networks.** *Proceedings of the International Wireless Communi-*

- cations and Mobile Computing Conference(IWCMC), Vancouver, Canada, 2006.*
[18](#)
- [37] ZUOYIN TANG; GLOVER, I.A.; EVANS, A.N.; JIANHUA HE. **Energy Efficient Transmission Protocol for Distributed Source Coding in Sensor Networks.** *Communications, 2007. ICC '07. IEEE International Conference on*, pages 3870–3875, June 2007. [18](#)
- [38] WEI WANG; DONGMING PENG; HONGGANG WANG; SHARIF, H.; HSIAO-HWA CHEN. **Taming Underlying Design for Energy Efficient Distributed Source Coding in Multirate Wireless Sensor Network.** *Vehicular Technology Conference, 2007. VTC2007-Spring. IEEE 65th*, pages 124–129, April 2007. [18](#)
- [39] XIAOXIA ZHANG; LIANG-LIANG XIE; AND XUEMIN SHEN. **An Energy-Efficient Bit Allocation Scheme in Wireless Sensor Networks.** *Global Telecommunications Conference (GLOBECOM 2010), 2010 IEEE*, pages 1–5, Dec 2010. [18](#)
- [40] BICEN, A.O.; AKAN, O.B.. **Energy-efficient RF source power control for opportunistic distributed sensing in wireless passive sensor networks.** *Computers and Communications (ISCC), 2012 IEEE Symposium on*, pages 000738–000743, July 2012. [18](#)
- [41] JIE HAO, ZHENG YAO, AND BAOXIAN ZHANG. **A gradient-based multi-path routing protocol for low duty-cycled wireless sensor networks.** *Communications (ICC), 2012 IEEE International Conference on*, pages 233–237, June 2012. [18](#)
- [42] WANG, A.Y.; SODINI, C.G.. **A simple energy model for wireless microsensor transceivers.** *Global Telecommunications Conference, 2004. GLOBECOM '04. IEEE*, **5**:3205–3209 Vol.5, Nov 2004. [18](#), [63](#), [65](#)
- [43] SHANNON, C.E.. **A mathematical theory of communication.** *Bell System Technical Journal, The*, **27**(4):623–656, Oct 1948. [21](#), [22](#)
- [44] MACKAY, D. J. C.. **Information Theory, Inference, and Learning Algorithms.** *Information Theory, IEEE Transactions on*, **50**(10), Oct 2004. [22](#)
- [45] LANDAUER, R.. **Irreversibility and heat generation in the computing process.** *IBM Journal of Research and Development*, **44**(1.2):261–269, Jan 2000. [23](#)
- [46] JOHN PROAKIS. **Digital Communications.** *McGraw-Hill Education; 5th edition*, 2007. [26](#), [27](#), [30](#), [39](#), [43](#), [44](#), [45](#), [47](#), [66](#), [67](#), [90](#), [104](#)

- [47] KATARIYA, A.; YADAV, A.; JAIN, N.; TOMAR, G.. **BER Performance Criteria Based on Standard IEEE 802.11a for OFDM in Multipath Fading Environments.** *Computational Intelligence and Communication Networks (CICN), 2011 International Conference on*, pages 238–241, Oct 2011. [26](#)
- [48] FENGZHONG QU; LIUQING YANG; SWAMI, A.. **Battery Power Efficiency of PPM and OOK in Wireless Sensor Networks.** *Acoustics, Speech and Signal Processing, 2007. ICASSP 2007. IEEE International Conference on*, 3:III–525–III–528, April 2007. [27](#)
- [49] MAHBOOB, M.. **Signalling and detection of parallel Triple Layer Wireless Sensor Networks with M-ary orthogonal modulation.** *Communications and Vehicular Technology in the Benelux (SCVT), 2012 IEEE 19th Symposium on*, pages 1–6, Nov 2012. [27](#)
- [50] MARVIN K. SIMON; MOHAMED-SLIM ALOUINI. **Digital communication over fading channels.** *Wiley, New York*, 2000. [30](#)
- [51] ERIN, C.; ASADA, H.H.; KAI-YEUNG SIU. **Minimum energy coding for RF transmission.** *Wireless Communications and Networking Conference, 1999. WCNC. 1999 IEEE*, pages 621–625 vol.2, 1999. [31](#)
- [52] PRAKASH, Y.; GUPTA, S.K.S.. **Energy efficient source coding and modulation for wireless applications.** *Wireless Communications and Networking, 2003. WCNC 2003. 2003 IEEE*, pages:212–217 vol.1, March 2003. [32](#), [33](#)
- [53] FISCHIONE, C.; JOHANSSON, K.H.; SANGIOVANNI-VINCENTELLI, A.; ARES, B.Z.. **Minimum Energy coding in CDMA Wireless Sensor Networks.** *Wireless Communications, IEEE Transactions on*, pages:985–994, Feb 2009. [32](#)
- [54] JAEWEON KIM; ANDREWS, J.G.. **An energy efficient source coding and modulation scheme for wireless sensor networks.** *Signal Processing Advances in Wireless Communications, 2005 IEEE 6th Workshop on*, pages 710–714, June 2005. [34](#), [36](#)
- [55] LIN, S.; COSTELLO, D. J.. **Error Control Coding: Fundamentals and Applications.** *Pearson Prentice-Hall*, 2004. [37](#)
- [56] ERIN, C.; ASADA, H.H.. **Energy optimal codes for wireless communications.** *Decision and Control, 1999. Proceedings of the 38th IEEE Conference on*, pages:4446–4453 vol.5, 1999. [41](#), [89](#)
- [57] RAPPAPORT, T.S.. **Wireless Communications, Principles and Practice.** *Prentice Hall*, 1996. [42](#)

- [58] TANG, Q.; GUPTA, S.K.S.; SCHWIEBERT, L.. **BER performance analysis of an on-off keying based minimum energy coding for energy constrained wireless sensor application.** *Communications, IEEE International Conference on*, pages:2734–2738, 2005. [48](#), [89](#)
- [59] QIN WANG; HEMPSTEAD, M.; WOODWARD YANG. **A Realistic Power Consumption Model for Wireless Sensor Network Devices.** *Sensor and Ad Hoc Communications and Networks, 2006. SECON '06. 2006 3rd Annual IEEE Communications Society on*, pages:286–295, Sept 2006. [59](#)
- [60] POLASTRE, J.; SZEWCZYK, R.; CULLER, D.. **Telos: enabling ultra-low power wireless research.** *Information Processing in Sensor Networks, 2005. IPSN 2005. Fourth International Symposium on*, pages 364–369, April 2005. [59](#)
- [61] HEINZELMAN, W.R.; CHANDRAKASAN, A.; BALAKRISHNAN, H.. **Energy-efficient communication protocol for wireless microsensor networks.** *System Sciences, 2000. Proceedings of the 33rd Annual Hawaii International Conference on*, pages 10 pp. vol.2-4-7, Jan 2000. [59](#)
- [62] CHIPCON. **SmartRF CC2420, 2.4GHz IEEE 802.15.4/ZigBee-ready RF Transceiver.** [59](#)
- [63] CHIPCON. **Wakeup receiver-aided communication terminals.** [59](#)
- [64] CHEE, Y.H.; RABAEY, J.; NIKNEJAD, A.M.. **A class A/B low power amplifier for wireless sensor networks.** *Circuits and Systems, 2004. ISCAS '04. Proceedings of the 2004 International Symposium on*, pages:IV–409–12 Vol.4, May 2004. [59](#)
- [65] AKSIN, D.; GREGORI, S.; MALOBERTI, F.. **High-efficiency power amplifier for wireless sensor networks.** *Circuits and Systems, 2005. ISCAS 2005. IEEE International Symposium on*, pages 5898–5901 Vol. 6, May 2005. [59](#)
- [66] FRANCESCO, M.; ANASTASI, G.; CONTI, M.; PASSARELLA, A.. **Energy Conservation in Wireless Sensor Networks: A survey.** *Ad Hoc Networks*, pages:537–568, 2009. [60](#)
- [67] SHUGUANG CUI; GOLDSMITH, A.J.; BAHAI, A.. **Energy-efficiency of MIMO and cooperative MIMO techniques in sensor networks.** *Selected Areas in Communications, IEEE Journal on*, **22**(6) pages:1089–1098, Aug 2004. [61](#), [66](#)
- [68] POTTIE, G.; KAISER, W.. **Wireless Integrated Network Sensors.** *Communication of ACM*, **43**:51–58, May 2000. [61](#)

- [69] QIULING TANG; LIUQING YANG; GIANNAKIS, G.B.; TUANFA QIN. **Battery Power Efficiency of PPM and FSK in Wireless Sensor Networks.** *Wireless Communications, IEEE Transactions on*, **6**(4):1308–1319, April 2007. [62](#)
- [70] SHUGUANG CUI; GOLDSMITH, A.J.; BAHAI, A.. **Modulation optimization under energy constraints.** *Communications, 2003. ICC '03. IEEE International Conference on*, **4**:2805–2811 vol.4, May 2003. [66](#), [67](#)
- [71] WANG, A.Y.; SODINI, C.G.. **On the Energy Efficiency of Wireless Transceivers.** *Communications, 2006. ICC '06. IEEE International Conference on*, **8**:3783–3788, June 2006. [66](#)
- [72] SHUGUANG CUI; GOLDSMITH, A.J.; BAHAI, A.. **Energy-constrained modulation optimization for coded systems.** *Global Telecommunications Conference, 2003. GLOBECOM '03. IEEE*, **1**:372–376 Vol.1, Dec 2003. [67](#)
- [73] DALY, D.C.; CHANDRAKASAN, A.P.. **An Energy-Efficient OOK Transceiver for Wireless Sensor Networks.** *Solid-State Circuits, IEEE Journal of*, **42**(5):1003–1011, 2007. [85](#)
- [74] CHEE, Y.H.; NIKNEJAD, A.M.; RABAHEY, J.. **An Ultra-Low-Power Injection Locked Transmitter for Wireless Sensor Networks.** *Solid-State Circuits, IEEE Journal of*, **41**(8):1740–1748, 2006. [85](#)
- [75] RAJA, M.K.; YONG PING XU. **A 52 pJ/bit OOK transmitter with adaptable data rate.** *Solid-State Circuits Conference, 2008. A-SSCC '08. IEEE Asian*, pages 341–344, 2008. [85](#), [98](#), [99](#), [100](#)
- [76] RAJA, M.K.; DINGJUAN CHUA; YONG PING XU. **A 52 pJ/bit 433-MHz low power OOK transmitter.** *Analog Integrated Circuits and Signal Processing*, **70**(1):57–67, January 2012. [98](#)
- [77] YUE PENG; ANDRIEUX, G.; DIOURIS, J.-F.. **Realistic Energy Consumption Model for On-Off Keying Based Minimum Energy Coding.** *Vehicular Technology Conference (VTC Spring), 2014 IEEE 79th*, pages 1–5, 2014. [105](#)
- [78] TAN, Y.K.; HOE, K.Y.; PANDA, S.K.. **Energy Harvesting using Piezoelectric Igniter for Self-Powered Radio Frequency (RF) Wireless Sensors.** *Industrial Technology, 2006. ICIT 2006. IEEE International Conference on*, pages 1711–1716, 2006. [125](#)
- [79] LAMBERT J.H. **Observationes variae in mathesin puram.** *Acta Helveticae physico-mathematico-anatomico-botanico-medica, Band III*, pages 128–168, 1758. [143](#)

- [80] CORLESS, R. M.; GONNET, G. H.; HARE, D. E. G.; JEFFREY, D. J.; KNUTH, D. E.. **On the Lambert W function.** *Advances in Computational Mathematics*, pages 5: 329–359., 1999. [143](#)
- [81] CORLESS, R. M.; GONNET, G. H.; HARE, D. E. G.; JEFFREY, D. J.; KNUTH, D. E.. **Lambert’s W function in Maple.** *The Maple Technical Newsletter (MapleTech)*, pages 9: 12–22, 1993. [143](#)

Thèse de Doctorat

Yue PENG

Optimisation énergétique des communications entre objets communicants

Energy optimisation of communication techniques between communicating objects

Résumé

Les progrès technologiques ont permis le développement d'applications de capteurs sans fil. Les capteurs densément distribués impliquent le plus souvent de faibles débits de données et de faibles portées de transmission. L'efficacité énergétique demeure une contrainte importante pour la conception des réseaux de capteurs sans fil. Pour ces applications, les noeuds sont généralement déployés avec des ressources énergétiques réduites et le remplacement d'une batterie peut être coûteux. Plusieurs méthodes peuvent être utilisées pour minimiser la consommation d'énergie dans ces réseaux. Dans cette thèse, nous nous concentrons sur la couche physique et sur la réduction de la consommation d'énergie des méthodes de transmission en utilisant des modulations à faible énergie. Une première étude nous permet de déduire que pour un canal BBAG, le codage à minimum d'énergie basé sur la modulation OOK est efficace énergétiquement, mais au prix d'une efficacité spectrale réduite. Seule la puissance de transmission est considérée et la consommation des circuits électroniques n'est pas prise en compte. Ensuite, des modèles de consommation d'énergie différents sont introduits afin d'obtenir une analyse de l'efficacité énergétique de transmetteurs réalistes. Le fait que le codage à minimum d'énergie améliore l'efficacité énergétique est confirmé et les limites des circuits électroniques pratiques sont mises en évidence. Enfin, le protocole réseau est abordé par l'introduction du protocole de contrôle d'erreurs ARQ. Finalement, l'efficacité énergétique d'une télécommande autonome est améliorée en utilisant la modulation orthogonale OOK et un véritable démonstrateur est présenté.

Mots clés

Réseaux de capteurs sans fil, efficacité énergétique, OOK, codage à minimum d'énergie.

Abstract

Technological advances have resulted in the development of wireless sensor applications. The densely distributed sensors, generally used for data gathering, environmental monitoring, industrial automation or surveillance, involve often low data rates and low transmission ranges. Despite the progress in software and hardware technologies, the energy efficiency is still one of the important constraints for the design of Wireless Sensor Network (WSN). For wireless sensor applications, nodes are usually deployed with reduced energy resources and without capability of battery replacement. Several techniques could be used to minimize the energy consumption of WSN. In this thesis we focus the physical layer and we propose to reduce the energy consumption by using low energy coding schemes. Firstly, a study allows us to deduce that in AWGN channel, Minimum-Energy Coding based on OOK modulation is energy efficiency, but at the price of lower spectrum efficiency. Only the transmission power is considered and the consumption of electronic circuits is not taken into account. Then, different energy consumption models are introduced to achieve energy efficiency analysis using realistic devices. The fact that Minimum-Energy coding based on OOK improves the energy efficiency performance is confirmed and the limits of practical circuits are highlighted. At last, the network protocol is addressed by introducing the ARQ error control protocol. Finally, the energy efficiency of an autonomous remote control is improved by using OOK orthogonal modulation and a real demonstrator is realized.

Key Words

Wireless sensor networks (WSNs), Energy efficiency, OOK, Minimum energy coding.